STATIC AND DYNAMIC RESPONSE OF A MODEL CURVED GIRDER BRIDGE

RAMENDRA SUNDAR GHOSH

DISSERTATION

IN THE

FACULTY OF ENGINEERING

Presented in partial fulfilment of the requirements for the

Degree of MASTER OF ENGINEERING

at

Sir George Williams University

Montreal, Canada

September, 1972.

ABSTRACT

An analysis of the static and dynamic response of a single span horizontally curved girder bridge is presented. Static and dynamic loads were applied to a one-eighth scale model, and experimental values obtained for deflections and strains. The combined torsional and flexural natural frequencies were obtained both analytically and experimentally.

The static analysis was carried out with and without a concrete slab deck. Without the concrete slab, the bridge was treated as a plane grid with curved elements. With the concrete slab, the bridge was treated as a beam of composite cross-section. A comparison is made between the computed and experimental response of the model curved bridge, and good agreement is obtained.

ACKNOWLEDGEMENT

The writer wishes to express his indebtedness and gratitude to Dr. Matthew McC. Douglass for his guidance and encouragement during the course of this work and most of all for providing the inspiration and helpful assistance during the preparation of this dissertation.

The author would also like to sincerely thank Mr. Adham Khalil who rendered invaluable help and guidance in setting up the experiment at all stages and in helping to conduct the experiment.

The writer also wishes to sincerely thank the following individuals and organizations for the help they have provided.

To Mr. E. Heasman, the Civil Engineering technician, for providing help in the experimental work.

To Mr. J. Hopkins for helping with the computer work.

To the staff of the Structures Laboratory for helpful assistance.

In addition, gratitude is due to Miss Sharon Flood, who typed the manuscript.

Montreal, Canada R.S. Ghosh

September 1972.

TABLE OF CONTENTS

LIST OF FIGURES

LIST OF PHOTOGRAPHS

NOTATION

A	=	$\frac{L}{\pi R}$, central included angle parameter
B	=	bimoment
C	=	viscous damping coefficient
Cn, Cns	=	transverse displacement amplitudes of the nth and nsth mode, respectively
$C_b(Z)$	=	Viscous damping coefficient for the transverse displacement
CO(Z)	=	viscous damping coefficient for the torsional rotation
D	=	$\frac{L}{\pi \rho_o}$, ratio of span to polar radius of gyration about shear centre
Dn, Dns	=	torsional rotation amplitudes if nth and nsth mode
DI	=	dimensionless dynamic increment, defined as the difference between the instantaneous value of a dynamic effect and the corresponding static effect, normalised with respect to the maximum static value of that effect
DI	=	DI for deflection
DI	=	DI for rotation
DI_M	=	DI for bending moment
DI_S	=	DI for St. Venant's torsional moment
DI_W	=	DI for warping torsional moment
DI_B	=	DI for bimoment
E	=	modulus of elasticity of the bridge material
f(z,t)	=	external load in the y-direction per unit length
$\mathcal{F}$	=	Rayleigh's dissipation function
G	=	Modulus of shear rigidity

I_x	=	moment of inertia of the cross-section of the bridge
I_w	=	warping constant
J	=	St. Venant's torsional constant
L	=	length of curved bridge along the centre line between supports
m_b	=	the beam mass per unit length
m_n, m_{ns}	=	model mass participating respectively in the nth and nsth mode
n	=	an interger denoting the order of the natural mode of vibration
P	=	magnitude of constant force
Q	=	transverse shear force
U	=	strain energy
V	=	speed of vehicle
Yn, Yns	=	eigenfunctions for the transverse displacement
ρ_o	=	the polar radius of gyration of the bridge cross-section about its shear centre
ϕn, ϕns	=	eigenfunctions for the torsional rotation
ωn, ωns	=	coupled natural frequencies of the curved beam
ω_v	=	the nth uncoupled flexural natural frequency of a straight beam of the same length as the centre line length of the curved beam
$\omega\phi$	=	the nth uncoupled torsional natural frequency of a straight beam of the same length as the centre line length of the curved beam

CHAPTER 1

INTRODUCTION

1.1 General

In recent years there has been an increasing demand for highway interchanges in cities. With the tight geometric restrictions necessary in such areas a demand for curved bridges has developed. There are many advantages in the use of curved girders. Steel girder bridges are particularly attractive where clearance is critical.

Many curved girder bridges have been built using steel girders, but in general the girders have been straight with only the reinforced concrete deck being curved. However a curved girder bridge has certain advantages. e.g.

1. The number of Piers required is less, because straight girders which are really chords of the bridge have to be short to follow the curve of the bridge.
2. There is continuity in curved girder bridges providing reduction in moments, whereas straight girders must be simple beams.
3. The overhanging slab from the outside girder varies for the straight beams, whereas it is constant for curved girders.

4. The appearance of curved girders is much better than straight ones, particularly when viewed from below.

A review of the literature discloses several theoretical and analytical approaches to the computation of the dynamic response of various types of bridges under moving loads, but literature on curved girder bridges is sparse. Few papers on dynamic analysis of curved bridges are available.

The object of this investigation is to find out the response of a curved girder bridge under the action of both static and dynamic loads. An actual bridge was designed for highway H-20 loading and an 1/8" scale model was used for investigation of its static and dynamic behaviour.

An analysis has been developed for the natural frequency of a curved girder bridge consisting of steel girders and composite decking.

A static analysis of the bridge grid has been also carried out to verify the analysis developed by previous investigators.

1.2 Previous Study

Fickel[1] obtained the expression for the influence lines of a curved girder for statically determinate and indeterminate systems. Close[2] derived an expression for the deflection of a curved cantilever beam. In both of the

above two investigations the deflection is assumed to result from deformations due to bending and St. Venant's torsion, without taking warping into consideration, even though non-uniform torsion exists in a non-circular section with restraint against warping. A publication by United Steel Corporation[33] gives two methods of design and analysis. Both are based on limiting assumptions. The segments of curved girders between diaphragms are assumed to be either completely free to warp or completely restrained.

Lavelle[3] developed a procedure for analysing curved girders using a stiffness matrix. He also developed a computer programme to analyse curved girder bridges under static loading. Han Chin Wu[4] developed a method of determining normal stresses caused by warping. C.B. Clark[5] analysed a model structure and found the work of Lavelle and Wu to be in satisfactory agreement with his experimental results.

Dabrowski[6] analysed a curved girder of thin walled open cross-section symetric, about one axis only. The structure is restrained against translation at the supports while rotation is permitted about all but the longitudinal axis. This is an extension of the analysis of Vlasov[7] who assumed cross-section to be doubly symetric.

Culver [8] determined the natural frequency of a curved beam using the governing differential equations

developed by Vlasov. The cross-sectional shape is assumed to be constant along the entire length of the member and doubly symmetric i.e. the shear centre and centroid coincide. Both prismatic and thin walled open cross-sections have been considered for vibrations normal to the plane of curvature. For the case of a simply supported beam, he assumed the normal mode functions for deflections in the form of sine curves and obtained a solution for Vlasov's equations. For the case of fixed-end curved beams he obtained an approximate solution for the natural frequencies using the Rayleigh-Ritz method.

Yonezawa[9] used the solutions for orthotropic fan shaped plates which are simply supported at two opposite straight edges and rigidly attached to elastic beams at the other curved edges for the static case of a uniformly distributed load and for the case of free vibrations. He applied those solutions to the numerical analysis of curved girder bridges.

In the problem of free vibrations both an exact solution (by the Frobenius Method) and an approximate one (by the Galerkin Method) were obtained.

The dynamic response of beams subjected to travelling loads is being studied for a century. In 1847 Willis[10] established the governing equation of motion of a mass load traversing a simply supported beam having uniform stiffness

with negligible mass and damping.

Kryloff[11] first solved the problem of a force having no mass travelling with a constant velocity over a member having a uniformly distributed mass.

Timoshenko[12] solved the same beam with an additional pulsating force crossing the beam.

In 1935 Lowan[13] considered the effect of a constant force traversing the beam at a variable rate.

Inglis[14] solved the problem of a smoothly rolling mass and a pulsating force crossing a beam having uniform mass and stiffness and also possessing viscous damping. He assumed the load distribution and deflection to be represented by a half sine curve.

Jeffcott[15] solved the general case of a mass travelling over a beam of uniform mass and stiffness. He solved the governing linear differential equation with variable co-efficients by an iterative method.

Shallenkamp[16] found a solution in terms of a Fourier series with unknown co-efficients which were determined by solving a system of linear algebraic equations, obtained through the use of generalised co-ordinates and linear superposition principles.

In 1950 Ayre[17] et al solved the problem of a pure force passing over a two span continuous beam. A subsequent experimental investigation was made[18] for

comparison with the Shallenkamp solution for a simple span and for the pure force solution for a two span continuous member.

In 1961 Licari[19] and Wilson obtained a mathematically exact solution to the problem of a beam of uniform mass and stiffness with viscous damping traversed by a moving mass system. The system consisted of unsprung and sprung, damped components in addition to a pulsating pure force. The solution is presented as an infiinte series having co-efficients obtained through the condition of compatibility between the beam and the vehicle.

Looney [20,21] and Biggs[22,23] solved by numerical methods the differential equations describing the transient response of a single span beam subjected to a moving sprung and unsprung mass system. It is assumed in these analyses that the deflection of the structure could be described by the first mode of vibration.

Wen[24] extended this method in analysing the case of a two axle vehicle by assuming the deflected shape of the span to be equal to the static deflection ot the instantaneous position of the vehicle.

Fleming and Romualdi[25] analysed a multispan system by replacing the spans by lumped mass systems excited by forcing functions dependent on the position of the moving mass load.

Tung[26] et al solved numerically the governing

differential equation of motion of a single span member derived from an energy consideration.

The work of Duncan[27] and Bishop et al[28,29] describing the use of dynamic receptances in the analysis of vibrating systems was expanded by Skeer[30] to incorporate a moving forcing function exerted on a beam and plate system.

Christiano[31] studied the dynamic response of horizontally curved girder bridges subjected to moving loads.

He formulated the differential equations of motion of the bridge by adapting the static case derived by Dabrowski. The equations are solved by using an extension of the work by Licari and Wilson who analysed the dynamic behaviour of a straight beam subjected to a similar forcing function. The accelerations of the unsprung mass are expressed in terms of a Fourier sine series with unknown co-efficients. The compatibility condition between the bridge and vehicle are used to establish a system of linear differential equations from which the co-efficients are obtained.

Due to non-coincidence of the shear centre and the centroid of the cross-section, there results a triple coupling phenomenon of the bending (about two orthogonal directions) and twisting modes of vibration. His investigations employed the following assumptions regarding the bridge model: the distribution of flexural, torsional and

warping rigidities and the mass of the beam is uniform along the length of the span. The effect of bridge damping is neglected. The vehicle is idealised to be a single axle one with two wheels and having sprung and unsprung components of mass.

Vashi and Heins Jr.[32] investigated the dynamic behaviour of a curved bridge.

In their analysis the flexural and torsional damping in the bridge is considered to be viscous and uniformly distributed along the span. The co-efficients of viscous damping in flexure and torsion are assumed to be proportional to the beam mass and the mass polar moment of inertia respectively. The vehicle is represented as a single axle as well as a two axle sprung mass-load having sprung and unsprung components of mass. The suspension system includes a constant frictional force and a periodic force simulating the effects of flat spots in tires. The two axle representation permits investigation of the effects of pitching motion and the axle spacing on the response of the curved beam.

In this investigation a scaled model of a curved girder highway bridge has been tested to find its response to both static and dynamic loading, and the combined natural frequencies of vibration have been measured for both the vertical and twist modes.

CHAPTER II

2.1 Design and Fabrication of the Model

The curved bridge was designed for H20-S16 loading. The bridge is for single lane traffic and has a simply supported span of 90'-0" along the curve and a radius of curvature of 90'-0". An 1/8 scale model is shown in Fig. 1. The bridge consists of two main steel girders with intermediate cross girders. The concrete deck is of composite construction having studs connected to the top of the curved girders.

The design was based on a simplified method as outlined in a publication by the United States Steel Corporation[33]. This method has sufficient engineering accuracy for practical design. The first step of the simplified method is to isolate each curved girder under consideration and straighten it out to its full developed length. The external load is then applied to the girder considering it supported at its developed span lengths and the moment diagram is constructed by standard procedures for beams. This diagram is called primary moment diagram.

The next step is to construct a similar diagram having as its ordinates the ordinates of the primary moment diagram divided by the horizontal radius of the curved girder.

This is referred to as the M/R diagram and its purpose is explained with the help of Fig. 4.

A portion of the flange of a straight girder is shown in Fig. 4(a). Ignoring flexural stress carned by the web, the internal force at any point along the flange is equal to the moment at that point divided by the depth of the beam.

$$F = M/d \qquad \ldots(1)$$

By curving the flange along an arc of radius R, as would be the case in a curved girder, radial components of these internal forces are developed as a distributed force, q. This is shown in Fig. 4(b).

The magnitude of q can best be derived by the equilibrium condition for a very small segment of a girder as shown in Fig. 4(c), where the direction of q is reversed. Radial force q and axial force F, vary along the girder length. However, for a small segment of the girder, and F may be considered constant. Writing the equilibrium equation nn the Y direction.

$2qR\Delta\theta = 2F \sin\Delta\theta$

For small angles:

$\Delta\theta = \sin\Delta\theta$

Reducing: $2qR = 2F$

or $q = \frac{F}{R}$ $\qquad \ldots(2)$

Combining equations (1) and (2)

$$q = \frac{M}{dR} \quad ; \text{or} \qquad \ldots(3)$$

$$d = M/R \qquad \ldots(4)$$

The M/d internal forces developed in the top and bottom flanges are equal in magnitude but opposit in direction in the two flanges. Consequently, their radial components q are also equal in magnitude but opposite in direction, representing a couple (or a torque) equal to (qd). Therefore, the M/R diagram is, in fact, a torque diagram per unit length acting on the girder due to curvature. The M/R diagram is now applied as a distributed load acting laterally on the developed length of the girder which is now considered supported at each point of torsional restraint, or in other words, at each diaphragm or floor beam.

Since the M/R loading is really torque per foot, it is evident that the support reactions at the floorbeams due to this lateral loading are then the concentrated resisting torques developed by the floorbeams to restrain twisting of the curved girder. Although the girder is actually continuous over the support at each floorbeam, this continuity was ignored and the reactions at the floorbeams due to the M/R loading determined by simple beam

action would be sufficiently accurate. After computing the reactions, the shear diagram was constructed. The shear diagram is the internal torque of the curved girder diagram.

After applying these steps to both girders of the system and obtaining the concentrated torques at both ends of the floorbeams, the end shears of each floorbeam were computed by the equations of static equilibrium. These end shears were then applied as vertical concentrated loads to the girder which was again considered supported at its developed span length. This method of convergence was repreated twice and the results were considered sufficiently accurate.

2.2 Fabrication of the Specimen

The steel used for fabrication was ASTM Standard A36, Structural Steel The curved girders were heat curved since the curvature of the girders was very high.

All Connections were welded. Small studs were welded to top flanges to act as shear connectors. The model is shown in Figure 1.

CHAPTER III

THEORETICAL PROGRAM

3.1 Static Analysis

The curved girder bridge was first analyzed as a grid without the concrete slab. Matrix analysis of the grid was made using the stiffness method. A computer program developed by Lavelle[3] was used to analyze the grid. The details of the derivation are given in Appendix A. It outlines the general procedure for a stiffness matrix with modification being made for the member stiffness matrix of individual curved elements. This program gives the moment, shear and torque for each individual elements.

The stresses resulting from the non-uniform torsion was obtained by the method used by Wu.[4] Non-circular sections when twisted, undergo longitudinal warping as well as angular distortions. Plane sections before twisting do not remain plane after twisting. If this warping tendency is not restrained, the member will exhibit a constant unit angle of twist and will therefore be subjected to pute torsion. If however, the warping distorsion is resisted in any way, longitudinal normal stresses are produced in addition to the torsional shearing stresses.

The angle of twist per unit length will no longer be constant. The detailed derivation is given

in Appendix B.

The curved bridge was then analyzed with the concrete deck. The method developed by Dabrowski was used. A brief outline is given below.

Consider the element shown in Fig. 2. The element is of length dz, which is the product of the radius and the central angular increment $d\alpha$. The cross section is assumed to be non-deformable, and has a vertical axis of symmetry. A point on the element is defined by its location relative to the right hand co-ordinate system, the origin of which is at the centroid of the cross section. The displacement of the shear center, which is considered to be a distance Yo above the centroid, is defined by components U, V and W in the X, Y and Z directions respectively, The displacement of any point on the cross-section may be defined relative to the shear centre through the angle of twist, $\emptyset$.

The external forces Px, Py, Pz acting in the X, Y and Z directions respectively in addition to the external torque P$\emptyset$, about the Z axis, are applied at the shear centre, and are shown acting in the positive direction. The internal shear forces Qx and Qy and the twisting moment H, also act through the shear centre, however the normal force N and the bending moments Mx and My, are transmitted through the centroid of the cross-section.

Equilibrium Equations

The conditions of equilibrium are given as follows:

$$\sum F_x = Q_x' + \frac{N}{R} + p_x = 0 \qquad (3.1.1a)$$

$$\sum F_Y = -Q_y' + p_y = 0 \qquad (3.1.1b)$$

$$\sum F_z = N' - \frac{Q_x}{R} + p_z = 0 \qquad (3.1.1c)$$

$$\sum M_x = M_x' + \frac{1}{R}(H + Q_x y_o) + Q_y = 0 \qquad (3.1.1d)$$

$$\sum M_y = M_y' + Q_x = 0 \qquad (3.1.1e)$$

$$\sum M_z = H' - \frac{1}{R}(M_x + N y_o) + p_\phi = 0 \qquad (3.1.1f)$$

where the prime (') denoted differentiation with respect to Z. The shear forces Qx and Qy may be eliminated from the above equations, resulting in four independent equations having four unknowns as follows:

$$N' + \frac{M_y'}{R} + p_z = 0 \qquad (3.1.2a)$$

$$M_x'' + \frac{1}{R}\left(H' - \frac{N}{R} y_o - p_x y_o\right) + p_y = 0 \qquad (3.1.2b)$$

$$M_y'' - \frac{N}{R} - p_x = 0 \qquad (3.1.2c)$$

$$H' - \frac{1}{R}(M_x + N y_o) + p_\phi = 0 \qquad (3.1.2d)$$

Force Deformation and Moment-Curvature Relations

The normal force N, the bending moments Mx and My, and the twisting moment H , are related to the displacement components U, V, W and ϕ, by

$$N = EA\left(w' - \frac{u}{R} - \phi\frac{y_o}{R}\right) \qquad (3.1.3a)$$

$$M_x = -EI_x\left(v'' - \frac{\phi}{R}\right) \qquad (3.1.3b)$$

$$M_y = EI_y\left[u'' + \frac{v}{R^2} - \frac{\phi}{R^2}(y_o + r_y)\right] \qquad (3.1.3c)$$

$$H = -EI_w\left(\phi''' + \frac{v'''}{R}\right) + GK_t\left(\phi' + \frac{v'}{R}\right) \qquad (3.1.3d)$$

where

A = area of cross section

E = Young's modulus

G = Shear modulus

Ix = Moment of inertia about X axis

Iy = Moment of inertia about Y axis

Iw = Warping constant

Kt = St. Venant torsion constant and

$$r_y = \frac{1}{I_y}\int y x^2 \, dA$$

Substitution of Equations (3.1.3) into Equations (3.1.2) would result in a set of four coupled differential equations in U, V, W and Ø. In order to simplify the method of solution however, it is assumed that the normal force N, can be neglected in Equations (3.1.2). The solution of the above is given in reference (6).

3.2 Dynamic Analysis

The dynamic analysis is based on a method developed by Vashi[32]. A brief outline of the method is presented below.

3.2.1 Mathematical Models

The mathematical analysis of the problem of the dynamic behaviour of horizontally curved bridges requires idealization of the actual bridge vehicle system. This idealization is based upon the following simplifications and assumptions regarding the behaviour of the bridge and the vehicle unit.

1. Bridge

a. Usual curved beam theory of thin-walled symmetrical cross-sections is assumed to be applicable. It is assumed that during vibration, the deflection of all girders at any transverse section of the bridge is constant. Accordingly, an actual bridge which may consist of a floor system and stringers is represented by a single

curved beam of equivalent rigidity and mass, as shown in Fig. 3.

b. Cross-sectional dimensions of the bridge are assumed to be small, compared to the horizontal radius of curvature and the length of the beam.

c. Centroid and shear centre are assumed to coincide. Although this is not true of a highway bridge cross-section, the noncoincidence of centroid and shear centre results in an inappreciable error because of the slenderness of the beam.

d. The distribution of flexural, torsional and warping rigidities and the mass of the beam is uniform along the span length.

e. Effects of shearing deformation, flexural rotatory inertia and axial forces are assumed to be negligible.

f. Bridge damping is viscous and uniformly distributed along the span. The co-efficients Cb(Z) and Cθ(Z) of viscous damping in flexure and torsion, respectively are assumed to be proportional to the beam mass and the mass polar moment of inertia.

g. The beam is assumed to be simply supported. For a simple support, it is assumed that the flexural and warping normal stresses are zero at the support. The designation "simple support" requires that such a support

resists a torque i.e. prevents rotation.

h. Bridge deck is assumed to be smooth and free of irregularities.

3.2.2 Vehicle as a Constant Force

The problem of the vibration of a multi-wheel vehicle with many degrees of freedom is very complicated. The width of the vehicle and consequently the effects of rolling cannot be considered in the analysis because of the idealization of the bridge as a curved beam.

An actual highway vehicle which possesses sprung and unsprung components of mass can be idealised as a single axle sprung mass in Figure 5.

Because of the vehicle mass, the contact forces between the vehicle and the bridge will vary considerably. However, it has been shown in Reference (32) that the extent to which the constant force solution correlates with the sprung mass load solutions depends primarily on the frequency ratio σ_y. Also, for small values of all sprung mass load solutions approach the constant force solutions irrespective of the value of the mass ratio, RS, and the contact forces remain almost constant and undergo a variation which is less than 10% of the static load. Therefore, the vehicle will be idealised as a constant force on the bridge. It will also be assumed that the constant force will pass through the shear centre of every

cross-section, as it traverses the bridge at a constant speed, travelling from left to the right along the bridge span.

Displacement Equations of Flexural-Torsional Bridge Motion

Vlasov's Theory (7) of flexural-torsional motion of the elastic horizontally curved beam takes into account the flexural and torsional deformations and accordingly contains two dependent variables instead of the one transverse displacement described in the classical theory of flexure of straight beams.

Fig. 6 shows an element of a horizontally curved beam with a set of reference axes passing through the shear centre of the beam cross-section. The parameters and θ denote respectively the vertical displacement of the shear centre in the Y direction and the angle of twist of the beam cross-section. R is the constant radius of curvature of the centre line of the beam (Z axis).

The equilibrium of the forces moments and torques acting on the sides of an element of the curved beam as shown in Fig. 7 give the following three equations.

$$\frac{\partial Q}{\partial z} + f(z,t) - m_b \ddot{\eta} = 0 \qquad (3.2.1a)$$

$$\frac{\partial M}{\partial z} - Q + \frac{T}{R} = 0 \qquad (3.2.1b)$$

$$\frac{\partial T}{\partial z} - \frac{M}{R} + m(z,t) = m_b \rho^2 \ddot{\theta} \qquad (3.2.1c)$$

The functions Q, M and T denote the transverse shear force, the bending moment and the torsional moment, respectively.

The terms f(z,t) and m(z,t) represent the external load intensity in the Y direction and the externally applied torsional moment per unit length respectively. The terms $m_b\ddot{\eta}$ and $m_b\rho^2\ddot{\theta}$ are the inertia forces of translation and rotation during vibration. m_b and ρ_o are respectively, the beam mass per unit length and the polar radius of gyration about the shear centre. The number of dots above η and θ indicates the order of differentiation with respect to line, t.

The internal bending and torsional moments as described by Vlasov can be expressed in terms of η and θ and used as follows:

$$M = - EI_x \left(\eta'' - \frac{\theta}{R}\right) \qquad (3.2.2a)$$

$$T = GK_t \left(\frac{\eta'}{R} + \theta'\right) - EI_w \left(\frac{\eta''}{R} + \theta'''\right) \qquad (3.2.2b)$$

The total torsional moment T defined by Eq. (3.2.2b) is obtained by summing the St. Venant's torsional moment S with the warping torsional moment W, which are as follows:

$$S = GK_t \left(\frac{\eta'}{R} + \theta'\right) \qquad (3.2.2c)$$

$$W = -EI_w \left(\frac{\eta''}{R} + \theta'''\right)$$

The terms E x, GKt and EIw are flexural torsional and warping rigidities respectively. The number of primes above η and θ indicates the order of differentiation with respect to the Z co-ordinate.

Eliminating the term Q in Eq. (3.2.1a) and (3.2.1b) and substituting Eqs. (3.2.2a) and (3.2.2b) into resulting Equation and Eq. (3.2.1c) gives

$$\left(\frac{EI_w}{R^2}+EI_x\right)\eta'''' - \frac{GK_t}{R^2}\eta'' + \frac{EI_w}{R}\theta''' - \frac{EI_x+GK_t}{R}\theta'' + m_b\ddot{\eta} = f(z,t) \tag{3.2.3a}$$

$$\frac{EI_w}{R}\eta'''' - \frac{EI_x+GK_t}{R}\eta'' + EI_w\theta'''' - GK_t\theta'' + \frac{EI_x}{R^2}\theta + m_b\rho_o^2\ddot{\theta} = m(z,t) \tag{3.2.3b}$$

These equations form a set of two linear, simultaneous partial differential equations for flexural torsional motions of a horizontally curved beam with any support conditions. subjected to the forcing functions f(z,t) and m(z,t).

For a simple support boundary conditions, the displacement η, the rotation θ, the normal flexural stress σ_f, and the normal warping stress σ_w, all vanish at the boundary. The first two conditions can be symbolically written as

$$\eta(0,t) = \eta(L,t) = 0 \tag{3.2.4a}$$

$$\theta(0,t) = \theta(L,t) = 0 \tag{3.2.4b}$$

Remembering that the normal flexural stress is proportional to the bending moment M defined by Eq. 3.2.2a and the normal warping stress σ_w is proportional to the bimoment B defined as

$$B = -EI_w\left(\frac{\eta''}{R} + \theta''\right)$$

and utilizing Eqs. (3.2.4a) and (3.2.4b) the remaining two conditions are satisfied if:

$$\eta''(0,t) = \eta''(L,t) = 0 \qquad (3.2.4c)$$

$$\theta''(0,t) = \theta''(L,t) = 0 \qquad (3.2.4d)$$

Here L denotes the length of the curved beam between the supports along the Z axis.

C. Free Vibrations

The free vibration problem is specified by Eqs. (3.2.3a) and (3.2.3b) in their homogeneous form, i.e. with $f(z,t) = m(z,t) = 0$, and by boundary conditions given by Eqs.(3.2.4a, b,c and d). For harmonic vibrations, one can take

$$\eta(z,t) = \sum_{n=1}^{\infty} Y_n(z)\,\sin(\omega_n t + \epsilon_n) \qquad (3.2.5a)$$

$$\theta(z,t) = \sum_{n=1}^{\infty} \phi_n(z)\,\sin(\omega_n t + \epsilon_n) \qquad (3.2.5b)$$

Substituting Eqs. (3.2.5 a, b) into Eqs. (3.2.3 a, b)

with f(z,t) = m(z,t) = 0 results in a pair of ordinary differential equations which can be solved for the eigenfunctions Yn and Øn. However, for the simple support boundary conditions the eigenfunctions have the simple form:

$$Y_n(z) = C_n \sin \frac{n\pi z}{L} \tag{3.2.6a}$$

$$\phi_n(z) = D_n \sin \frac{n\pi z}{L} \tag{3.2.6b}$$

Substituting Eqs.(3.2.6a,b) into Eqs.(3.2.6a, b) and the resulting equations into Eqs.(3.2.3a,b) with f(z.t) = m(z,t) = o gives

$$\left[1+\frac{D^2}{A^2}\left(\frac{\omega_r}{\omega_\theta}\right)^2\left\{1-\left(\frac{\omega_n}{\omega_r}\right)^2\right\}\right]C_n + R\left[1+\left(\frac{D}{n}\right)^2\left(\frac{\omega_r}{\omega_\theta}\right)^2\right]D_n = 0 \tag{3.2.7a}$$

$$\left[1+\left(\frac{D}{n}\right)^2\left(\frac{\omega_r}{\omega_\phi}\right)^2\right]C_n + R\left[1+\left(\frac{\omega_r}{\omega_\phi}\right)^2\left\{\frac{A^2D^2}{n^4}-\left(\frac{\omega_n}{\omega_r}\right)^2\right\}\right]D_n = 0 \tag{3.2.7b}$$

Here the following notation has been used.

$$\omega_r = \left(\frac{n\pi}{L}\right)^2\sqrt{\frac{EI_x}{m_b}}$$

$$\omega_\phi = \frac{n\pi}{L^2}\sqrt{\frac{n^2\pi^2 EI_w + GK_t}{m_b\rho_o^2}L^2}$$

$$A = \frac{L}{\pi R}$$

$$D = \frac{L}{\pi\rho_o}$$

Equating the determinant of the co-efficient matrix of

Eqs.(3.2.7a, b) to zero and solving for Wn yield

$$\omega_{ns} = \frac{2\pi}{T_B} n^2 \sqrt{\rho_{ns}}$$

(S = 1 & 2 for each n = 1,2.....

(3.2.8)

where

$$\left.\begin{matrix}\rho_{n1}\\ \rho_{n2}\end{matrix}\right\} = \frac{1}{2}\left[C \mp \sqrt{C^2 - 4\left(\frac{\omega_\phi}{\omega_r}\right)^2\left\{1-\left(\frac{A}{n}\right)^2\right\}^2}\right.$$

$$C = 1 + \frac{A^2 D^2}{n^4} + \left(1 + \frac{A^2}{D^2}\right)\left(\frac{\omega_\phi}{\omega_r}\right)^2$$

$$T_B = \frac{2L^2}{\pi}\sqrt{\frac{m_b}{EI_x}}$$

It should be noted that ω_ϕ, ω_V and T_B, as defined above represent the nth uncoupled torsional natural frequency, the nth uncoupled flexural natural frequency and the fundamental flexural natural period of a straight beam of the same length as the centre line length L, of the curved beam. It is seen from Eq.(3.2.8) that for each n, there are two frequencies, Wn1 and Wn2. The corresponding amplitude ratios

$$\left(\frac{D_n}{C_n}\right)_s = \frac{K_{ns}}{R}$$

$$K_{ns} = -\frac{1 + \frac{D^2}{A^2}\left(\frac{\omega_r}{\omega_\phi}\right)^2\left\{1-\left(\frac{\omega_{ns}}{\omega_r}\right)^2\right\}}{1 + \left(\frac{D}{n}\right)^2\left(\frac{\omega_r}{\omega_\phi}\right)^2}$$

S = 1, and 2 for each n = 1, 2, ... (3.2.9b)

General Formulation of Forced Vibration with Damping

Any deflection of a curved beam can be represented by a double infinite series of its eigenfunctions. As was shown in Section C, the eigenfunctions for a simply supported curved beam are proportional to $\sin \frac{n\pi Z}{L}$ and, for each n, there are two frequencies ω_{n1} and ω_{n2}. In this case, it is convenient to assume

$$\eta(Z,t) = \sum_{n=1}^{\infty} \sum_{S=1}^{2} Y_{ns}(Z)\, q_{ns}(t) \qquad (3.2.11a)$$

$$\theta(Z,t) = \sum_{n=1}^{\infty} \sum_{S=1}^{2} \phi_{ns}(Z)\, q_{ns}(t) \qquad (3.2.11b)$$

where

$$Y_{ns}(Z) = \sin \frac{n\pi Z}{L} \qquad (3.2.12a)$$

$$\phi_{ns}(Z) = \frac{K_{ns}}{R} \sin \frac{n\pi Z}{L} \qquad (3.2.12b)$$

The unknown functions $g_{ns}(t)$ are called the normal co-ordinates.

For a beam undergoing combined bending and torsional displacements, the kinetic energy K, the strain energy U and thr Rayleigh dissipation function F are

$$K = \frac{1}{2}\int_0^L m_b (\dot{\eta})^2 dZ + \frac{1}{2}\int_0^L m_b \rho_o^2 (\dot{\theta})^2 dZ \qquad (3.2.13a)$$

$$U = \frac{1}{2}\int_0^L EI_x\left(\eta'' - \frac{\theta}{R}\right)^2 dz + \frac{1}{2}\int_0^L GK_t\left(\frac{\eta'}{R}+\theta'\right)^2 dz + \frac{1}{2}\int_0^L EI_w\left(\frac{\eta''}{R}+\theta''\right)^2 dz \qquad (3.2.13b)$$

$$F = \frac{1}{2}\int_0^L C_b(z)(\dot{\eta})^2 dz + \frac{1}{2}\int_0^L C_\theta(z)(\dot{\theta})^2 dz \qquad (3.2.13c)$$

Substituting Eqs. (3.2.11a,b) into Eqs. (3.2.13a, b) and making use of the orthogonality equations (3.2.10a,b,c, d and e) it can be shown that the energy expressions for K and U reduce to

$$K = \frac{1}{2}\sum_{n=1}^{\infty}\sum_{s=1}^{2} m_{ns}\,\dot{q}_{ns}^2(t) \qquad (3.2.14a)$$

$$U = \frac{1}{2}\sum_{n=1}^{\infty}\sum_{s=1}^{2} m_{ns}\,\omega_{ns}^2\,q_{ns}^2(t) \qquad (3.2.14b)$$

$$m_{ns} = \frac{m_b L}{2}\left\{1+\left(\frac{AK_{ns}}{D}\right)^2\right\} \qquad (3.2.14c)$$

The use of assumptions stated in Section A, regarding the damping characteristics of bridge yields

$$C_b(z) = \mu_b m_b \;,\; C_\theta(z) = \mu_\theta m_b \rho_o^2 \qquad (3.2.15a)$$

where μ_b and μ_θ are constants of proportionality. Further it is assumed that μ_b and μ_θ are nearly equal and therefore

$$\mu_b \simeq \mu_\theta = \mu \qquad (3.2.15b)$$

Utilizing Eqs.(3.2.11),(3.2.15) and (3.2.10) the Rayleigh dissipation function given by Eq.(3.2.13c) can be written as

$$\mathcal{F} = \frac{\mu}{2} \sum_{s}^{\infty} \sum_{s=1}^{2} m_{ns} \dot{q}_{ns}^{2}(t) = \mu K \qquad (3.2.16)$$

For systems with viscous damping, Lagrange's equation of motion can be written as

$$\frac{d}{dt}\left(\frac{\partial R}{\partial \dot{q}_{ns}}\right) - \frac{\partial K}{\partial q_{ns}} + \frac{\partial U}{\partial q_{ns}} + \frac{\partial F}{\partial \dot{q}_{ns}} = Q_{ns}$$

(S = 1 and 2 for each n = 1, 2, ... (3.2.17)

where Q_{ns} is the generalised force corresponding to the nsth generalised displacement g_{ns}. Substituting the series expressions for K, U and F from equations(3.2.14a,b) and (3.2.16) into Eq. (3.2.17) gives:

$$\ddot{q}_{ns} + \mu \dot{q}_{ns} + \omega_{ns}^{2} q_{ns} = \frac{Q_{ns}}{m_{ns}}$$

(S = 1 and 2 for each n = 1, 2 ..... (3.2.18)

which represents a two fold infinite set of velocity-uncoupled equations, and is similar to that of a one-degree-of-freedom system with viscous damping.

For a single constant force P moving across the the bridge with constant speed V, the generalised force Q_{ns} is given by

$$Q_{ns} = P Y_{ns} \quad (z = Vt)$$

(S = 1 and 2 for each n = 1, 2..... (3.2.19)

Substituting for Q_{ns} from Eq.(3.2.19) into Eq. (3.2.17) gives:

$$\ddot{q}_{ns} + \mu \dot{q}_{ns} + \omega_{ns}^2 q_{ns} = \frac{P}{m_{ns}} \sin \frac{n\pi Vt}{L}$$

(S = 1 and 2 for each n = 1, 2 ..... (3.2.20)

The orthogonality relations for the eigenfunctions $Y_{ns}(Z)$ and $\phi_{ns}(Z)$ of a curved beam with arbritary support conditions and arbritary variation of mass and stiffnesses were developed by Vashi in reference32 . These relations for S = 1 and S = 2 are

$$\int_0^L m_b (Y_{ns} Y_{ms} + \rho_o^2 \phi_{ns} \phi_{ms}) \, dz = 0 \quad \text{for } m \neq n \quad (3.2.10a)$$

$$= m_{ns} \text{ for } m = n \quad (3.2.10b)$$

$$\int_0^L EI_x \left(Y''_{ns} - \frac{\phi_{ns}}{R}\right)\left(Y''_{ms} - \frac{\phi_{ms}}{R}\right) dz + \int_0^L GK_t \left(\frac{Y'_{ns}}{R} + \phi'_{ns}\right)\left(\frac{Y'_{ms}}{R} + \phi'_{ms}\right) dz + \int_0^L EI_w \left(\frac{Y''_{ns}}{R} + \phi''_{ns}\right)\left(\frac{Y''_{ms}}{R} + \phi''_{ms}\right) dz$$

$$= 0 \text{ for } m \neq n \quad (3.2.10c)$$

$$= m_{ns} \omega_{ns}^2 \text{ for } m = n \quad (3.2.10d)$$

where

$$m_{ns} = \int_0^L m_b \left(Y_{ns}^2 + \rho_o^2 \phi_{ns} \right)^2 dz \qquad (3.2.10e)$$

3.3 Solution of Equation of Motion

The solution of Eq.(3.2.20)may be written as the sum of the soltuion of the associated homogeneous equation and a convolution integral.

This leads to

$$q_{ns}(t) = e^{-\frac{\mu}{2}t}\left(A_{ns}\cos\bar{\omega}_{ns}t + B_{ns}\sin\bar{\omega}_{ns}t\right) + \frac{P}{m_{ns}\bar{\omega}_{ns}}\int_0^t \sin\frac{n\pi v\tau}{L}\, e^{-\frac{\mu}{2}(t-\tau)}\sin\bar{\omega}_{ns}(t-\tau)\,d\tau$$

(S = 1 and 2 for each n = 1, 2..... ∞ (3.3.1)

where W_{ns} is the damped natural frequency given by

$$\bar{\omega}_{ns} = \sqrt{\omega_{ns}^2 - \left(\frac{\mu}{2}\right)^2} \qquad (3.3.2)$$

Substituting Eq.(3.3.1) into Eq.(3.2.11a, b) gives the general solution of the forced vibration problem in the form

$$\eta(z,t) = \sum_{n=1}^{\infty}\sum_{s=1}^{2} Y_{ns}(z)\left[e^{-\frac{\mu t}{2}}\left(A_{ns}\cos\bar{\omega}_{ns}t + B_{ns}\sin\bar{\omega}_{ns}t\right) + \frac{P}{m_{ns}\bar{\omega}_{ns}}\int_0^t \sin\frac{n\pi v\tau}{L}\, e^{-\frac{\mu}{2}(t-\tau)}\sin\bar{\omega}_{ns}(t-\tau)\,d\tau\right] \qquad (3.3.3a)$$

$$\theta(z,t) = \sum_{n=1}^{\infty}\sum_{s=1}^{2} \phi_{ns}(z)\left[e^{-\frac{\mu t}{2}}(A_{ns}\cos\bar{\omega}_{ns}t + B_{ns}\sin\bar{\omega}_{ns}t) + \frac{P}{m_{ns}\bar{\omega}_{ns}}\int_0^t \sin\frac{n\pi V\tau}{L} e^{-\frac{\mu}{2}(t-\tau)} \sin\bar{\omega}_{ns}(t-\tau)\,d\tau\right] \quad (3.3.3b)$$

where Y_{ns} and ϕ_{ns} are as defined by Eqs. (3.2.12a,b).

For maximum effects, bridge damping will be neglected and hence $\mu = 0$. Further, for zero initial conditions of the bridge displacement and velocity, the constants A_{ns} and B_{ns} are all identically zero. As a result, the general solution given by Eq (3.3.3a, b) after a considerable amount of simplification by substituting the values of ω_{ns} and M_{ns} from Eqs. (3.2.8) and (3.2.14c) can be written as

$$\eta(z,t) = \frac{PL^3}{\pi^4 EI_x}\sum_{n=1}^{\infty}\sum_{s=1}^{2} \frac{\sin\frac{n\pi z}{L}}{RM_{ns}} G_{ns}(t) \quad (3.3.4a)$$

$$\theta(z,t) = \frac{PL^3}{\pi^4 EI_x R}\sum_{n=1}^{\infty}\sum_{s=1}^{2} \frac{k_{ns}\sin\frac{n\pi z}{L}}{RM_{ns}} G_{ns}(t) \quad (3.3.4b)$$

Here, the following notation has been used

$$G_{ns}(t) = \frac{\sin 2\pi n\alpha\frac{t}{T_B}}{n^2(n^2\rho_{ns}-\alpha^2)} - \frac{\alpha\sin 2\pi n^2\sqrt{\rho_{ns}}}{n^3\sqrt{\rho_{ns}}\,(n^2\rho_{ns}-\alpha^2)}$$

$$\alpha = \frac{VT_B}{2L} = \text{speed parameter}$$

$$RM_{ns} = \frac{m_{ns}}{m_b L} = \frac{1}{2}\left[1 + \left(\frac{Ak_{ns}}{D}\right)^2\right]$$

B. Dynamic Increments for Displacements and Stress Resultants

For highway bridges, the parameter α is a small quantity relative to unity, and the contribution of the terms in Eqs. (3.3.4a,b) for $n > 1$ may be neglected in comparison to that for $n = 1$. Considering, therefore, only the term $m = 1$ Eqs. (3.3.4a,b) reduce to

$$\eta(z,t) = \frac{PL^3 \sin\frac{\pi z}{L}}{\pi^4 E I_x} \sum_{s=1}^{2} \frac{G_{1s}(t)}{R M_{1s}} \qquad (3.3.5a)$$

$$\theta(z,t) = \frac{PL^3 \sin\frac{\pi z}{L}}{\pi^4 E I_x R} \sum_{s=1}^{2} \frac{k_{1s} G_{1s}(t)}{R M_{1s}} \qquad (3.3.5b)$$

The static or crawl deflection at any section at a distance Z from the left support at any time t is obtained by taking $\alpha = 0$ but retaining the term $\sin 2\pi\alpha \frac{t}{T_B}$ in Equation (3.3.5a,b), This yields

$$\eta_{st}(z,t) = \frac{PL^3 \sin\frac{\pi z}{L}}{\pi^4 E I_x} \left[\sum_{s=1}^{2} \frac{1}{\rho_{1s} R M_{1s}}\right] \sin 2\pi\alpha \frac{t}{T_B} \qquad (3.3.6a)$$

$$\theta_{st}(z,t) = \frac{PL^3 \sin\frac{\pi z}{L}}{\pi^4 E I_x R}\left[\sum_{s=1}^{2}\frac{K_{1s}}{\rho_{1s} R M_{1s}}\right]\sin 2\pi\alpha\frac{t}{T_B} \qquad (3.3.6b)$$

Subtracting Eqs. (3.3.6a,b) from Eqs. (3.3.5a,b) gives

$$\eta(z,t) - \eta_{st}(z,t) = \frac{PL^3 \sin\frac{\pi z}{L}}{\pi^4 E I_x}\sum_{s=1}^{2}\frac{H_{1s}(t)}{R M_{1s}} \qquad (3.3.7a)$$

$$\theta(z,t) - \theta_{st}(z,t) = \frac{PL^3 \sin\frac{\pi z}{L}}{\pi^4 E I_x R}\sum_{s=1}^{2}\frac{K_{1s} H_{1s}(t)}{R M_{1s}} \qquad (3.3.7b)$$

where

$$H_{1s}(t) = \frac{\alpha^2 \sin 2\pi\alpha\frac{t}{T_B}}{\rho_{1s}(\rho_{1s}-\alpha^2)} - \frac{\alpha \sin 2\pi\sqrt{\rho_{1s}}\frac{t}{T_B}}{\sqrt{\rho_{1s}}(\rho_{1s}-\alpha^2)}$$

These equations define the instantaneous values of the dynamic increment at a section specified by the co-ordinate Z, which, when nondimensionalized with respect to the corresponding maximum static effect, become

$$DI_\eta = \frac{\eta(z,t) - \eta_{st}(z,t)}{\eta_{st,max}} = \frac{\sum_{s=1}^{2}\frac{H_{1s}(t)}{R M_{1s}}}{\sum_{s=1}^{2}\frac{1}{\rho_{1s} R M_{1s}}}$$

$$DI_\theta = \frac{\theta(z,t) - \theta_{st}(z,t)}{\theta_{st,max}} = \frac{\sum_{s=1}^{2} \frac{K_{1s} H_{1s}(t)}{R M_{1s}}}{\sum_{s=1}^{2} \frac{K_{1s}}{\rho_{1s} R M_{1s}}} \qquad (3.3.8b)$$

The subscripts η and θ refer to the transverse deflection and torsional rotation respectively.

The nondimensional dynamic increments for bending moment M, St. Venant's torsional moment S, warping torsional moment W and bimoment B can be derived in a manner similar to that used above for obtaining DI_η and DI_θ, by substituting the required derivatives of the displacements into the definitions of these stress resultants. The dynamic increment for the bending moment DI_M can be obtained as

$$DI_M = \frac{\sum_{s=1}^{2} \frac{1 + A^2 K_{1s}}{R M_{1s}} H_{1s}(t)}{\sum_{s=1}^{2} \frac{1 + A^2 K_{1s}}{\rho_{1s} R M_{1s}}} \qquad (3.3.8c)$$

It can be shown that the dynamic increments DI_S, DI_W and DI_B associated respectively with the St. Venant's torque; warping torque and bimoment are equal and are given by

$$DI_S = DI_W + DI_B = \frac{\sum_{s=1}^{2} \frac{1 + K_{1s}}{R M_{1s}} H_{1s}(t)}{\sum_{s=1}^{2} \frac{1 + K_{1s}}{\rho_{1s} R M_{1s}}} \qquad (3.3.8d)$$

From Eqs. (3.3.8c,d) an upperbound to the maximum value of DI_M, DI_S, DI_W and DI_B can be obtained by taking the sum of the absolute values of the individual terms. This approach yields:

$$DI_{M_{max}} = \frac{\sum_{s=1}^{2} \frac{1+A^2 K_{1s}}{\rho_{1s} RM_{1s}} \frac{\alpha}{(\sqrt{\rho_{1s}}-\alpha)}}{\sum_{s=1}^{2} \frac{1+A^2 K_{1s}}{\rho_{1s} RM_{1s}}} \qquad (3.3.9a)$$

$$DI_S, \text{ max.} = DI_W, \text{ max.} = DI_B, \text{ max.}$$

$$= \frac{\sum_{s=1}^{2} \frac{(-1)^{s+1}(1+K_{1s})}{\rho_{1s} RM_{1s}} \frac{\alpha}{\{\sqrt{\rho_{1s}}-(-1)^{s+1}\alpha}}{\sum_{s=1}^{2} \frac{1+K_{1s}}{\rho_{1s} RM_{1s}}}$$

These formulas are useful in predicting the general level of response due to a single moving constant force.

CHAPTER IV

EXPERIMENTAL PROGRAM

4.1.1 Static Test Procedure

The static test was carried out first. The curved girders and cross beams were tested as a grid. Budd Metafilm strain gauges Type C6-145 and deflection dial gauges were used at locations shown in Fig. 13. The static load was applied by a Gilmore Loading System. The actuator was placed on top of a semi-circular wedge piece to approach a concentrated loading condition. Loads of 3000 lbs. and 4500 lbs. were applied at locations shown in Fig. 13, and the strains and deflections were recorded. A strain gauge recorder was used to record the strains. Then the Gilmore actuator was moved to the next position and the same procedure was repeated.

4.1.2 Test Results

The test results are shown in Fig. 8, 9 and 10. Solid lines represent the experimental values, while theoretical values are shown by dotted lines. "I.G." indicates the girder nearest the centre of curvature and "O.G." signifies the farthest girder.

4.1.3 Test Evaluation

Fig. 9 shows the vertical deflections of the girders as measured by the dial indicators. The curves

shown in the Figure 9 are for the bridge without a slab. The curves shown in Fig. 10 are for the bridge with the concrete slab.

For loads applied to the outside girder at 1/4L and 1/2L the actual deflections are more than the computed deflections. For the outside girder loaded at mid span the discrepancy between measured and computed vertical deflections is 10 percent. For loads on the inner girder good correlation is obtained between the measured and computed deflection. The correlation between the experimental and theoretical analyses is on the whole good.

The stress distribution for static loading for the bridge without the concrete deck is shown in Fig. 8a and 8b. The theoretical stress (shown in parentheses) are compared with those obtained from the measured strains and are also shown at the location of strain gauges. The stresses are greater when the load is on the outside girder than when the load is on the inner girder.

4.2.1 Dynamic Test Procedure

Dynamic tests were performed on the laboratory model by running the load carriage across the bridge and measuring the strains at the midspan. The load carriage is shown in Photograph 16. The wheel spacing is shown in Fig. 12. The load carriage was fitted with a wire rope and pulled by a overhead trolley at a constant velocity. The load carriage was fitted with rollers which pressed against a flat iron

guide (4" x 1/2") bent to the same curvature as the bridge and clamped at the ends with C-clamps. The load carriage was pulled and its velocity was recorded with a stop watch. The strain gauge was connected to the strain-indicator (Budd Type) which was again connected to the oscilloscope. The oscilloscope was adjusted for the same velocity as the load carriage and the load carriage was pulled and the oscillograph reading was photographed on a Polaroid Land film.

Natural Frequency

For measuring the natural frequency the set up shown in Fig. 11 was used. A Bruel & Kjaer Accelerometer type 4312 was mounted magnetically under the cross beam at the centre.

The Accelerometer was connected to a Preamplifier (Bruel & Kjaer 2616) also connected to the oscilloscope. The bridge was then excited by a hammer blow and the response recorded in the oscilloscope was photographed. The same procedure was repeated three times and the results were found to be consistent.

To verify the results further, the bridge model was again excited by the Gilmore Loading System at a certain frequency and the response in the oscilloscope was photographed. The frequency of excitation was changed again and the same procedure was repeated. The frequency at the maximum response is the natural frequency.

4.2.2 Test Results

The test results are shown on Photograph. Photograph 1 shows the calibration of the oscilloscope for known strain. Photograph 2 shows the stress variation at strain gauge No. 26 as the load carriage moves along the span.

Photographs 3 to 10 are records of the natural frequencies. Photograph 3 shows the period of oscillation. Photograph 4 to 10 shows the response in the oscilloscope when the model is shaken by the Gilmore Loading System at known frequencies.

4.2.3 Test Evaluation

For the dynamic load increments the results have been evaluated for the condition when the travelling load is at 1/4 span and at 1/2 span points, in order to compare these with theoretical calculations, the experimental values being 9% and 12% more than the computed values.

Very good and consistent results have been obtained for natural frequencies. The natural frequencies have been determined in two different ways and the results are consistent. The theoretical value obtained by Vashi's (32) method was 26.2 and 64 while the experiment yielded a value of 25.5 and 62.

CHAPTER V

SUMMARY AND CONCLUSION

The theoretical analysis of curved bridge grid utilising the stiffness method takes into account the curvature of the individual elements and hence is a method sufficiently accurate for design purposes. The torsional rigidity of the elements is considered, incorporates the St. Venant torsional rigidity but does not take into account the warping torsional rigidity. The torsional rigidity does not contribute much to the results, although it is important in a curved bridge since the beam elements are subjected to considerable twist. The stresses due to non-uniform torsion were evaluated and in some cases this added 15% more to the stress caused by flexure. The procedure adopted for finding the normal stress (Reference 4) is very involved and difficult to use in the design office.

The bridge with the concrete deck was analyzed by the method used by Dabrowski. Reasonable correlation has been obtained between the computed and experimental results. This shows that the whole curved bridge consisting of the steel beams and concrete deck can be considered as a curved beam, provided that there are adequate shear connectors. The accuracy will depend on the geometrical properties of the bridge. For a very short span bridge, the theory may

not be valid, but it is valid for most practical bridges.

For the dynamic load increments the test was performed with an unsprung mass only. In the analysis, the vehicle was treated as a single moving constant force where the force exerted by the vehicle is essentially constant. The experimental results agree well with the computed values. The flexural-torsional response of a horizontally curved bridge due to sprung mass loads is extremely complex because of its dependence on various parameters, although an actual highway vehicle possesses both sprung and unsprung masses and the test vehicle consisted of an unsprung mass. It has been shown in Reference . that for a combination of a small value of frequency ratio and a large value of mass ration RS or conversely, the peak values of the dynamic increments for the displacement and the stress resultants can be approximated by a constant force solution.

The natural frequencies of the bridge found experimentally agreed very well with the computed values. This shows that the idealization of the curved bridge as discussed in Chapter III is logical.

BIBLIOGRAPHY

1. Fickel, H.H., "Analysis of Curved Girders," Journal of the Structural Division, ASCE, Vol. 85, No. ST7, Proc. Paper 2164, September 1959.

2. Close, R.A., "Deflection of Circular Curved I-Beams," Journal of the Structural Division, ASCE, Vol. 90, No. ST1, Proc. Paper 3804, February 1964.

3. Lavelle, F.H. and Bolck, J.S., "A Program to Analyze Curved Girder Bridges," University of Rhode Island, Rhode Island, December 1965.

4. Wu, Han-Chin, and Clarke, C.B., "Normal Stresses in Beams Due to Non-uniform Torsion," Eng. Bulletin, No. 10, University of Rhode Island, Rhode Island, November 1966.

5. Clarke, C.B., "Laboratory Tests of Horizontally Curved Steel Girders," Presented at the January 31 to February 4, 1966 ASCE Structural Engineering Conference, at Miami Beach, Fla.

6. Dabrowski, R., "Zur Berechnung Van Gekrummten Dunnwandigen Trager mit offenem Profil," Der Stahlbau, Wilhelm Ernst and Sohn, Berlin-Wilmersdorf, Germany, December 1964.

7. Vlasov, V.Z., "Thin Walled Elastic Beams," Second Edition, Natural Science Foundation, Washington, D.C., 1961.

8. Culver, C.G., "Natural Frequency of Horizontally Curved Beams," Journal of the Structural Division, Proc. ASCE, April 1967.

9. Yonezawa, H., "Moments and Free Vibrations in Curved Girder Bridges," Journal of the Engineering Mechanics Division, ASCE, Vol. 88, February 1962.

10. Willis, R., "Appendix to the Report of the Commissioners... to Inquire into Application of Iron to Railway Structures," London, England, 1847.

11. Kryloff, A.N., "Uber der erzwungenen Schwingungen von gleich formigen," Mathematische Annalen, 61, 1905.

12. Timoshenko, S.P., "On the Forced Vibration of Bridges," Philosophical Magazine, 43, 1922.

13. Lowan, A.N., "On Transverse Oscillations of Beams Under the Action of Moving Variable Loads," Philosophical Magazine, 19, Series 7, 1935.

14. Inglis, C.E., "Theory of Transverse Oscillations in Girders and Its Relation to Live Loads and Impact Allowances," Proceedings of the Institution of Civil Engineers, London, England, 218, 1924.

15. Jeffcott, H.H., "On the Vibration of Beams Under the Action of Moving Loads," Philosophical Magazine, 8, Series 7, 1929.

16. Schallenkamp, A., "Schwingungen Von Tragern bei bewegten Lasten," Ingenieur-Archiv, 8, 1937.

17. Ayre, R.S., G. Ford, and L.S. Jacobsen, "Transverse Vibration of a Two-Span Beam Under the Action of a Moving Constant Force," Journal of Applied Mechanics, 17, 1950.

18. Ayre, R.S., L.S. Jacobsen, C.S. Hsu, "Transverse Vibration of One and of Two-Span Beams Under the Action of a Moving Mass Load," Proceedings of the First U.S. National Congress on Applied Mechanics, 1951.

19. Licari, J.S. and E.W. Wilson, "Dynamic Response of a Beam Subjected to a Moving Forcing System," Proceedings, Fourth U.S. National Congress of Applied Mechanics, 1961.

20. Looney, C.T.G., "High Speed Computer Applied to Bridge Impact," Proceedings, ASCE, 84, ST5, September 1958.

21. Looney, C.T.G., "Impact on Railway Bridges," Bulletin 352, University of Illinois, Urbana, Illinois.

22. Biggs, J.M., "Vibrations of Simple Span Highway Bridges," Highway Research Board Bulletin 124, 1956.

23. Biggs, J.M. and H.S. Suer, "Vibrations of Simple Highway Bridges," Transactions, ASCE, 124, 1959.

24. Wen, R.K., "Dynamic Response of Beams Traversed by Two Axles," Proceedings, ASCE, 86, EM5, October 1960.

25. Fleming, J.F. and J.P. Romualdi, "Effects of Load Characteristics and Bridge Geometry Upon Highway Bridge Impact," Proceedings, ASCE, 87, ST4, October 1961.

26. Tung, T.P., L.E. Goodman, T.Y. Chen and N.M. Newmark, "Highway-Bridge Impact Problems," Highway Research Board Bulletin 124, 1956.

27. Duncan, W.J., "Mechanical Admittances and Their Applications to Oscillation Problems," Great Britain Aeronautical Research Comm., R & M 2000, 1947.

28. Bishop, R.E.D., "The Analysis and Synthesis of Vibrating Systems," Royal Aeronautical Society Journal, 58, 1954.

29. Bishop, R.E.D., "The Analysis of Vibrating Systems which Embody Beams in Flexure," Proceedings, Institute of Mechanical Engineers, 69, 1955.

30. Skeer, M., "The Dynamic Response of Beam and Plate Systems Subjected to Moving Mass Excitations," Ph.D. Thesis, Carnegie Institute of Technology, Pittsburgh, Pennsylvania, 1964.

31. Christiano, Paul P., "The Dynamic Response of Horizontally Curved Bridges Subject to Moving Loads," Ph.D. Thesis, Carnegie-Mellon University, Pittsburgh, Pa., 1967.

32. Vashi, K.M. and Heins, C.P., Jr., "Dynamic Behaviour of Horizontally Curved Highway Bridges," Progress Report, The Design of Curved Viaducts, University of Maryland, Maryland, September 1969.

33. United States Steel Corporation, "Analysis and Design of Horizontally Curved Steel Bridge Girders," ADUCO 91063, September 1963.

34. Borg, S.F. and Gennaro, J.J.,"Advanced Structural Analysis", D. Van Nostrand Co., Inc., Princeton, N.J., 1959.

35. Goldberg, J.E., "Torsion of I Type and H Type Beams," Paper No. 145, Proceedings, ASCE, August 1952.

36. Bornscheuer, F.W., "Systematische Darstellung des Biege- und Verfrehvorganges unter besonderer Beruecksichtigung der Woelbkrafttorsion," Stahlbau 21, Heft 1, Berlin 1952.

37. Lyse, I. and Johnston, B.G., "Structural Beams in Torsion," ASCE Trans. Vol. 101, 1936.

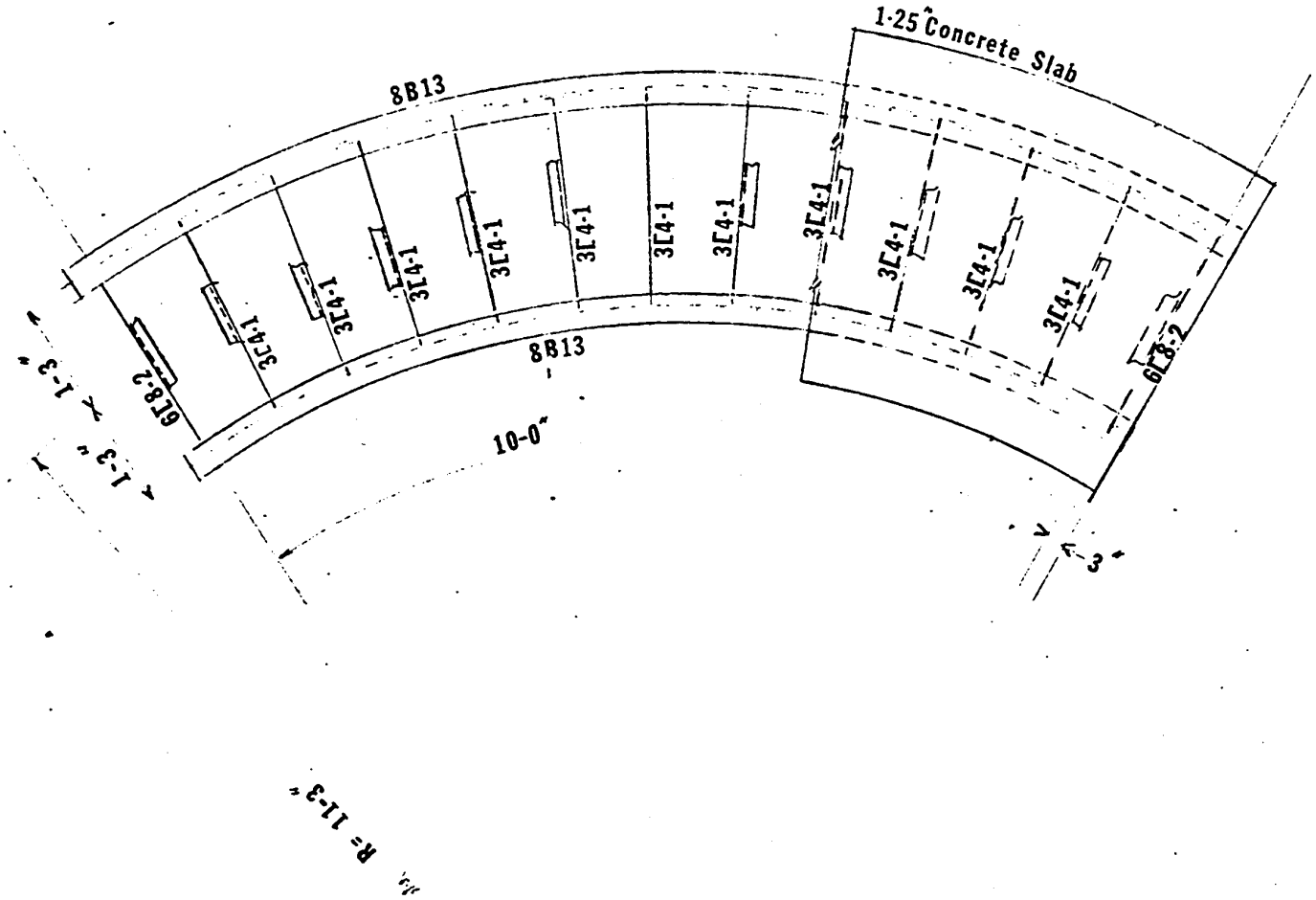

LABORATORY MODEL BRIDGE

FIGURE 1(a)

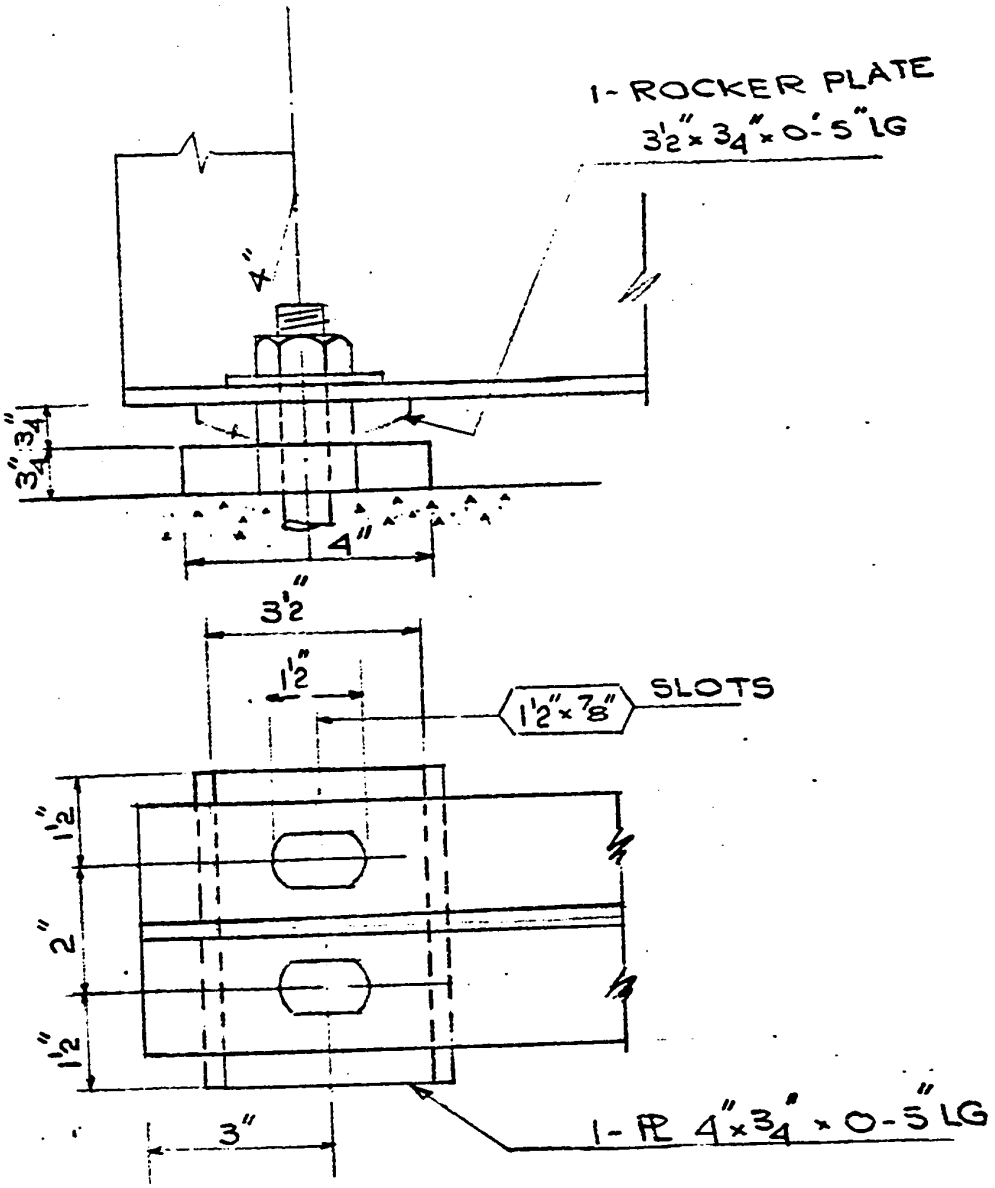

EXPANSION BEARING

FIGURE 1(b)

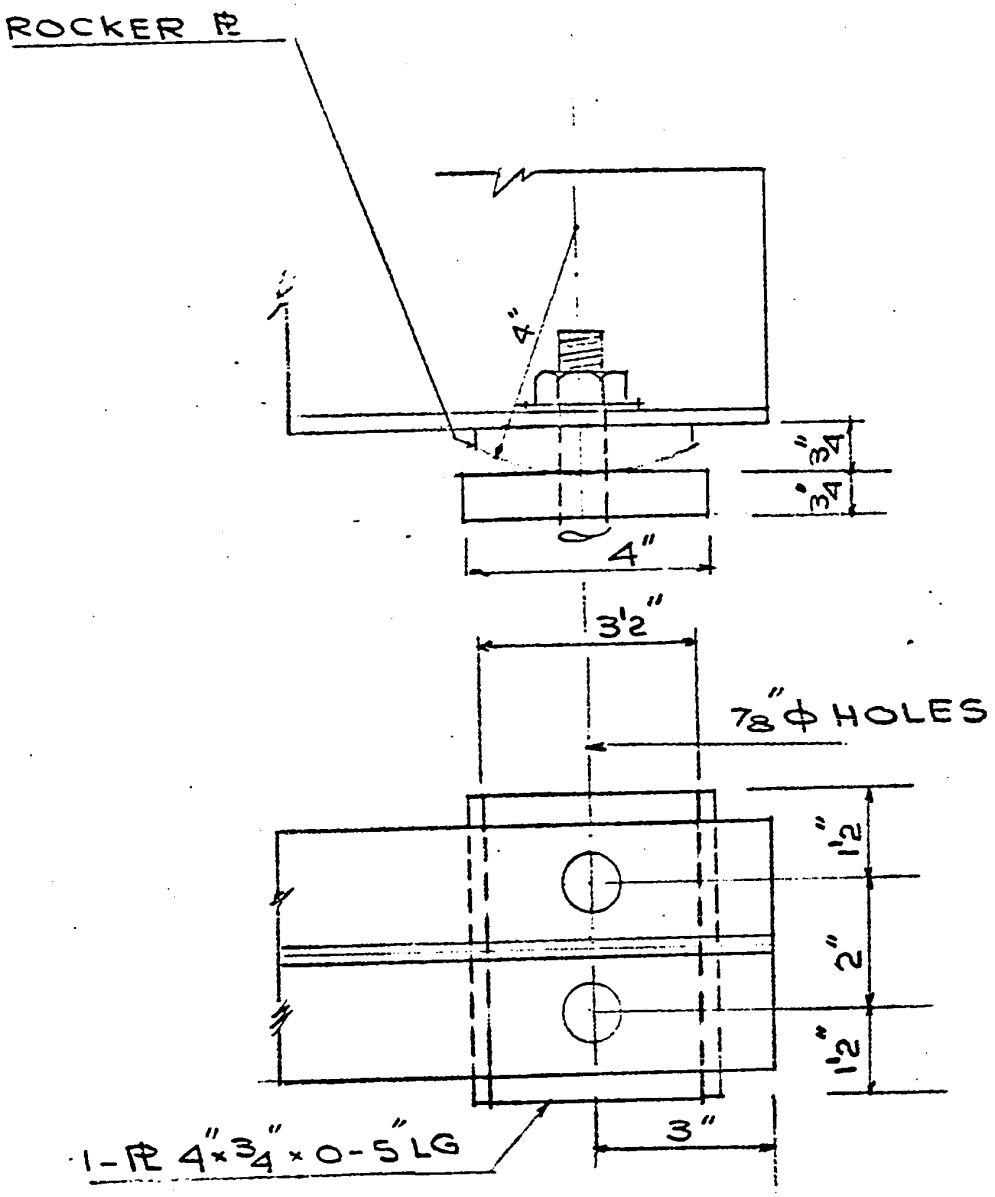

FIXED BEARING

FIGURE 1(c)

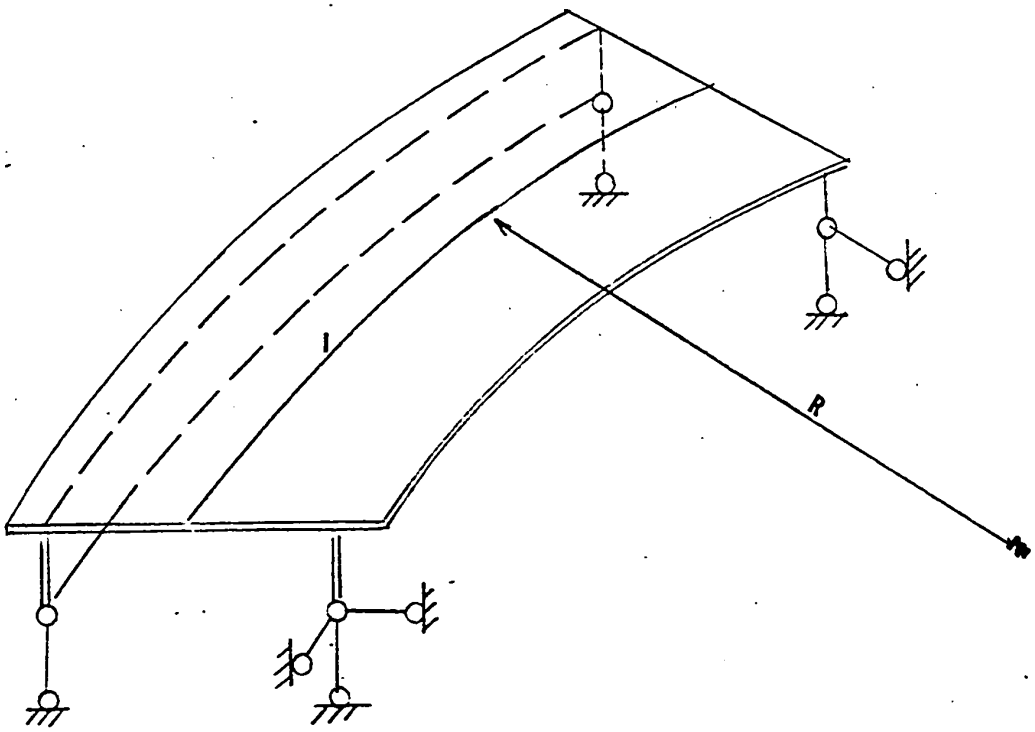

(a) Analytical Structural Model

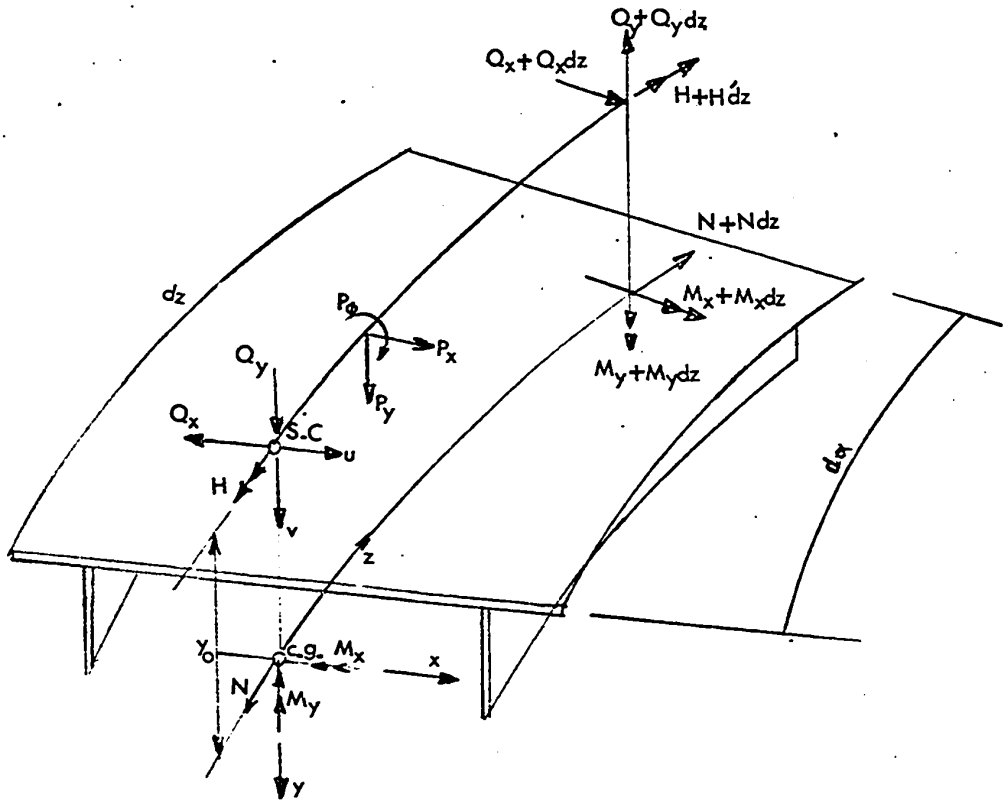

(b) Differential Element

ANALYTICAL MODEL OF HORIZONTALLY CURVED BRIDGE

FIGURE 2

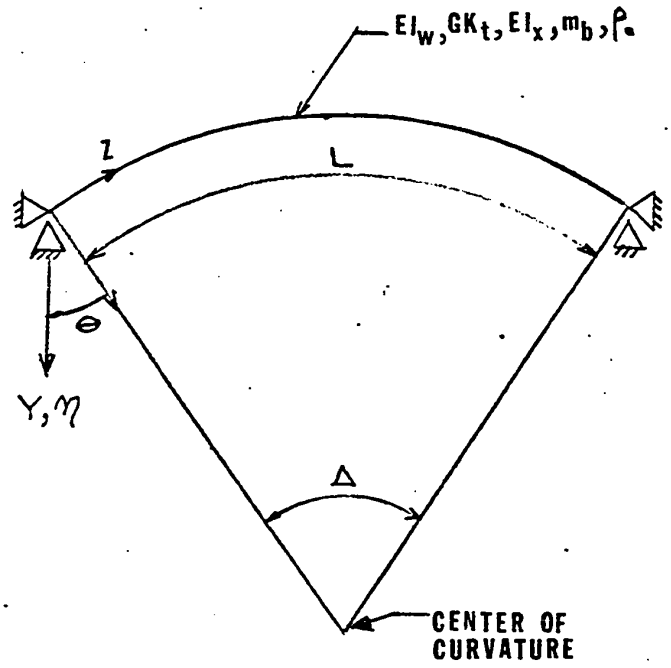

IDEALISATION OF A SIMPLY SUPPORTED HORIZONTALLY CURVED BRIDGE

FIGURE 3

PORTION OF STRAIGHT FLANGE - PLAN VIEW

(a)

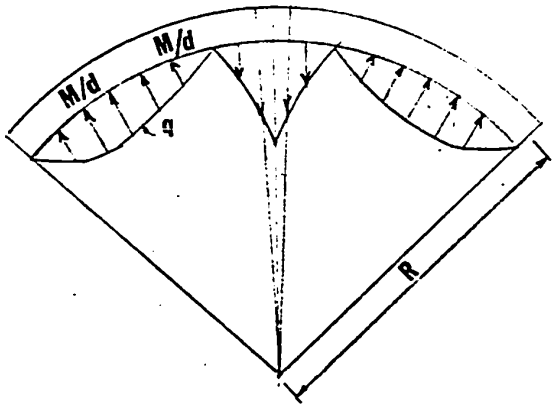

CURVED FLANGE-PLAN VIEW

(b)

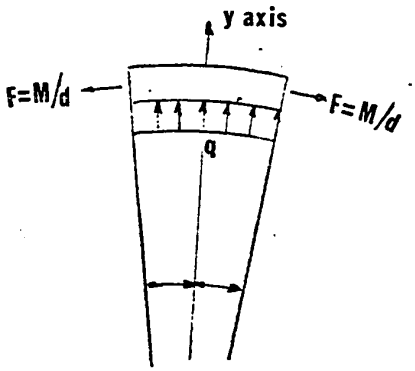

SMALL SEGMENENT OF CURVED FLANGE PLAN VIEW

(c)

FORCES IN FLANGE DUE TO CURVATURE

FIGURE 4

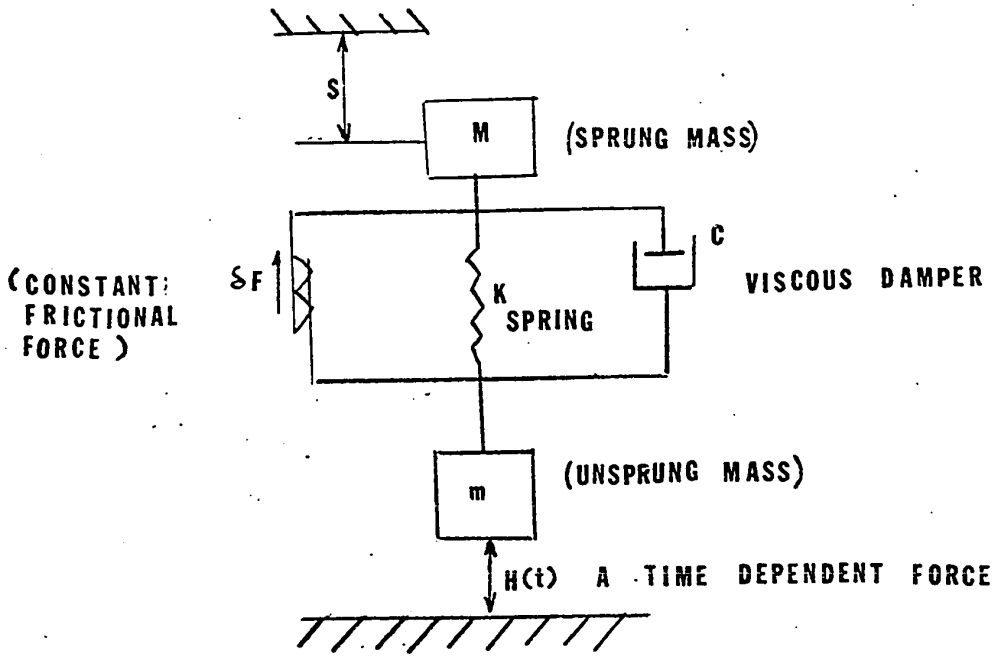

IDEALISATION OF A VEHICLE AS
A SINGLE-AXLE LOAD UNIT

FIGURE 5

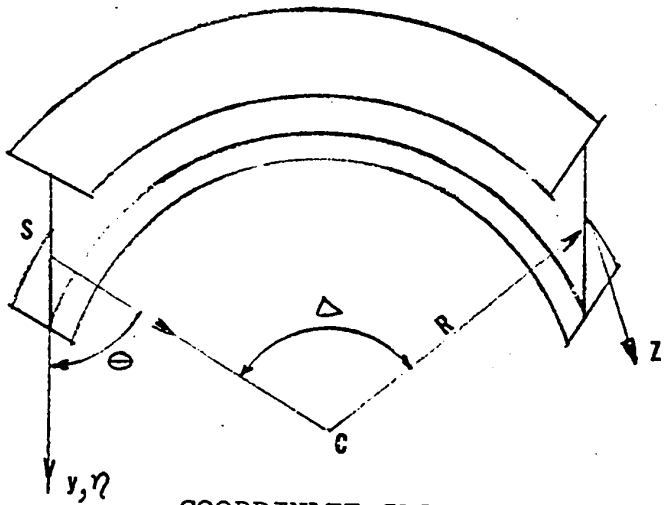

COORDINATE SYSTEM
FIGURE 6

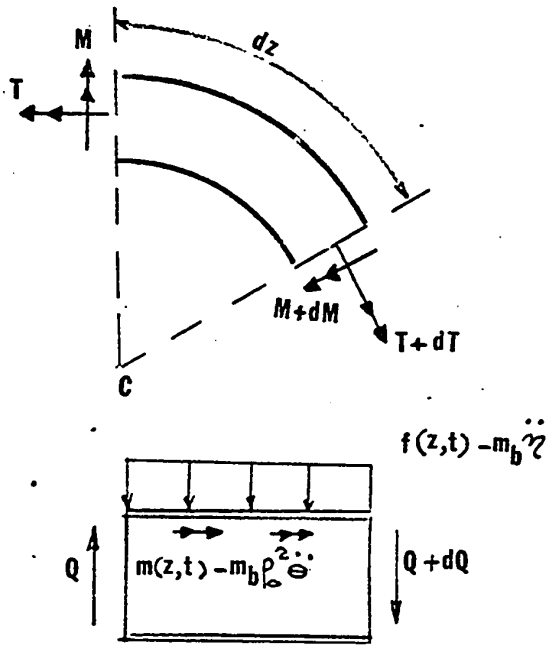

FORCES ON A CURVED ELEMENT

FIGURE 7

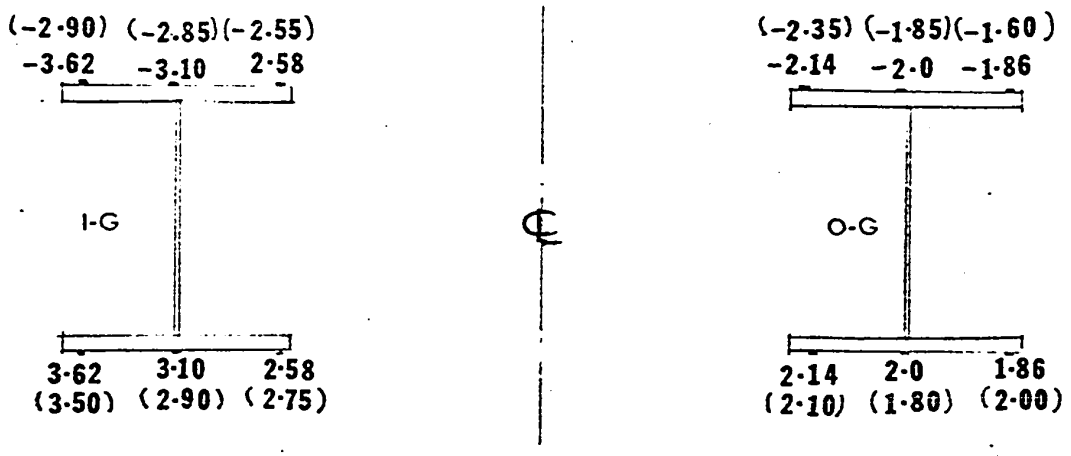

SECTION AT MIDDLE SPAN

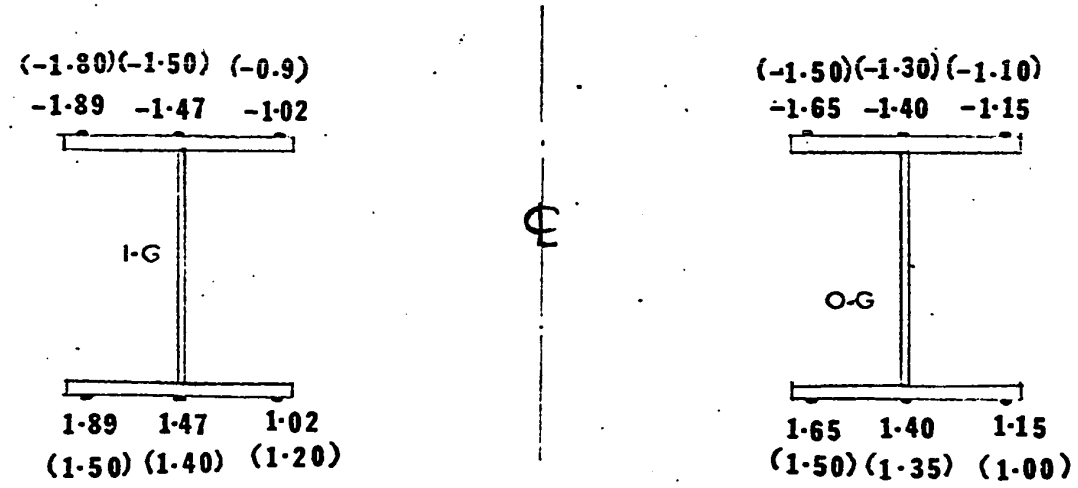

SECTION AT QUARTER SPAN JOINTS 19& 20

NORMAL STRESSES DUE TO LOAD ON JOINT 13

Note: Measured Values
Denoted by( )

FIGURE 8(a)

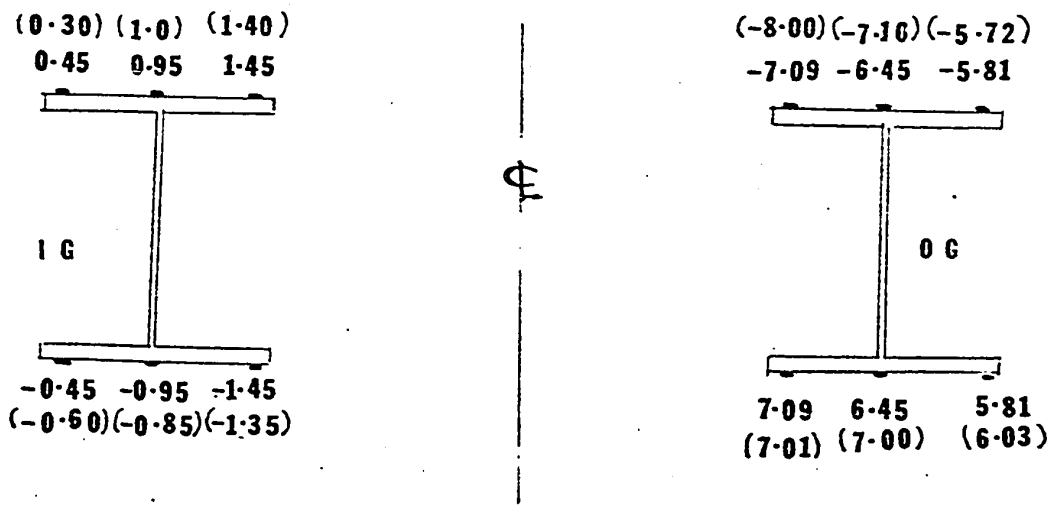

SECTION AT MIDDLE SPAN

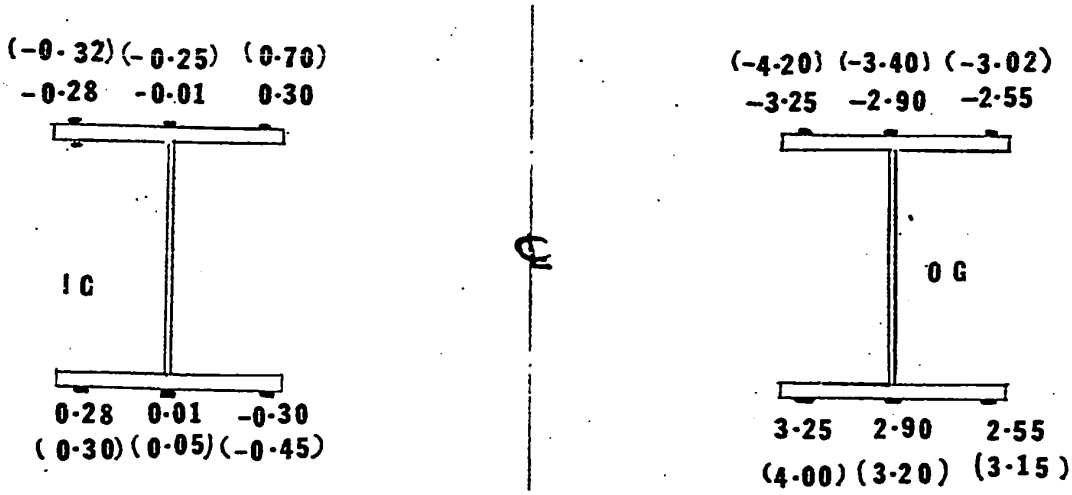

SECTION AT QUARTER SPAN JOINTS 19&20

NORMAL STRESSES DUE TO LOAD ON JOINT 14

Note: Measured Values
Denoted by ( )

FIGURE 8(b)

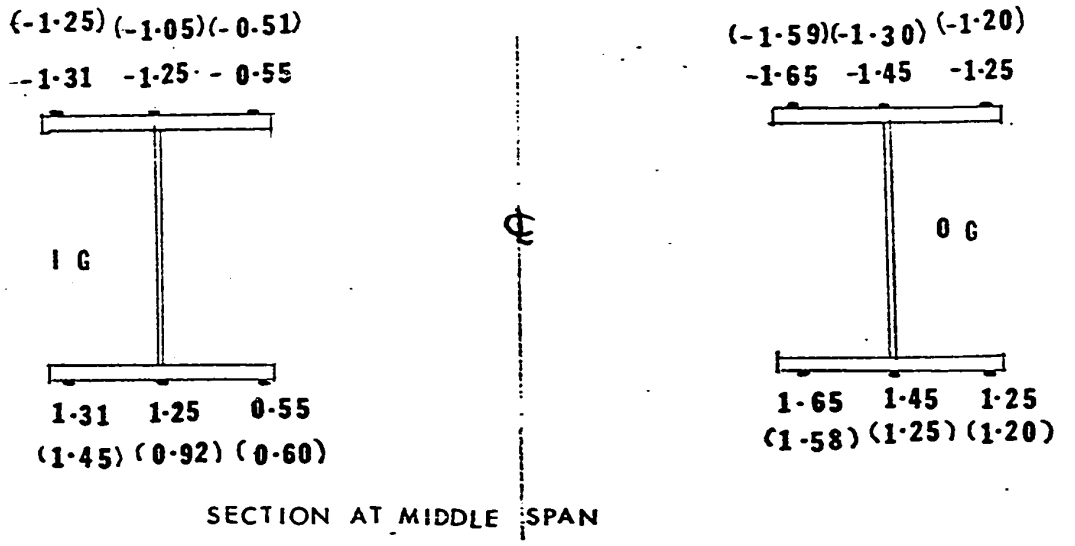

SECTION AT MIDDLE SPAN

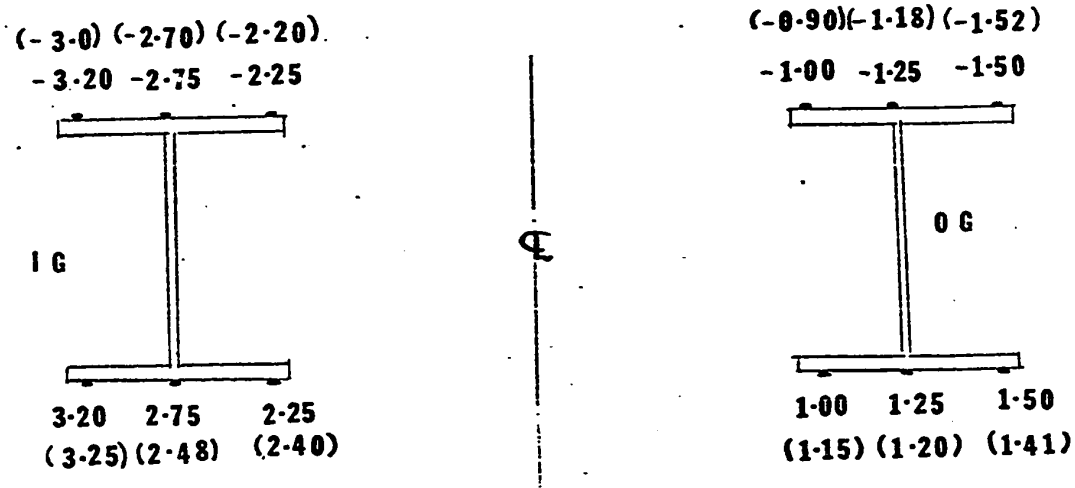

SECTION AT QUARTER SPAN JOINTS 19 & 20

NORMAL STRESSES DUE TO LOAD ON JOINT 19

Note: Measured Values
Denoted by ( )

FIGURE 8(c)

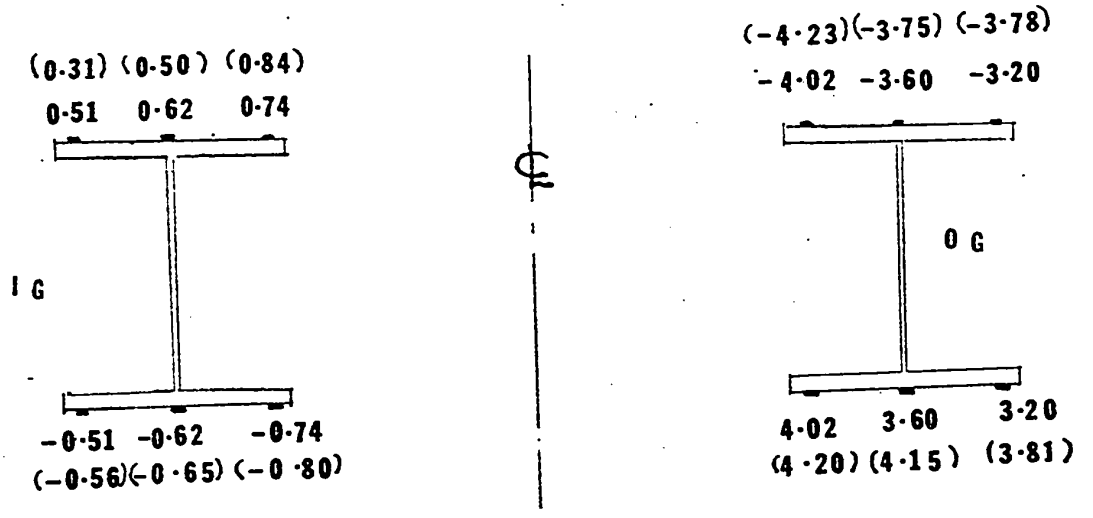

SECTION AT MIDDLE SPAN

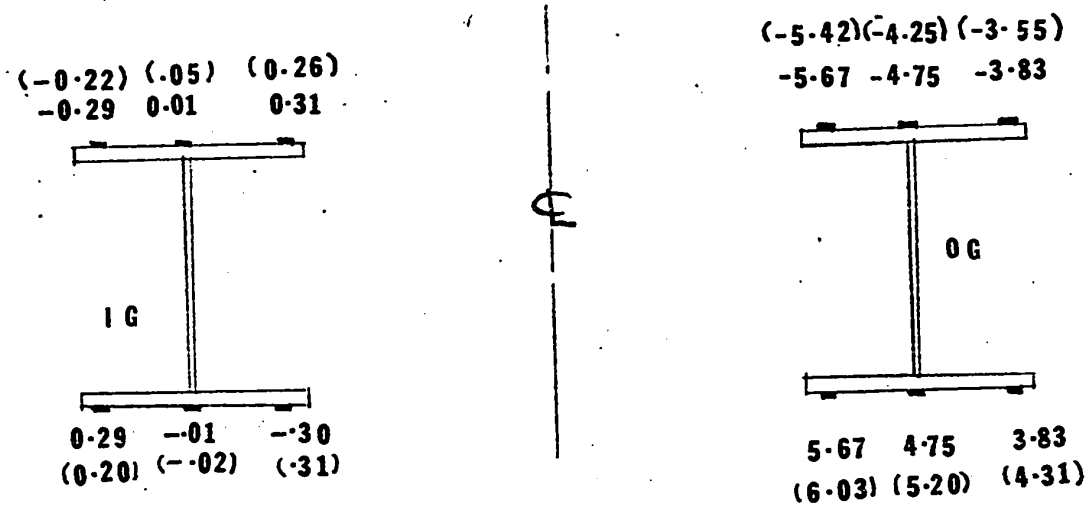

SECTION AT QUARTER SPAN JOINTS 19&20

NORMAL STRESSES DUE TO LOAD ON JOINT 20

Note: Measured Values
Benoted by ( )

FIGURE 8(d)

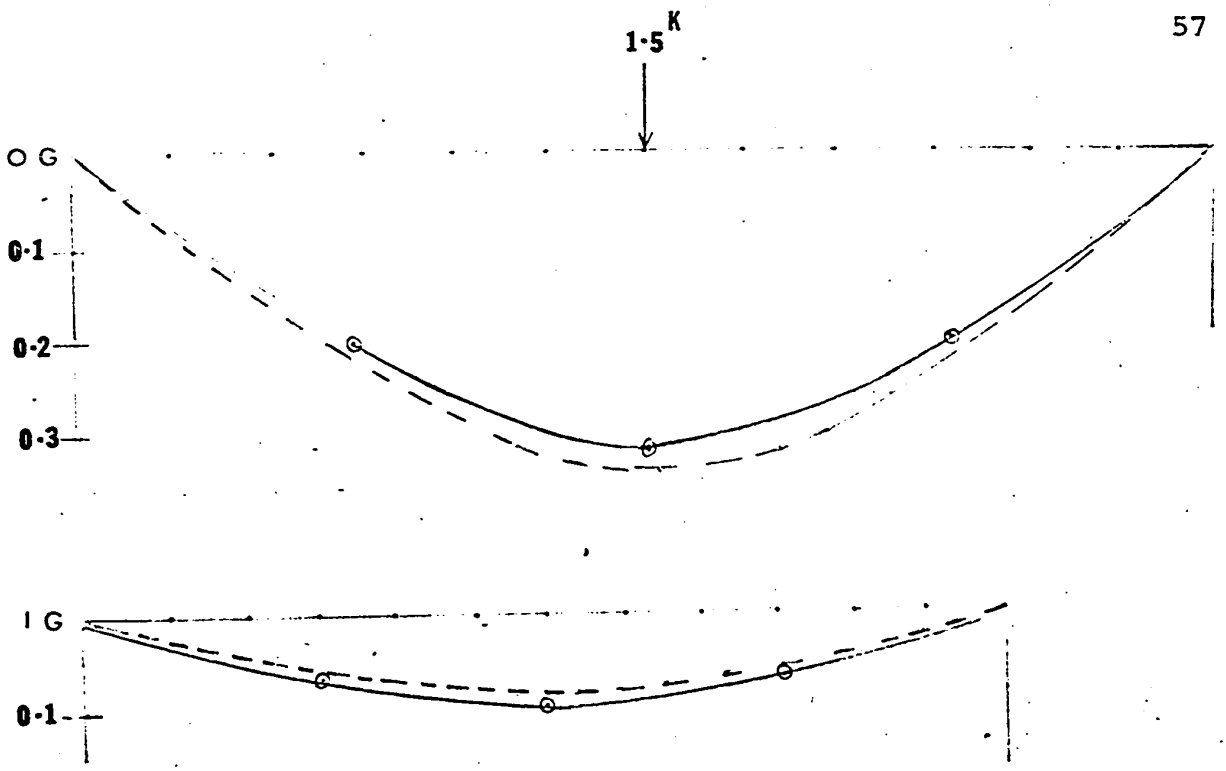

LOAD AT JOINT 14

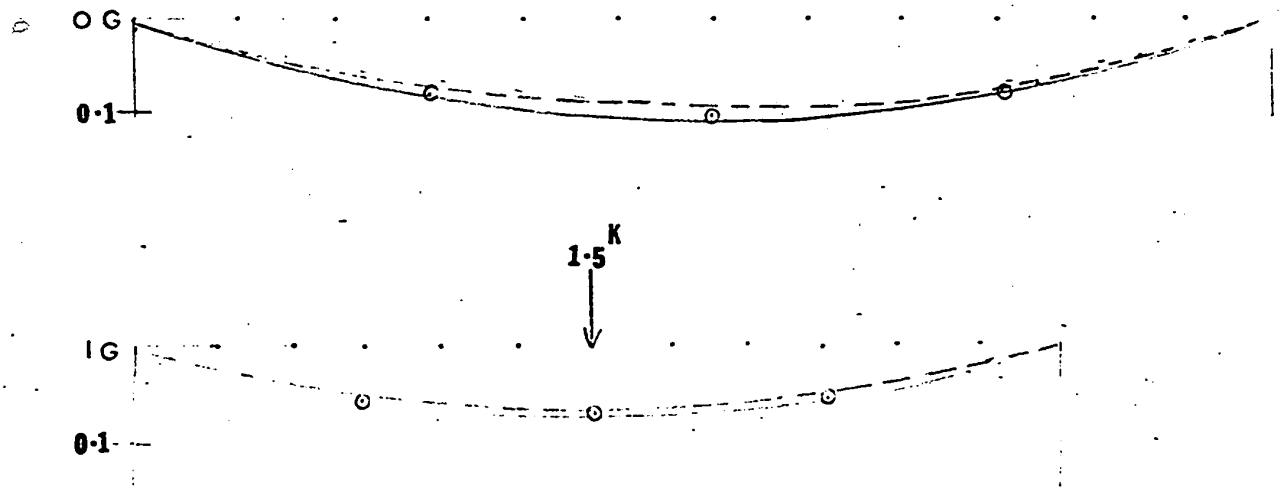

LOAD AT JOINT 13

DEFLECTION OF GIRDERS WITHOUT SLAB

FIGURE 9(a)

——— Test

------- Analysis

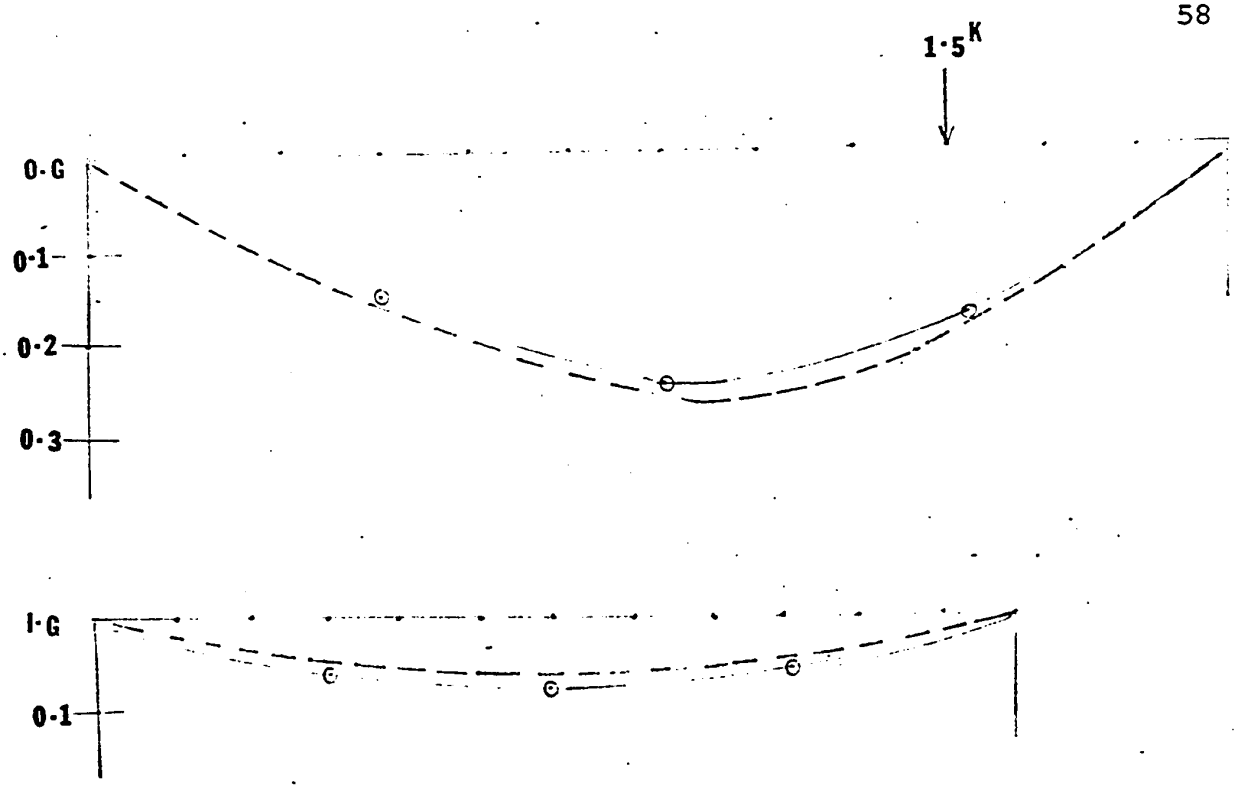

LOAD AT JOINT 20

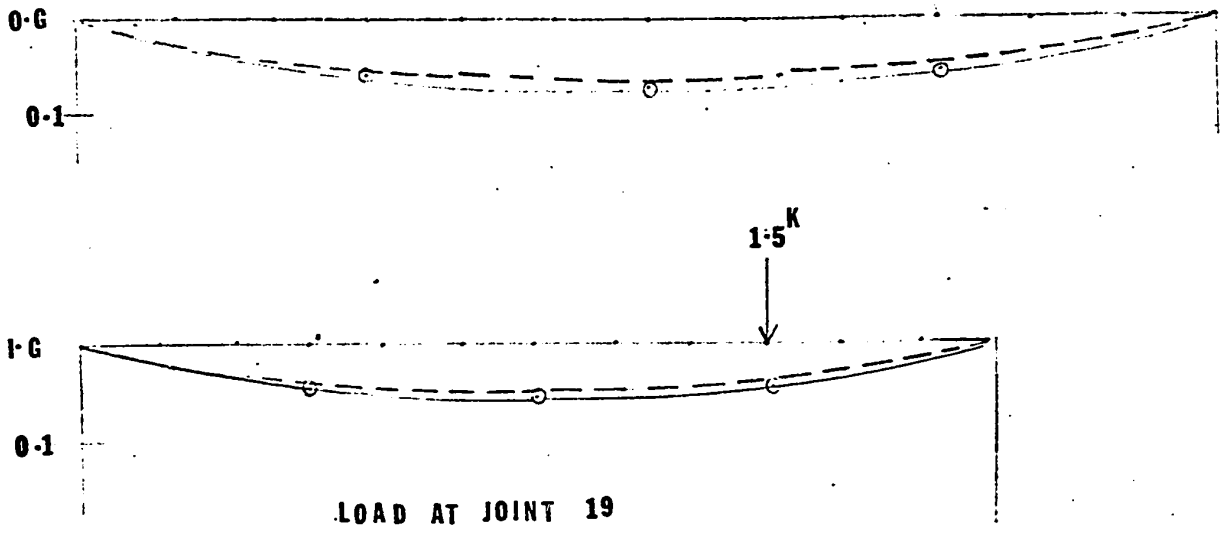

LOAD AT JOINT 19

(inch)

DEFLECTION OF GIRDERS WITHOUT SLAB

——— Test
---- Analysis

FIGURE 9(b)

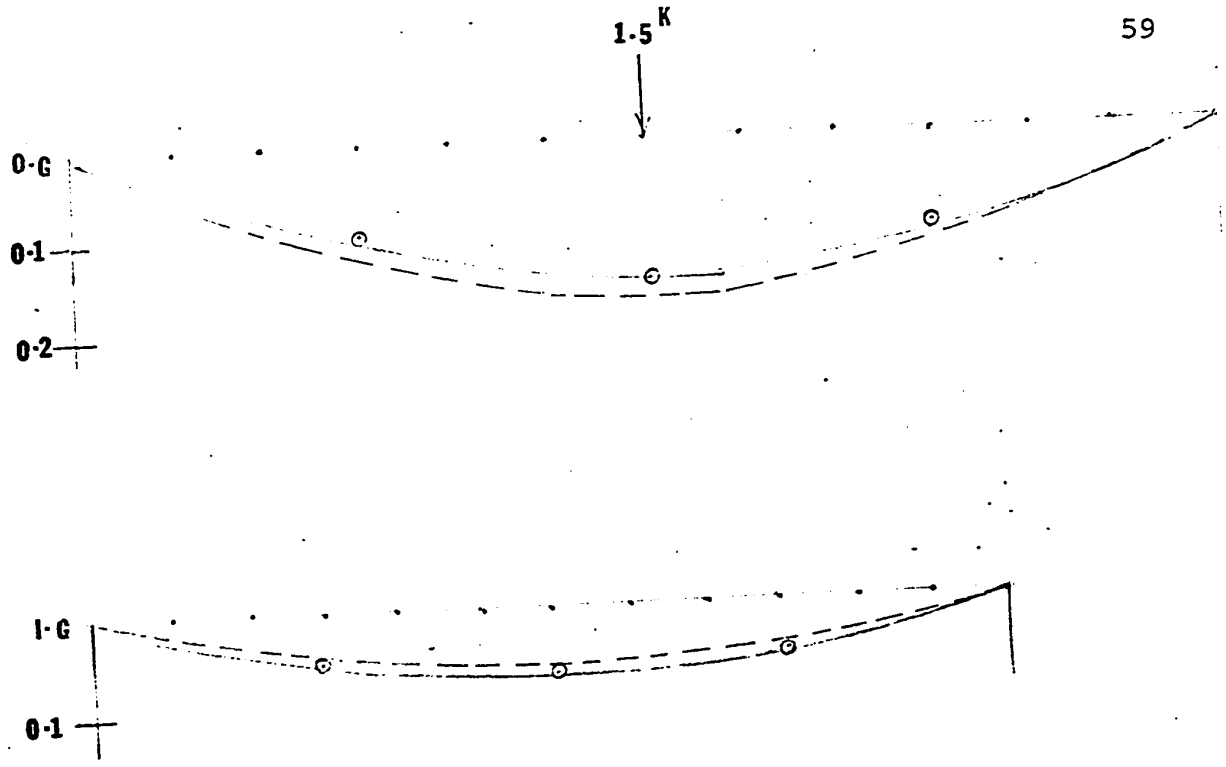

LOAD AT JOINT 14

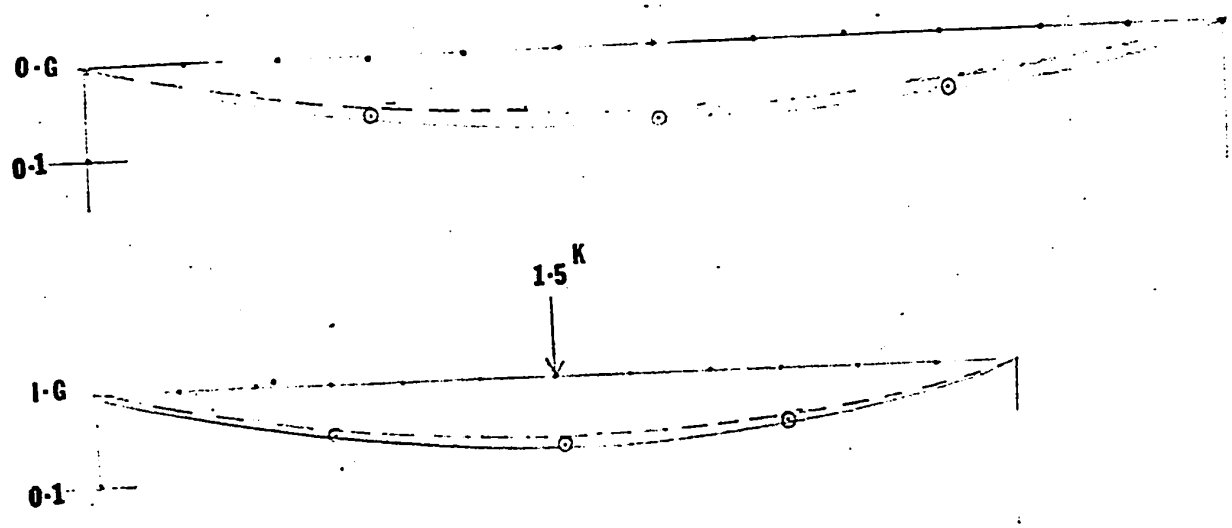

LOAD AT JOINT 13

DEFLECTION OF GIRDERS WITH SLAB

FIGURE 10

——— Test
------ Analysis

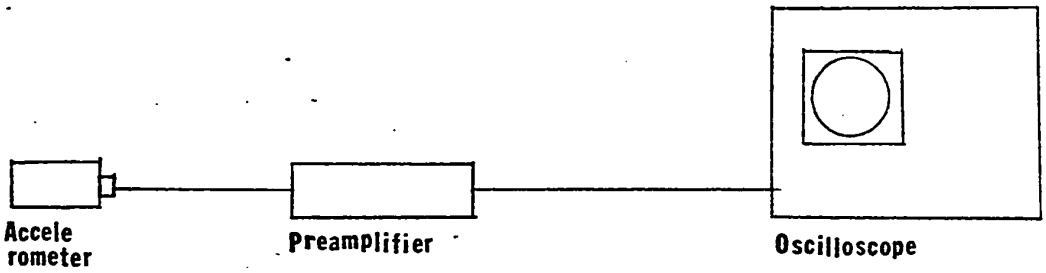

INSTRUMENTATION ARRANGEMENT FOR DYNAMIC TEST

FIGURE 11

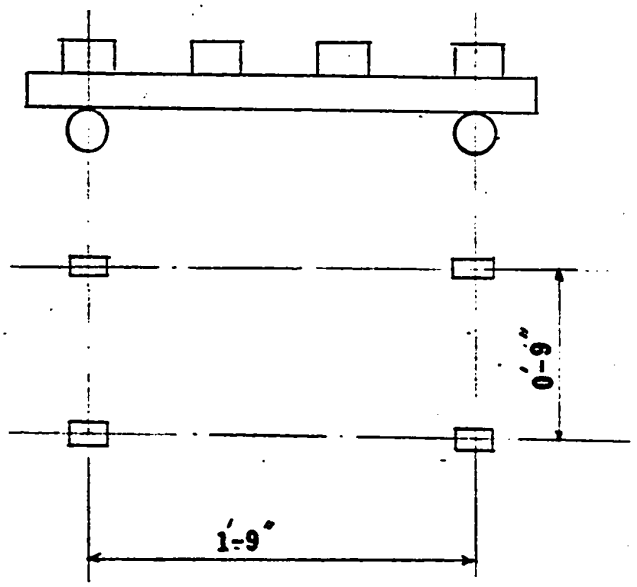

LOAD CARRIAGE

FIGURE 12

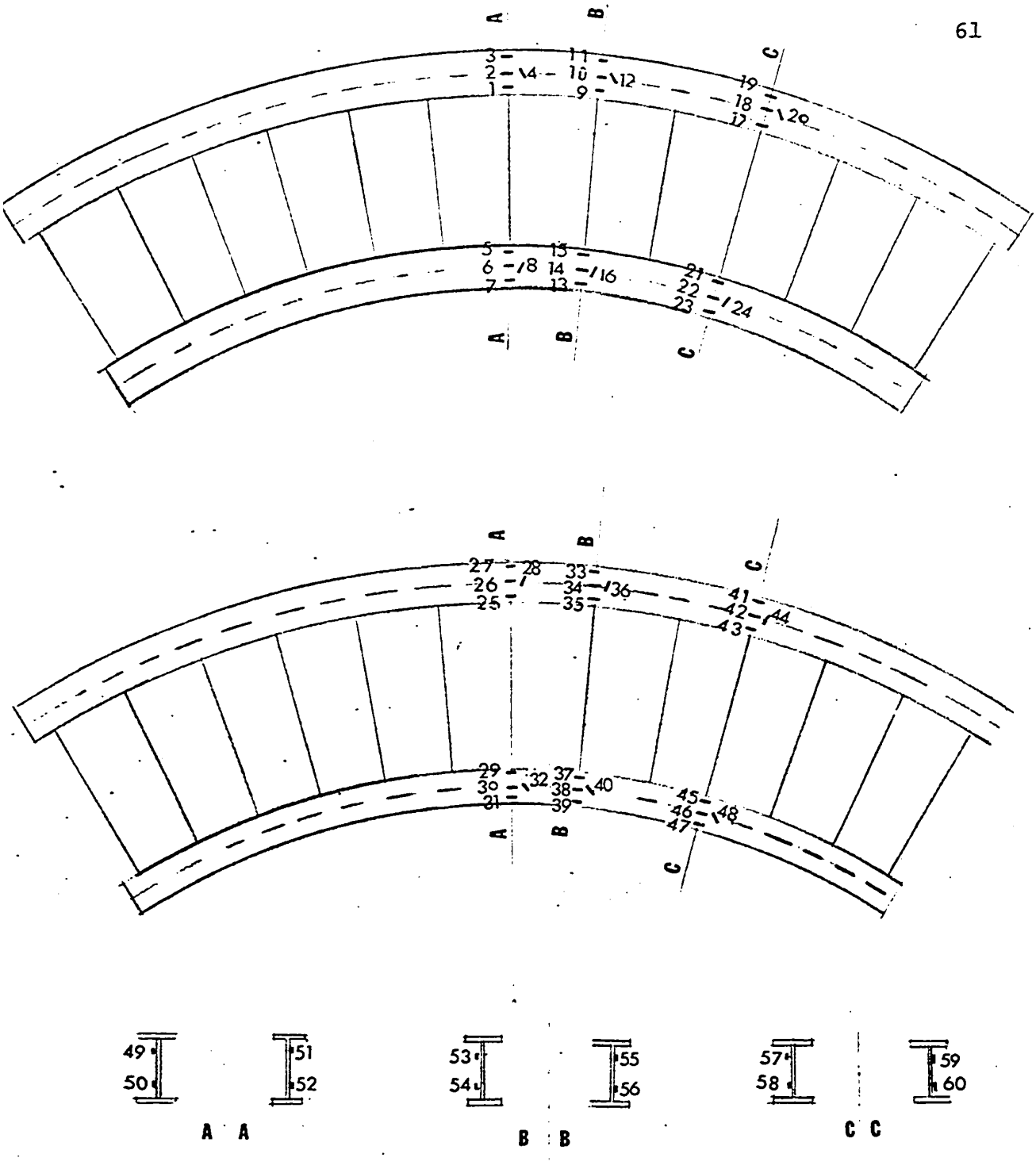

LOCATIONS OF STRAIN GAUGES

FIGURE 13(a)

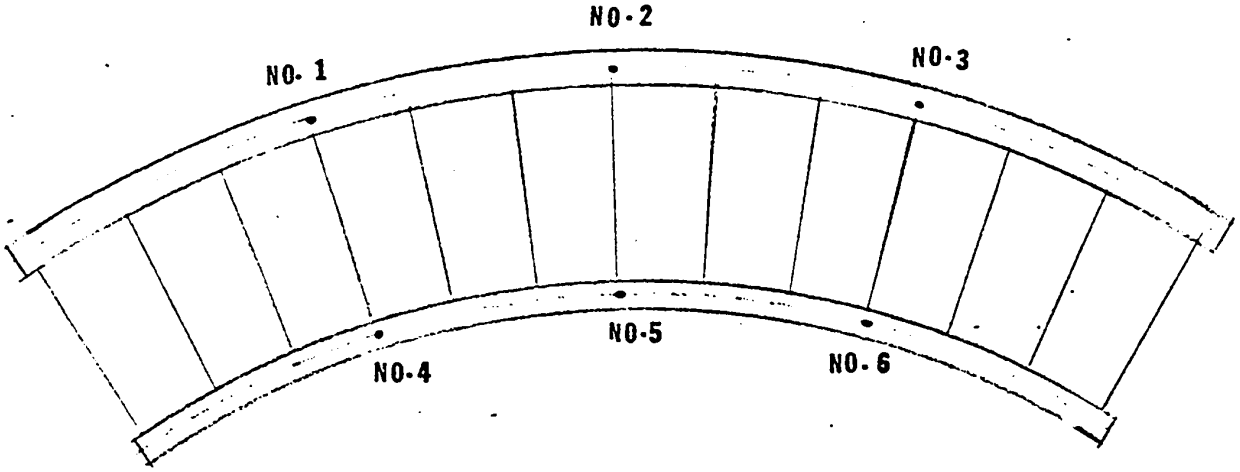

LOCATIONS OF DIAL INDICATORS

FIGURE 13(b)

APPENDIX A

ANALYSIS OF GRID STRUCTURES WITH CURVED MEMBERS

The curved girder bridge is taken as a planar frame loaded normal to its plane as shown in Fig. A.1.

A right-handed co-ordinate system is used. This is called the structure system and is denoted by the superscript ^{O}. Joints are established at supports and where members frame together. These are numbered consecutively from 1 to n (where n is the number of joints), in any convenient order. The members are numbered consecutively from 1 to n, in any convenient order.

Each vector of interest (force or deflection) at any joint has three components, one linear and two angular. These components are always considered in the standard order. Linear along Z axis, angular about X axis, angular about Y axis, a component being positive when its sense agrees with that of the corresponding reference axis. An angular vector is represented by a double headed vector normal to the plane of rotation, according to the right-hand rule (i.e. in the direction of the extended thumb of the right hand when the fingers of the right hand curl in the direction of rotation).

The directions of interest are established by

numbering the component directions consecutively from 1 to 3n, following the standard order at each joint taken in numerical order where n is the number of joints. Thus referring to Fig. A.2, the directions of interest at any joint J are 3J-2, 3J-1, and 3J.

For any loading applied to the structure, three equations of equilibrium are written for each joint. This can be expressed as one matrix equation, which, assuming that loads are applied only at joints, takes the form:

$$W^o + R^o - K^o \Delta^o = 0 \qquad \ldots(1)$$

where K^o is the structure stiffness matrix (order 3n).

W^o is the load matrix consisting of the loads at all joints.

R^o is the structure reaction matrix, consisting of the reactions at all joints.

Δ^o is the deflection matrix consisting of the deflections at all joints.

W^o, R^o, and Δ^o are of order (3n) x 1, with the elements being components given in the order of the directions of interest.

An ordered direction restraint list is made of the directions in which free directions are prevented. If there are r restraints, then Eq. 1 represents 3n equations in terms of r unknown reactions and 3n-r unknown deflections. To

solve this equation, it is separated into an equivalent pair of matrix equations:

$$(CW)^{\circ} - (CKC)^{\circ}(C\Delta)^{\circ} = 0 \qquad \ldots(2)$$

$$(DW)^{\circ} + (DR)^{\circ} - (DKC)^{\circ}(C\Delta)^{\circ} = 0 \qquad \ldots(3)$$

where:

$(DW)^{\circ}$ and $(DR)^{\circ}$ are formed from W° and R° respectively by using components matching the direction restraint list (order = r x 1).

$(CW)^{\circ}$ and $(C\,R)^{\circ}$ are formed from W° and R° respectively by removing components matching the direction restraint list (order = (3h - r) x 1).

$(CKC)^{\circ}$ is formed from K° by remiving rows and columns matching the direction restraint list (order = (3n - r) x (3n - r)).

Equation 2 is solved to obtain the deflections

$$(C\Delta)^{\circ} = (CKC)^{\circ -1}(CW)^{\circ} \qquad \ldots(4)$$

This is substituted into equation 3 to obtain the reactions.

$$(CR)^{\circ} = (DKC)^{\circ}(C\Delta)^{\circ} - (DW)^{\circ}$$

From these results any other desired information can be readily obtained by simply statics.

Member Stiffness Matrix

Each member has its own stiffness matrix relating

its end forces and moments to deflections and rotations at the ends. Thus for a member ij we can write

$$M_{ij}^{m} = K_{ij}^{m} \Delta_{ij}^{m}$$

or

$$\begin{bmatrix} M_i^m \\ M_j^m \end{bmatrix} = \begin{bmatrix} K_{ii}^m & K_{ij}^m \\ K_{ji}^m & K_{jj}^m \end{bmatrix} \begin{bmatrix} \Delta_i^m \\ \Delta_j^m \end{bmatrix}$$

where:

M_a^m = 3 components of internal forces at end a (shear in Z^m direction, torque about X^m axis, moments about Y^m axis).

Δ_a^m = 3 components of deflection at a expressed in m-system.

K_{ab}^m = 3x3 stiffness submatrix relating Ma^m to Δb^m and $\bar{m}$ denotes a reference system related to end joints, as shown in Fig.A.3.

Joint i in Fig.A.3 is called the near end and joint j the far end. The near end of a curved member must be taken so that the member lies in the positive X^m-Y^m quadrant.

The member stiffness matrix can be expressed in terms of six parameters and the distance L as follows:

$$Kij^m = \left[\begin{array}{ccc|ccc} a & b & c & -a & -b & -c \\ b & d & e & -b & -d & -(e+bL) \\ c & e & f & -c & -e & -(f+cL) \\ \hline -a & -b & -c & a & b & -c \\ -b & -d & -e & b & d & (e+bL) \\ c & -(e+bL) & -(f+cL) & -c & (e+bL) & f \end{array}\right]$$

The parameters are computed from the following material and member properties which are assumed to be constant for the member:

E = modulus of elasticity

G = modulus of rigidity

I = moment of inertia of cross-section about Y^m axis

J = torsional constant of cross-section

For a curved member with radius R subtending a central angle θ these parameters are:

$$\left.\begin{array}{lll} a = \dfrac{d'f'}{g} & b = \dfrac{-b'f'}{g} & c = \dfrac{-c'd'}{g'} \\ d = \dfrac{a'f' - c'c'}{g} & e = \dfrac{b'c'}{g'} & f = \dfrac{a'd' - b'b'}{g'} \end{array}\right\} \quad (8)$$

where:

$$a' = \frac{R^3}{EI}\left\{\frac{\theta}{2} - \frac{\sin 2\theta}{4}\right\} + \frac{R^3}{GJ}\left\{\frac{3\theta}{2} - 2\sin\theta + \frac{\sin 2\theta}{4}\right\}$$

$$b' = \frac{R^2}{EI}\left\{\left[\frac{\theta}{2} - \frac{\sin 2\theta}{4}\right]\cos\frac{\theta}{2} - \frac{\sin^2\theta}{2}\sin\frac{\theta}{2}\right\}$$

$$+ \frac{R^2}{GJ}\left\{\left[\frac{\theta}{2} + \frac{\sin 2\theta}{4}\right]\cos\frac{\theta}{2} - \left[2 - \frac{\sin^2\theta}{2}\right]\sin\frac{\theta}{2}\right\}$$

$$c' = \frac{R^2}{EI}\left\{\frac{\sin^2\theta}{2}\cos\frac{\theta}{2} + \left[\frac{\theta}{2} - \frac{\sin 2\theta}{4}\right]\sin\frac{\theta}{2}\right\}$$

$$+ \frac{R^2}{GJ}\left\{\left[\frac{\theta}{2} + \frac{\sin 2\theta}{4}\right]\sin\frac{\theta}{2} - \frac{\sin^2\theta}{2}\cos\frac{\theta}{2}\right\}$$

$$d' = \frac{R}{EI}\left\{\left[2\sin^2\frac{\theta}{2} - 1\right]\frac{\sin 2\theta}{4} - \frac{\sin^3\theta}{2} + \frac{\theta}{2}\right\}$$

$$+ \frac{R}{GJ}\left\{\left[1 - 2\sin^2\frac{\theta}{2}\right]\frac{\sin 2\theta}{4} + \frac{\sin^3\theta}{2} + \frac{\theta}{2}\right\}$$

f' is formed by interchanging EI and GJ in expression for d'.

$$g' = a'd'f' - b'b'f' - c'c'd'$$

Coordinate Transformations

The components of vectors in an m system are related to the components in the O-system by a rotation matrix.

$$\pi^{mo} = \begin{bmatrix} \omega^{mo} & 0 \\ 0 & \omega^{mo} \end{bmatrix} \qquad \ldots 9(a)$$

$$\omega^{mo} = \begin{bmatrix} 1 & 0 & 0 \\ 0 & \cos\alpha^{om} & \sin\alpha^{om} \\ 0 & -\sin\alpha^{om} & \cos\alpha^{om} \end{bmatrix} \qquad \ldots 9(b)$$

α^{om} being measured from the O-system to the m system (see Fig.A.3) using the right hand rule to determine the signs. From which:

$$\Delta^{m}_{ij} = \pi^{mo}\, \Delta^{o}_{ij} \qquad \ldots 9(c)$$

$$M^{o}_{ij} = \pi^{om}\, M^{m}_{ij} \qquad \ldots 9(d)$$

For this type of matrix, π^{om} and π^{mo} are mutual transposes as well as mutual inverse.

Combining Eq. 6a and Eq. 9c we obtain

$$M^{m}_{ij} = (K^{m}_{ij}\, \pi^{mo})\, \Delta^{o}_{ij} = K^{mo}_{ij}\, \Delta^{o}_{ij}$$

This enables us to find Mij^m directly once the joint deflections are determined combining Eq. 9d and Eq. 10.

$$M^{\circ}_{ij} = (\pi^{\circ m} k^{m}_{ij} \pi^{m\circ}) \Delta^{\circ}_{ij} = k^{\circ}_{ij} \Delta^{\circ}_{ij}$$

and we see that

$$k^{\circ}_{ij} = (\pi^{m\circ})^{t} k^{m}_{ij} \pi^{m\circ}$$

Structure Stiffness Matrix

The structure stiffness matrix K° of Eq. 1 is assembled by summing the 3x3 submatrices of the individual member stiffness matrices as defined in Eq. 12. Thus,

$$\begin{bmatrix} \sum k^{\circ}_{11} & k^{\circ}_{12} & k^{\circ}_{13} & \cdot & \cdot & k^{\circ}_{1n} \\ k^{\circ}_{21} & \sum k^{\circ}_{22} & k^{\circ}_{23} & \cdot & \cdot & k^{\circ}_{2n} \\ k^{\circ}_{31} & k^{\circ}_{32} & \sum k^{\circ}_{33} & \cdot & \cdot & k^{\circ}_{3n} \\ \cdot & \cdot & \cdot & & & \cdot \\ k^{\circ}_{n1} & k^{\circ}_{n2} & k^{\circ}_{n3} & \cdot & \cdot & \sum k^{\circ}_{nn} \end{bmatrix}$$

where Kij° = 0 if no single member frames between i and J.

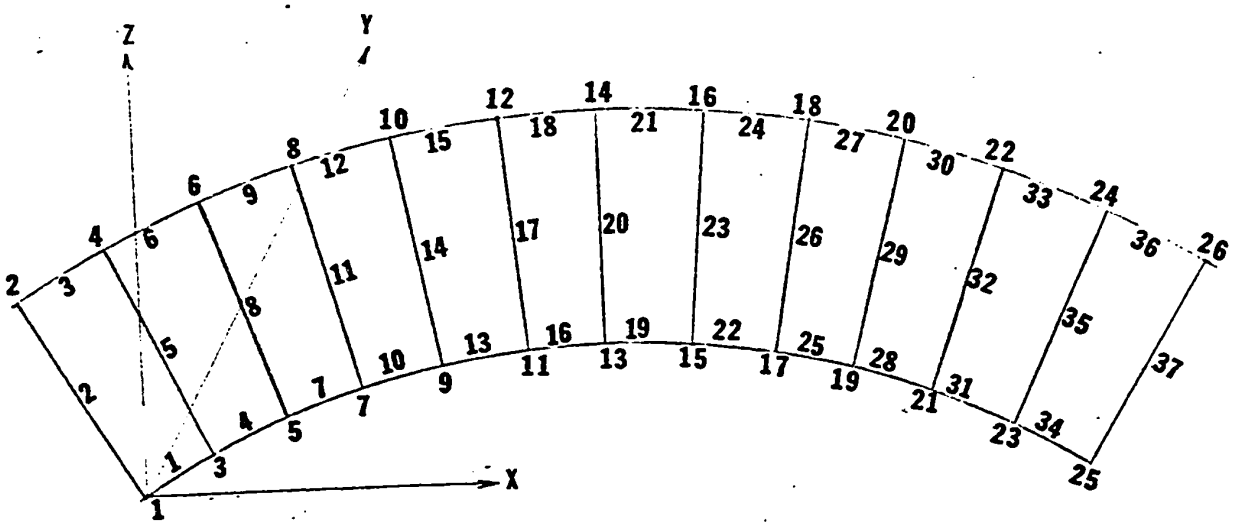

JOINT AND MEMBER NUMBERS

FIGURE A.1

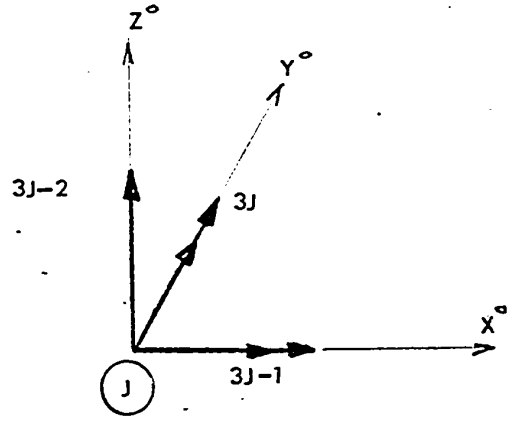

DIRECTIONS OF INTEREST AT JOINT j

FIGURE A.2

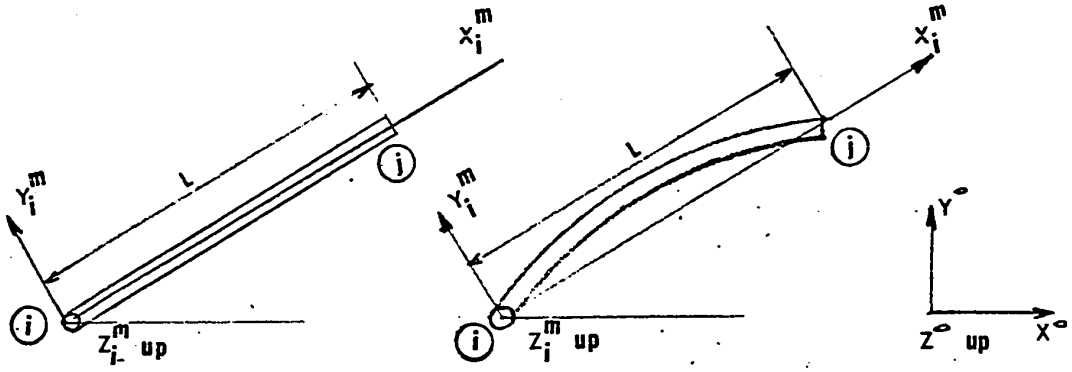

Straight Member Curved Member

MEMBER REFERENCE SYSTEM

FIGURE A.3

APPENDIX B

NON UNIFORM TORSION

Non-circular sections when twisted undergo longitudinal warping as well as angular distortions. Plane sections before twisting do not remain plane after twisting. If this warping tendency is not restrained, the member will exhibit a constant unit angle of twist and will therefore be subjected to pure torsion. If, however, the warping distortion is resisted in any way, longitudinal normal stresses are produced in addition to the torsional shearing stresses. The angle of twist per unit of length will no longer be constant. Therefore, non-uniform torsion is considered to exist in a member of non-circular section with restraint against warping.

Most of the papers discussing non-uniform torsion Theory [34, 35, 7] assume that the non-uniform torsion is obtained from the bending of the flanges of an I section about its minor principal axis, therefore, the theory is restricted to this type of section. The general theory of non-uniform torsion which can be applied to all kinds of thin walled open sections was developed by W.F. Bornscheur[36] and was later discussed by V.Z. Vlasov[26]. H.C. Wu[4] used the above mentioned theory in solving torsion problems. He used a method of analogy to solve the problem.

Torsional Constant

The St. Venant torsion theory gives the following result for a member subjected to a torsional moment

$$MP = GJ\emptyset'$$

where MP = primary twisting moment (resisting moment of unrestrained cross-section)

G = shear modulus of elasticity

J = torsional constant for the cross-section

$\emptyset' = \frac{d\emptyset}{dx}$ = angle of rotation per unit length, along the longitudinal axis

St. Venant found that for a rectangular section, for large ratios of b/h the value of J was given by the expression

$$J = 1/3(b - 0.63h)^{h3}$$

in which b is the length and h is the width of the rectangular section. For a narrow rectangle, 0.63H may be neglected, and hence

$$J \quad 1/3bh^3$$

For a rolled section such as an I section or channel, etc. which may be regarded as made up of narrow rectangles, the value of J will be approximately

$$J = 1/3 \quad (b - 0.63h)^{h3}$$

More accurate formulas for J have been presented by Inge Lyse and Bruce G. Johnston[37].

Warping Function

If a straight bar of thin-walled open section is subjected to a bending-moment, a plane section before bending will remain plane after bending. If it is subjected to twisting moment then a plane section before twisting will no longer be plane after twisting. Therefore, in the case of a member acted upon by both bending and twisting force systems (no restraint at both ends), the plane cross-section will become a space curved surface.

If an orthogonal rectilinear co-ordinate system (X-Y-Z) has been chosen, with the longitudinal axis of the beam lying in the X direction, the deformation of any section of the beam when acted upon by both bending and twisting moments, can be defined by three components i.e. Y, Z and W. The Y and Z components have the dimension in inches and perpendicular to each other, the component, W (in inches), denotes the displacement of the middle fibre of the cross-section in the X direction.

Let us consider now a thin-walled open cross-section of arbritary shape (Fig.B.2).

The following assumptions are made. The deformations due to primary (St. Venant's) shearing stresses will be considered, whereas those due to secondary (warping) shearing stresses will be neglected. For thin-walled open sections the primary shearing stresses (τ_p) are linearly

distributed between the two edges (Fig.B.1). Therefore, the shearing stress τ_p and its shearing strain γ vanish at the middle line of the cross section.

Figure B.2 shows a middle plane of an arbitrary shaped open section with length dx. During torsion the cross-sections rotate with respect to an axis through point D parallel to the longitudinal axis, and are twisted through an angle $d\phi$ between the two adjacent sections separated by length dx. We cut two rectangular elements dx ds from the middle plane and realize that they still have their rectangular form after deformation, since no shearing strains due to primary shearing stresses have been produced at the middle plane (Fig.B.1).

The element (I) whose tangent makes an angle ψ_1 with the line DS will incline during torsion, and produce a warping displacement -dw, whereas the element (II) whose angle of inclination ψ II = 0, produces no warping displacement in the longitudinal direction of the member. From element (I) (Fig.B.2) we can write the relations

$$-dw = \alpha\, ds, \quad \alpha = \frac{dU}{dx}$$

$$dU = da \sin\psi, \quad da = r\, d\phi$$

therefore

$$-dw = \alpha\, ds = \frac{dU}{dx} ds = \frac{da \sin\psi}{dx} ds = \frac{r\, d\phi \sin\psi}{dx} ds$$

$$\therefore \quad dw = -\frac{d\phi}{dx} (r \sin\psi)\, ds$$

Moreover, we know that

$$\frac{d\phi}{dx} = \phi' = \theta \quad \text{and} \quad r \sin\psi = r_t$$

hence $dw = -\theta r_t \, ds$

by integration we then obtain

$$w = w_b - \theta \int_0^S r_t \, ds, \text{ in inches} \qquad \ldots(5)$$

where S is measured counterclockwise from an arbitrary point B on the middle line of the cross-section. Wb denotes the displacement in the X direction of point B where S is equal to zero, and θ is the angle of twist per unit length. For St. Venant's torsion θ is a constant, therefore we can write θ in front of the integral.

The following function is introduced to simplify Eq. 5.

$$w = \int_0^S r_t \, ds \qquad \ldots(6)$$

where W is called the warping function and represents the shaded area F in Fig.B.2(a) swept by the radius r as we move along the middle line of the cross section from the point S = 0 up to the point S under consideration. The value of W is taken as positive when the radius r is rotating counterclockwise about D. At the point S = 0 which is chosen arbitrarily, W = 0.

In the previous discussion, it was assumed that the cross section rotated with respect to an arbitrary point D.

Let us now investigate the effect of warping of a displacement of the rotation centre. Assume, for example, that the centre of rotation is moved from Dm to Dn (Fig.B.3a).

Considering an element ds of the middle line of the cross section we can write the following from Fig.B.3.

$$r_{tm} + z_m \sin\beta + y_m \cos\beta = r_{tn} + z_n \sin\beta + y_n \cos\beta$$

$$r_{tn} = r_{tm} + (z_m - z_n)\sin\beta + (y_m - y_n)\cos\beta$$

$$r_{tn} = r_{tm} + (z_m - z_n)\frac{dy}{ds} + (y_m - y_n)\frac{dz}{ds}$$

$$w_n = \int_0^S r_{tn}\,ds = \int_0^S r_{tm}\,ds - (z_m - z_n)\int_{y_b}^{y} dy + (y_m - y_n)\int_{z_b}^{z} dz \qquad \ldots(7)$$

$$w_n = w_m - (z_m - z_n)(y - y_b) + (y_m - y_n)(z - z_b)$$

If we take Dm as the origin of the co-ordinate system, Eq. (7) becomes

$$w_n = w + z_n(y - y_b) - y_n(z - z_b) \qquad \ldots(8)$$

Then the warping functions having the centre of gravity G and the shear centre S as its centre of rotation, can be written:

$$w_g = w + z_o(y - y_b) - y_o(z - z_b) \qquad \ldots(9)$$

$$w_s = w + z_s(y - y_b) - y_s(z - z_b) \qquad \ldots(10)$$

Transformation of Co-ordinates

In the previous article the co-ordinate system (X-Y-Z) was chosen with its origin at an arbitrary point O. The warping function W was referred to an arbritary chosen point D. The following properties refer to this co-ordinate system.

Area - integral of order zero

$$A = \int_A dA \qquad \ldots(11)$$

Area - integral of first order

$$Ay = \int_A y\,dA \qquad \ldots(12)$$

$$Az = \int_A z\,dA \qquad \ldots(13)$$

$$Aw = \int_A W\,da \qquad \ldots(14)$$

Area - integral of second order

$$Ayz = \int_A yz\,dA \qquad \ldots(15)$$

$$Ayw = \int_A yw\,dA \qquad \ldots(16)$$

$$Azw = \int_A zw\,dA \qquad \ldots(17)$$

$$Ayy = \int_A y^2\,dA \qquad \ldots(18)$$

$$Azz = \int_A z^2\,dA \qquad \ldots(19)$$

$$Aww = \int_A w^2\,dA \qquad \ldots(20)$$

The above integrals will be transformed into some other co-ordinates systems in order to simplify canculations. The transformation can be divided into two steps.

A. First Transformation

If we introduce a new rectangular co-ordinate system $\hat{X}$-$\hat{Y}$-$\hat{Z}$ with its axes $\hat{X}$, $\hat{Y}$, $\hat{Z}$, parallel to X, Y, and Z but its origin coinciding with the centre of gravity of the cross

section, we have the following relations:

$$A_{\hat{y}} = \int_A \hat{y}\, dA = 0 \qquad \ldots(21)$$

$$A_{\hat{z}} = \int_A \hat{z}\, dA = 0 \qquad \ldots(22)$$

$$\hat{y} = y - y_o \qquad \ldots(23)$$

$$\hat{z} = z - z_o \qquad \ldots(24)$$

where Yo and Zo are the co-ordinates of the translation of the origin substituting Eq. (23) in Eq. (21)

$$A_{\hat{y}} = \int \hat{y}\, dA = \int_A (y-y_o)dA = \int_A y\, dA - y_o \int_A dA = 0$$

hence $$y_o = \frac{\int_A y\, dA}{\int_A dA} = \frac{A_y}{A} \qquad \ldots(25)$$

similarly $$z_o = \frac{A_z}{A} \qquad \ldots(26)$$

We transform the warping function W to $\hat{W}$ with a new reference plane having a distance Wo (given in inches square) from the original plane along the longitudinal X-axis in order to get the relation

$$A_{\hat{w}} = \int \hat{w}\, dA = 0 \qquad \ldots(27)$$

where $$\hat{w} = w - w_o, \qquad \ldots(28)$$

and W and $\hat{W}$ are both referred to the same rotation centre D. Substituting Eq. (28) in Eq. (27) we have

$$w_o = \frac{\int_A w\,dA}{\int_A dA} = \frac{A_w}{A} \qquad \ldots(29)$$

Considering the change of rotation centre from Dm to Dn and also from Eq. (7) we have

$$\hat{w}_n = w_n - w_{n_o} = w_n - \frac{A_{w_n}}{A}$$

$$= w_m - (z_m - z_n)(y - y_b) + (y_m - y_n)(z - z_b) - \frac{A_{w_n}}{A} \qquad \ldots(29)$$

moreover,

$$\hat{w}_n = (w_m - w_{m_o}) - (z_m - z_n)(y - y_b - y_o + y_b) + (y_m - y_n)(z - z_b - z_o + z_b)$$

$$\hat{w}_n = \hat{w}_m - (z_m - z_n)\hat{y} + (y_m - y_n)\hat{z}$$

We observe that the "old" co-ordinates have disappeared in all the terms of Eq. (30) except the term $\hat{w}_m$. Using this equation we are able to transform Eqs. (9) and (10) into the new co-ordinate system.

$$\hat{w}_q = \hat{w} + z_o\hat{y} - y_o\hat{z}$$

$$\hat{w}_s = \hat{w} + z_s\hat{y} - y_s\hat{z}$$

From the well known formula for the product of inertia we have the general expression.

$$A_{\hat{u}\hat{v}} = A_{uv} - \frac{A_u A_v}{A} \qquad \ldots(33)$$

Using this, the six transformed area-integrals of second order can be written as follows:

$$A_{\hat{y}\hat{z}} = \int_A \hat{y}\hat{z}\, dA = A_{yz} - \frac{A_y A_z}{A} \qquad \ldots(34)$$

$$A_{\hat{y}\hat{w}} = \int_A \hat{y}\hat{w}\, dA = A_{yw} - \frac{A_y A_w}{A} \qquad \ldots(35)$$

$$A_{\hat{z}\hat{w}} = \int \hat{z}\hat{w}\, dA = A_{zw} - \frac{A_z A_w}{A} \qquad \ldots(36)$$

$$A_{\hat{y}\hat{y}} = \int \hat{y}^2 dA = A_{yy} - \frac{A_y A_y}{A} \qquad \ldots(37)$$

$$A_{\hat{z}\hat{z}} = \int \hat{z}^2 dA = A_{zz} - \frac{A_z A_z}{A} \qquad \ldots(38)$$

$$A_{\hat{w}\hat{w}} = \int \hat{w}^2 dA = A_{ww} - \frac{A_w A_w}{A} \qquad \ldots(39)$$

B. Second Transformation

The X-Y-Z co-ordinate system is rotated about the centre of gravity G through an angle α (Fig.B.4) so that another product of inertia is zero i.e.

$$A_{\bar{y}\bar{z}} = 0 \qquad \ldots(40)$$

The axes of these directions are called the principal axes and are denoted $\bar{X}$-$\bar{Y}$-$\bar{Z}$. From Fig. B.4 we can write the well known relations

$$\bar{y} = \hat{y}\cos\alpha + \hat{z}\sin\alpha \quad \text{in inches} \qquad \ldots(41)$$

$$\bar{z} = \hat{z}\cos\alpha - \hat{y}\sin\alpha \quad \text{in inches} \qquad \ldots(42)$$

$$\tan 2\alpha = \frac{2A_{\hat{y}\hat{z}}}{A_{\hat{y}\hat{y}} - A_{\hat{z}\hat{z}}} \qquad \ldots(43)$$

$$A_{\bar{y}\bar{y}} = \tfrac{1}{2}(A_{\hat{y}\hat{y}} + A_{\hat{z}\hat{z}}) + \tfrac{1}{2}\sqrt{(A_{\hat{y}\hat{y}} - A_{\hat{z}\hat{z}})^2 + 4A_{\hat{y}\hat{z}}^2} \qquad \ldots(44)$$

$$A_{\bar{z}\bar{z}} = \tfrac{1}{2}(A_{\hat{y}\hat{y}} + A_{\hat{z}\hat{z}}) - \tfrac{1}{2}\sqrt{(A_{\hat{y}\hat{y}} - A_{\hat{z}\hat{z}})^2 + 4A_{\hat{y}\hat{z}}^2} \qquad \ldots(45)$$

As for the warping function, we transform its reference point to a point S on the Y-Z plane, so that the following relations exist:

$$A_{\bar{y}\bar{w}} = 0 \qquad \ldots(46)$$

$$A_{\bar{z}\bar{w}} = 0 \qquad \ldots(47)$$

where $\bar{W}$ is the new transformed warping function having S as its reference point.

From the fact both the integrals of Eq. (46) and Eq. (47) vanish, we know that the value of the integral $A_{\bar{W}\bar{W}}$ is a minimum. This gives the maximum normal stress due to warping.

If a transvers force is applied at the shear centre S of the cross section, there will be bending of the bar without torsion. Hence on the basis of the reciprocal theorm

we conclude that the torque applied on the bar will produce no deflection of point S. The shear centre axis S-S therefore remains straight during torsion, and the cross section of the bar rotates with respect to that axis. We call that axis the principal axis or rotation, and its maximum normal stress produced during torsion is called the principal warping stress.

From the above discussions, we know that the maximum normal stress exists only when the cross section rotates about its shear centre. Since we assumed that the rotation centre of the warping function $\bar{W}$ was at point S in Fig. B.4 and have obtained the maximum normal stress from this assumption, we conclude that the point S in Fig.B.4 is the shear centre. Hence we write

$$\bar{w} = \hat{w}_s = \hat{w} + z_s\hat{y} - y_s\hat{z} \qquad \ldots(48)$$

The formulas for the calculation of Ys and Zs in Eq. (48) can be derived from the equations below which themselves were derived from Eq. (46) and Eq. (47)

$$A\hat{y}\bar{w} = 0 \qquad \ldots(49)$$

$$A\hat{z}\bar{w} = 0 \qquad \ldots(50)$$

from Eq. (49)

$$A_{\hat{y}\bar{w}} = \int \hat{y}\bar{w}\, dA = \int \hat{y}(\hat{w} + z_s\hat{y} - y_s\hat{z})\, dA = 0$$

$$\therefore \quad A_{\hat{y}\hat{w}} + z_s A_{\hat{y}\hat{y}} - y_s A_{\hat{y}\hat{z}} = 0 \qquad \ldots(51)$$

and similarly from Eq. (50)

$$A_{\hat{z}\hat{w}} + z_s A_{\hat{y}\hat{z}} - y_s A_{\hat{z}\hat{z}} = 0 \qquad \ldots(52)$$

solving Eq. (51) and Eq. (52) simultaneously we obtain the co-ordinates of the shear centre.

$$y_s = \frac{A_{\hat{z}\hat{w}} A_{\hat{y}\hat{y}} - A_{\hat{y}\hat{w}} A_{\hat{y}\hat{z}}}{A_{\hat{y}\hat{y}} A_{\hat{z}\hat{z}} - (A_{\hat{y}\hat{z}})^2} \qquad \ldots(53)$$

$$z_s = \frac{-A_{\hat{y}\hat{w}} A_{\hat{z}\hat{z}} + A_{\hat{z}\hat{w}} A_{\hat{y}\hat{z}}}{A_{\hat{y}\hat{y}} A_{\hat{z}\hat{z}} - (A_{\hat{y}\hat{z}})^2} \qquad \ldots(54)$$

After the transformation of co-ordinates to the principal co-ordinate system, all the area-integrals of second order, except $A_{\bar{w}\bar{w}}$, $A_{\bar{y}\bar{y}}$, and $A_{\bar{z}\bar{z}}$ are equal to zero. The moments of inertia $A_{\bar{y}\bar{y}}$ and $A_{\bar{z}\bar{z}}$ can be obtained very easily from the Eq. (44) and Eq. (45) whereas the warping constant $A_{\bar{w}\bar{w}}$ can be obtained as follows:

$$A_{\bar{w}\bar{w}} = \int_A \bar{w}^2\, dA = \int_A (\hat{w} + z_s\hat{y} - y_s\hat{z})^2\, dA$$

$$A_{\bar{w}\bar{w}} = A_{\hat{w}\hat{w}} + z_s^2 A_{\hat{y}\hat{y}} + y_s^2 A_{\hat{z}\hat{z}} + 2z_s A_{\hat{y}\hat{w}} - 2y_s A_{\hat{z}\hat{w}} - 2y_s z_s A_{\hat{y}\hat{z}}$$

$$= A_{\hat{w}\hat{w}} + z_s(z_s A_{\hat{y}\hat{y}} + 2A_{\hat{y}\hat{w}} - y_s A_{\hat{y}\hat{z}})$$

$$+ y_s(y_s A_{\hat{z}\hat{z}} - 2A_{\hat{z}\hat{w}} - z_s A_{\hat{y}\hat{z}})$$

now since

$$z_s A_{\hat{y}\hat{y}} + 2A_{\hat{y}\hat{w}} - y_s A_{\hat{y}\hat{z}}$$

$$= \frac{-A_{\hat{y}\hat{w}}A_{\hat{z}\hat{z}} + A_{\hat{z}\hat{w}}A_{\hat{y}\hat{z}}}{A_{\hat{y}\hat{y}}A_{\hat{z}\hat{z}} - (A_{\hat{y}\hat{z}})^2} + 2A_{\hat{y}\hat{w}} - \frac{A_{\hat{z}\hat{w}}A_{\hat{y}\hat{y}} - A_{\hat{y}\hat{w}}A_{\hat{y}\hat{z}}}{A_{\hat{y}\hat{y}}A_{\hat{z}\hat{z}} - (A_{\hat{y}\hat{z}})^2} A_{\hat{y}\hat{z}}$$

$$= \frac{(A_{\hat{y}\hat{z}})^2 - A_{\hat{y}\hat{y}}A_{\hat{z}\hat{z}}}{A_{\hat{y}\hat{y}}A_{\hat{z}\hat{z}} - (A_{\hat{y}\hat{z}})^2} A_{\hat{y}\hat{w}} + 2A_{\hat{y}\hat{w}}$$

$$= -A_{\hat{y}\hat{w}} + 2A_{\hat{y}\hat{w}} = A_{\hat{y}\hat{w}}$$

similarly

$$y_s A_{\hat{z}\hat{z}} - 2A_{\hat{y}\hat{w}} - z_s A_{\hat{y}\hat{z}} = -A_{\hat{z}\hat{w}}$$

$$A_{\bar{w}\bar{w}} = A_{\hat{w}\hat{w}} + z_s A_{\hat{y}\hat{w}} - y_s A_{\hat{z}\hat{w}} \qquad \ldots(55)$$

Normal Stresses and Deformations

After having the sectional properties and the concept of bending theory we are able to derive the formulas for calculating the normal stresses and the differential euqation for the component deformations. The procedure is as follows:

A. By using the six conditions of equilibrium, the internal moments and forces acting on an element of a twisted member are expressed in terms of the internal loading.

B. The relationship between stresses and moments and forces is found.

C. The relationship between the deformations and the stresses is determined.

D. Using the relations of (A), (B), and (C) three differential equations of deformation are then set up.

Before going into the derivation of the differential equations, we notice that the total twisting moment about the shear centre S is equal to the sum of the primary torque $M_{\bar{s}p}$ (which produces the St. Venant's torsion) and the secondary torque $M_{\bar{s}\bar{s}}$ which produces normal stresses.

$$M_{\bar{s}} = M_{\bar{s}p} + M_{\bar{s}\bar{s}} \qquad \ldots(56)$$

Figure B.6 shows the twisting moments acting on an element of length dx taken from a twisted bar. The term $M_{\bar{s}}.d\bar{x}$ represents the external twisting moment applied upon element about the S-S axis, which is parallel to the X axis.

In the calculation of normal stresses we can take the primary twisting moment $M_{\bar{s}p}$ of Eq. (56) as a part of the external loading, since this torque $M_{\bar{s}p}$ gives no normal stresses during torsion. Hence the twisting moments shown in Fig. B.5 may be replaced by those shown in Fig. B.6.

$$m_{\bar{w}}.d\bar{x} = m_{\bar{s}}\,d\bar{x} + \frac{dM_{\bar{s}p}}{d\bar{x}}.d\bar{x} \qquad \ldots(57)$$

Moreover in a form similar to the following integrals

$$M_{\bar{y}} = \int V_{\bar{y}} \cdot d\bar{x} + C$$

$$M_{\bar{z}} = \int V_{\bar{z}} \cdot d\bar{x} + C$$

We can write the integral which is called the warping moment integral

$$M_{\bar{w}} = \int M_{\bar{s}\bar{s}} d\bar{x} + C \qquad \ldots(58)$$

where C is a constant.

Figure B7 shows an element taken from a twisted bar; the moments and the longitudinal forces are shown acting on the centre of gravity G of the cross section. The shearing forces and twisting moments are acting on the shear centre S. The external loadings are small - $n_{\bar{x}}$, $q_{\bar{y}}$ $q_{\bar{z}}$ $m_{\bar{y}}$ $m_{\bar{z}}$, $m_{\bar{s}}$ also shown in the middle section of the element. By applying the six conditions of equilibrium we have the following equations from Fig. B.7:

$$\sum N_{\bar{x}} = 0 : (N_{\bar{x}})' + n_{\bar{x}} = 0 \qquad \ldots(59)$$

$$\sum V_{\bar{y}} = 0 : (V_{\bar{y}})' + q_{\bar{y}} = 0 \qquad \ldots(60)$$

$$\sum V_{\bar{z}} = 0 : (V_{\bar{z}})' + q_{\bar{z}} = 0 \qquad \ldots(61)$$

$$\sum M_{\bar{x}} = 0 : (M_{\bar{s}\bar{s}})' + m_{\bar{w}} = 0 \qquad \ldots(62)$$

$$\sum M_{\bar{y}} = 0 : \quad (M_{\bar{y}})' + m_{\bar{y}} - V_{\bar{y}} = 0 \qquad \ldots(63)$$

$$\sum M_{\bar{z}} = 0 \quad (M_{\bar{z}})' + m_{\bar{z}} - V_{\bar{z}} = 0 \qquad \ldots(64)$$

$(M\bar{y})'$ and $(M\bar{z})'$ in Eq. (63) and Eq. (64) can be separated into two terms:

$$(M_{\bar{y}})' = (M_{\bar{y}i})' + (M_{\bar{y}2})'$$

$$(M_{\bar{z}})' = (M_{\bar{z}1})' + (M_{z2})'$$

where $(M\bar{y}\bar{1})'$ and $(Mz\bar{1})'$ have the following relationships with the external loadings

$$(M_{\bar{y}1})' + m_{\bar{y}} = 0$$

$$(M_{\bar{z}1})' + m_{\bar{z}} = 0$$

substituting the above expressions into Eq. (63) and Eq. (64) we obtain

$$(M_{\bar{y}2})' - V_{\bar{y}} = 0 \qquad \ldots(65)$$

$$(M_{\bar{z}2})' - V_{\bar{z}} = 0 \qquad \ldots(66)$$

substituting Eq. (65) in (60), Eq. (66) in (61) and Eq. (58) in (62) we have

$$(M_{\bar{y}2})'' = -q_{\bar{y}} \qquad \ldots(67)$$

$$(M_{\bar{z}2})'' = -q_{\bar{z}} \qquad \ldots(68)$$

$$(M_{\bar{w}})'' = -m_{\bar{w}} \qquad \ldots(69)$$

In order to obtain the relationships between the stresses and the external loadings we have to express the left hand side of Eqs. (67), (68) and (69) in terms of the stresses.

We have the two well-known expressions for the two bending moments

$$M_{\bar{y}2} = \int \sigma . \bar{y} . dA + C \qquad \ldots(70)$$

$$M_{\bar{z}2} = \int \sigma . \bar{z} . dA + C \qquad \ldots(71)$$

where is the normal stress on the cross section and C is a constant. The expression for $M_{\bar{w}}$ in terms of the stresses will now be discussed. Let r_t and ds have the same meaning as in Fig.B2(a)except with the shear centre S as their rotation centre. Let t be the thickness of the thin-walled section and τ be the shearing stress. Then $\tau.t$ is the unit shearing force in force per unit length, and $(\tau t) r_t$ is the twisting moment about the shear centre S caused by this unit shearing force.

If we integrate this twisting moment over the whole cross section, i.e. from S = 0 to S = e (end), we shall get the total secondary torque about the shear centre. This is true because St. Venant's shearing stress (τ_p) due to bending produce no twisting moment about the shear

Centre.

$$M_{\bar{S}S} = \int_0^e (\tau t) r_t \, ds \qquad \ldots(72)$$

using the method of integration by parts, we can rewrite Eq. (72) as follows:

$$M_{\bar{S}S} = \left[(\tau t)\left(\int_0^s r_t ds\right)\right]_0^e - \int_0^e \left(\int_0^s r_t ds\right) \frac{\partial(\tau t)}{\partial s} \cdot ds$$

The first term of the above equation vanishes, because the unit shearing force (or shear flow) vahishes at the open ends of a thin-walled section (at S = 0 and S = e). Moreover, we have $\int_0^s r_t ds = \bar{w}$ the warping function referrred to shear centre S; hence Eq. (72) becomes

$$M_{\bar{S}S} = -\int_0^e \bar{w} \cdot \frac{\partial(\tau t)}{\partial s} \cdot ds \qquad \ldots(73)$$

Let Fig.B.8 be an element of a bar subjected to both twisting and bending. By using the equilibrium condition we get the expression.

$$\frac{\partial(\tau t)}{\partial s} = -\frac{\partial \sigma}{\partial \bar{x}} \cdot t$$

Substituting into Eq. (73):

$$M_{\bar{s}\bar{s}} = \int_0^e \bar{w} \cdot \frac{\partial \sigma}{\partial \bar{x}} \cdot t \cdot ds = \int_A \bar{w} \frac{\partial \sigma}{\partial \bar{x}} \cdot dA \qquad \ldots(74)$$

Equation (74) into (58)

$$M_{\bar{w}} = \int_0^{\bar{x}} M_{\bar{s}\bar{s}}\, d\bar{x} + C = \int_0^{\bar{x}} \int_A \bar{w} \cdot \frac{\partial \sigma}{\partial \bar{x}} \cdot dA \cdot d\bar{x} + C$$

changing the order of integration

$$M_{\bar{w}} = \int_A \int_0^{\bar{x}} \bar{w} \cdot \frac{\partial \sigma}{\partial \bar{x}} \cdot d\bar{x} \cdot dA + C$$

$$= \int_A \bar{w} \int_0^{\bar{x}} \frac{\partial \sigma}{\partial \bar{x}} \cdot d\bar{x} \cdot dA + C$$

$$M_{\bar{w}} = \int_A \bar{w} \sigma \, dA + C \qquad \ldots(75)$$

where the warping function $\bar{w}$ is independent of $\bar{x}$. By substituting Eq. (70) into (67), Eq. (71) into (68) and (75) into (69), we obtain the following relationships between stresses and the external loadings:

$$\frac{\partial^2}{\partial \bar{x}^2} \left(\int_A \sigma \cdot \bar{y} \, dA \right) = - q_{\bar{y}} \qquad \ldots(76)$$

$$\frac{\partial^2}{\partial \bar{x}^2} \left(\int_A \sigma \cdot \bar{z} \, dA \right) = - q_{\bar{z}} \qquad \ldots(77)$$

$$\frac{\partial^2}{\partial \bar{x}^2} \left(\int_A \sigma \cdot \bar{w} \, dA \right) = - m_{\bar{w}} \qquad \ldots(78)$$

Next, we express the normal stress σ in terms of the deformations. Let $\bar{\eta}$ and $\bar{\zeta}$ be the deflections of the $\bar{Y}$ and $\bar{Z}$ directions respectively, and $\bar{\phi}$ be the rotation of the bar about its shear centre. The total normal stress is equal to the sum of the bending parts $\sigma_{\bar{y}}$ and $\sigma_{\bar{z}}$ and the warping parts $\sigma_{\bar{w}}$, thus

$$\sigma = \sigma_{\bar{y}} + \sigma_{\bar{z}} + \sigma_{\bar{w}} \qquad \ldots(79)$$

The following stress due to bending are well-known:

$$\sigma_{\bar{y}} = -E\bar{\eta}''\bar{y} \qquad \ldots(80)$$

$$\sigma_{\bar{z}} = -E\bar{\zeta}''\bar{z} \qquad \ldots(81)$$

where E is the modulus of elasticity. But the normal stress dur to warping is relatively complicated. From Eq. (5) and Eq. (6) we have the warping displacement:

$$w = w_b - \theta \int_0^s r_t ds = w_b - \theta w$$

Using Eq. (29) the average value of W, denoted by w_o can be obtained.

$$w_o = \frac{1}{A}\int_A w\,dA = w_b - \frac{\theta}{A}\int w\,dA = w_b - \theta w_o$$

where A is the area of the cross section. Thus, the warping displacement, $\hat{W}$, in the X-Y-Z-W system can be obtained by subtracting the two above equations:

$$\hat{W} = w - w_o = \theta(w_o - w) = -\theta w \qquad \ldots(82)$$

where $\hat{w} = w - w_o$ $\ldots(28)$

For the warping torsion, the angle of twist per unit length, θ, is not a constant and is equal to $\frac{d\phi}{dx}$ or $\frac{d\hat{\phi}}{d\hat{x}}$ in the "$\wedge$" system.

Therefore,

$$\hat{W} = -\frac{d\hat{\phi}}{d\hat{x}}\,\hat{w}$$

and $$\frac{d\hat{W}}{d\hat{x}} = -\frac{d^2\hat{\phi}}{d\hat{x}^2}\cdot\hat{w}$$

Using Hook's Law and substituting in the above expression, we obtain the normal stress due to warping.

$$\sigma_W = E e_{\hat{w}} = E \cdot \frac{d\hat{W}}{d\hat{x}} = -E \cdot \frac{d^2\hat{\phi}}{d\hat{x}^2}\cdot\hat{w}$$

$$\sigma_{\hat{w}} = -E\hat{\phi}''\hat{w} \qquad \ldots(83)$$

Hence, we can see that the warping normal stress depends on the angle or rotation $\hat{\phi}$ and the warping function $\hat{W}$ only. Therefore we can write the expression for the

warping normal stress having the shear centre as its centre of rotation as follows:

$$\sigma_{\bar{w}} = -E\bar{\phi}''\bar{w} \qquad \ldots(84)$$

Adding Eq. (80), Eq. (81) and (84) we have from Eq. (79)

$$\sigma = -E(\bar{\eta}''\bar{y} + \bar{\varsigma}''\bar{z} + \bar{\phi}''\bar{w}) \qquad \ldots(85)$$

Substituting Eq. (85) in Eqs. (76), (77) and (78) and using the symbols of the area integral we can obtain three differential equations:

$$EA_{\bar{y}\bar{y}}\bar{\eta}'''' + EA_{yz}\bar{\varsigma}'''' + EA_{\bar{y}\bar{w}}\bar{\phi}'''' = q_{\bar{y}} \qquad \ldots(86)$$

$$EA_{\bar{y}\bar{z}}\bar{\eta}'''' + EA_{\bar{z}\bar{z}}\bar{\varsigma}'''' + EA_{\bar{z}\bar{w}}\bar{\phi}'''' = q_z \qquad \ldots(87)$$

$$EA_{\bar{y}\bar{w}}\bar{\eta}'''' + EA_{\bar{z}\bar{w}}\bar{\varsigma}'''' + EA_{\bar{w}\bar{w}}\bar{\phi}'''' = m_{\bar{w}} \qquad \ldots(88)$$

These equations can be simplified, since the area integrals $A_{\bar{y}z}$ and $A_{\bar{y}\bar{w}}$ and $A_{\bar{z}\bar{w}}$ are all equal to zero due to Eqs. (40), (46) and (47).

$$EA_{\bar{y}\bar{y}}\bar{\eta}'''' = q_{\bar{y}} \qquad \ldots(89)$$

$$EA_{\bar{z}\bar{z}}\bar{\zeta}'''' = q_{\bar{z}} \qquad \ldots(90)$$

$$EA_{\bar{w}\bar{w}}\bar{\phi}'''' = m_{\bar{w}} \qquad \ldots(91)$$

Eliminating $q_{\bar{y}}$, $q_{\bar{z}}$, $m_{\bar{w}}$ from Eqs. (67), (68), (69) and Eqs. (89), (90), and (91) we get

$$M_{\bar{y}2} = -E\bar{\eta}''A_{\bar{y}\bar{y}} \qquad \ldots(92)$$

$$M_{\bar{z}2} = -E\bar{\zeta}''A_{\bar{z}\bar{z}} \qquad \ldots(93)$$

$$M_{\bar{w}} = -E\bar{\phi}''A_{\bar{w}\bar{w}} \qquad \ldots(94)$$

$$\bar{\eta}'' = -\frac{M_{\bar{y}2}}{EA_{\bar{y}\bar{y}}} \qquad \ldots(95)$$

$$\bar{\zeta}'' = \frac{M_{\bar{z}2}}{EA_{\bar{z}\bar{z}}} \qquad \ldots(96)$$

$$\bar{\phi}'' = \frac{M_{\bar{w}}}{EA_{\bar{w}\bar{w}}} \qquad \ldots(97)$$

Therefore, Eq. (85) becomes

$$\sigma = \frac{M_{\bar{y}2}}{A_{\bar{y}\bar{y}}}\cdot\bar{y} + \frac{M_{\bar{z}2}}{A_{\bar{z}\bar{z}}}\cdot\bar{z} + \frac{M_{\bar{w}}}{A_{ww}}\cdot\bar{w} \qquad \ldots(98)$$

The first two terms of Eq. (98) are due to bending and the last term is due to warping.

The warping function $\bar{W}$ and the warping constant $A_{\bar{w}\bar{w}}$ have been discussed in Art. IV.

The following Article will be devoted to the discussion of the warping moment integral $M_{\bar{w}}$.

VI. Solutions to the Differential Equations

Equation (91) of Art. V is a differential equation for the rotation angle $\bar{\phi}$ caused by torsion. This differential equation will be solved in this Article for different loading conditions. After having obtained the expression of $\bar{\phi}$, the warping moment integral $M_{\bar{w}}$, and the normal stress $\sigma_{\bar{w}}$ can be found easily from Eqs. (94) and (84).

Rewriting Eqs. (91) and (57):

$$E A_{\bar{w}\bar{w}} \bar{\phi}''' = m_{\bar{w}} \qquad \ldots(91)$$

$$m_{\bar{w}} = m_{\bar{s}} + \frac{d M_{\bar{s}p}}{d\bar{x}} \qquad \ldots(57)$$

and substituting Eq. (57) into Eq. (91)

$$E A_{ww} \bar{\phi}''' = m_{\bar{s}} + \frac{d M_{\bar{s}p}}{d\bar{x}} \qquad \ldots(99)$$

The primary (st. Venant's) twisting moment is given in Art. II as:

$$M_{\bar{s}p} = G J \bar{\phi}' \qquad \ldots(100)$$

where G is the shear modulus of elasticity, and J is the torsional constant for the cross section defined in Art. II. Substituting Eq. (100) into (99), we have

$$EA\bar{w}\bar{w}\bar{\phi}'''' - GJ\bar{\phi}'' = m\bar{s} \qquad \ldots(101)$$

We notice that this differential equation has the same form as that for bending of a beam column.

$$EI\eta'''' - H\eta'' = p \qquad \ldots(102)$$

where η is the deflection of the beam; H is the axial tensile force and p is the external loading. Thus we can make an analogy and understand Eq. (101) as a differential equation for bending of a beam column as shown in Fig.B.9.

where GJ corresponds to the axial force H

$M\bar{s}$ corresponds to the loading P

EAww corresponds to the flexural rigidity EI

and $\bar{\phi}$ corrresponds to the deflection η.

To solve Eq. (102) we integrate it twice:

$$EI\eta'' - H\eta = \int(\int p\,dx)\,dx + C_1x + C_2$$

$$\eta'' - \frac{H}{EI}\eta = \frac{1}{EI}\left[\int(\int p\,dx)\,dx + C_1x + C_2\right] \qquad \ldots(103)$$

Homogeneous Solutions

$$\eta_H = K_1 e^{\beta x} + K_2 e^{-\beta x} = A \sinh \beta x + B \cosh \beta x \qquad \ldots(104)$$

where K1, K2, A and B are constants and $\beta = \sqrt{\frac{H}{EI}}$

Assume the particular integral is of the following form:

$$\eta_p = \frac{1}{EI}\left[C\int(\int p\,dx)dx + D\int p\,dx + Fp + Gx + K\right] \quad ;$$

substituting into Eq. (103) and assuming p a constant:

$$\frac{1}{EI}\left[C_p - \frac{H}{EI}\left\{C\int(\int p\,dx)dx + D\int p\,dx + Fp + Gx + K\right\}\right]$$

$$= \frac{1}{EI}\left[\int(\int p\,dx)\,dx + C_1 x + C_2\right] \quad ;$$

by comparing the co-efficients on both sides of the above equation we have

$$C = -\frac{EI}{H}, \quad D = 0, \quad F = -\frac{1}{\beta^4}, \quad G = -\frac{C_1 EI}{H}, \quad K = -\frac{C_2 EI}{H}$$

therefore,

$$\eta_p = \frac{1}{EI}\left[-\frac{EI}{H}\int(\int p\,dx)dx - \frac{1}{\beta^4}p - \frac{C_1 EI}{H}x - \frac{C_2 EI}{H}\right]$$

$$= \frac{1}{H}\left[\int(\int p\,dx)\,dx + C_1 x + C_2\right] - \frac{p}{\beta^4 EI}$$

$$\ldots(105)$$

It is known that the bending moment M° is of a simply supported beam type acted upon by a distributed

load p (without axial force) is

$$M^{\circ} = -\left[\int \left(\int p\,dx\right) dx + C_1 x + C_2\right] \qquad \ldots(106)$$

Differentiating with respect to x twice

$$\frac{d^2 M^{\circ}}{dx^2} = -p \qquad \ldots(107)$$

and using the relationship of $\beta = \sqrt{\frac{H}{EI}}$

we have

$$\beta^4 EI = \frac{H}{EI}\beta^2 EI = H\beta^2 \qquad \ldots(108)$$

Substituting Eqs. (106), (107) and (108) into (105),

$$\eta_p = \frac{1}{H}\left(M^{\circ} + \frac{1}{\beta^2}\frac{d^2 M^{\circ}}{dx^2}\right) \qquad \ldots(109)$$

and combining Eqs. (104), and (109) to obtain the general solution of Eq. (103):

$$\eta = \eta_H + \eta_p = A\sinh\beta x + B\cosh\beta x + \frac{1}{H}\left(M^{\circ} + \frac{1}{\beta^2}\frac{d^2 M^{\circ}}{dx^2}\right) \qquad \ldots(110)$$

By analogy the general solution of Eq. 101 can be written as follows:

$$\bar{\phi} = A\sinh\lambda\bar{x} + B\cosh\lambda\bar{x} + \frac{1}{GJ}\left(M^{\circ}_{\bar{w}} + \frac{1}{\lambda^2}\frac{d^2 M^{\circ}_{\bar{w}}}{d\bar{x}^2}\right) \qquad \ldots(111)$$

where A and B are constants, $M_{\bar{w}}^{\circ}$ is the warping moment integral, at GJ = 0, corresponding to Eq. (106):

$$M_{\bar{w}}^{\circ} = -\left[\int\left(m_{\bar{s}}\, d\bar{x}\right) d\bar{x} + C_1 x + C_2\right) \qquad \ldots(112)$$

and λ has the following expression corresponding to that of β.

$$\lambda = \sqrt{\frac{GJ}{EA_{ww}}} \qquad \ldots(113)$$

The solutions of Eq. (101) for two different kinds of loading will be discussed. For convenience, a vector symbol $\overset{\downarrow}{\phi}$ is introduced to represent a torque acting on a beam. Thus Fig.B10 can be represented by Fig.B11 where $\overset{\downarrow}{\phi}$ is a "positive" torque and $\overset{\uparrow}{\phi}$ a "negative" one.

A. Uniform Torque

A beam analogous to the beam column is loaded by a uniform torque of length C and an axial load GJ (Fig.B.12). Figures (b) and (c) are the shear and bending moment diagrams of this determinate analogous beam at GJ = 0.

From Eq. (111) and Fig.B.12, the expression of ϕ in each region can be written as follows:

Region I:

$$GJ\bar{\phi} = M_{\bar{w}}^{\circ} + \frac{d^2 M_{\bar{w}}^{\circ}}{\lambda^2 d\bar{x}^2} + GJ\left(A_1 \sinh\lambda\bar{x} + B_1 \cosh\lambda\bar{x}\right)$$

$$= M_{\bar{w}}^{\circ} + GJ\left(A_1 \sinh\lambda\bar{x} + B_1 \cosh\lambda\bar{x}\right) \qquad \ldots(114)$$

Region II:

$$GJ\bar{\phi} = M_{\bar{w}}^{\circ} - \frac{m_{\bar{s}}}{\lambda^2} + GJ\left(A_2 \sinh\lambda\bar{x} + B_2 \cosh\lambda\bar{x}\right) \qquad \ldots(115)$$

Region III:

$$GJ\phi = M^{\circ}_{\bar{w}} + GJ(A_3 \sinh \lambda \bar{x} + B_3 \cosh \lambda \bar{x}) \qquad \ldots(116)$$

Applying the boundary conditions to determine the 6 constants appearing in Eq. (114) and Eq. (115) and Eq. (116) At $\bar{X} = 0$ $\bar{\phi} = 0$ (deflection of the analogous beam should be equal to zero at the support). From Eq. (114)

$$0 = 0 + GJ B_1 \quad \therefore B_1 = 0$$

At $\bar{x} = l$, $\bar{\phi} = 0$ $\qquad \ldots(117)$

$$0 = GJ(A_3 \sinh \lambda l + B_3 \cosh \lambda l)$$

$$\therefore A_3 = -\frac{B_3 \cosh \lambda l}{\sinh \lambda l} \qquad \ldots(118)$$

At $\bar{X} = a$, $\bar{\phi}1 = \bar{\phi}$ 11 (Deflection at left = deflection at right).

$$(M^{\circ}_{\bar{w}})_a + GJ(A_1 \sinh \lambda a + B_1 \cosh \lambda a)$$
$$= (M^{\circ}_{\bar{w}}) - \frac{m_{\bar{s}}}{\lambda^2} + GJ(A_2 \sinh \lambda a + B_2 \cosh \lambda a).$$

substituting Eq. (117) and rewriting

$$(A_1 - A_2) \sinh \lambda a = -\frac{m_{\bar{s}}}{\lambda^2 GJ} + B_2 \cosh \lambda a). \qquad \ldots(119)$$

at x = a $\bar{\phi}1' = \bar{\phi}11'$ (slope at left = slope at right):

$$(M^{\circ}_{\bar{s}p})_a + \lambda GJ(A_1 \cosh\lambda a + B_1 \sinh\lambda a)$$
$$= (M^{\circ}_{\bar{s}p})_a + \lambda GJ(A_2 \cosh\lambda a + B_2 \sinh\lambda a)$$

substituting into Eq. (117) and rewriting,

$$(A_1 - A_2)\cosh\lambda a - B_2 \sinh\lambda a = 0 \qquad \ldots(120)$$

At x = a + c, $\bar{\phi}11 = \bar{\phi}111$

$$(M^{\circ}_{\bar{w}})_{a+c} - \frac{m_{\bar{s}}}{\lambda^2} + GJ\left[A_2 \sinh\lambda(a+c) + B_2 \cosh\lambda(a+c)\right]$$
$$= (M^{\circ}_{\bar{w}})_{a+c} + GJ\left[A_3 \sinh\lambda(a+c) + B_3 \cosh\lambda(a+c)\right.$$

or

$$(A_2 - A_3)\sinh\lambda(a+c) + (B_2 - B_3)\cosh\lambda(a+c) = \frac{m_{\bar{s}}}{\lambda^2 GJ} \qquad \ldots(121)$$

At $\bar{x} = a+c$, $\bar{\phi}'_{11} = \bar{\phi}'_{111}$

$$(M^{\circ}_{\bar{s}p})_{a+c} + \lambda GJ\left[A_2 \cosh\lambda(a+c) + B_2 \sinh\lambda(a+c)\right]$$
$$= (M^{\circ}_{\bar{s}p})_{a+c} + \lambda GJ\left[A_3 \cosh\lambda(a+c) + B_3 \sinh\lambda(a+c)\right]$$

or

$$(A_2 - A_3)\cosh\lambda(a+c) + (B_2 - B_3)\sinh\lambda(a+c) = 0 \qquad \ldots(122)$$

From Eq. (120)

$$A_1 - A_2 = \frac{B_2 \sinh\lambda a}{\cosh\lambda a} \qquad \ldots(123)$$

Substituting into Eq. (119) and simplifying we have

$$B_2 = \frac{m_s^- \cosh \lambda a}{\lambda^2 GJ} \qquad \ldots(124)$$

Eq. (124) into (123):

$$A_1 - A_2 = \frac{m_s^- \sinh \lambda a}{\lambda^2 GJ} \qquad \ldots(125)$$

$$B_2 - B_3 = \frac{m_s^-}{\lambda^2 GJ} \cosh \lambda (a+c). \qquad \ldots(126)$$

Eq. (124) into Eq. (126):

$$B_3 = \frac{m_s^- [\cosh \lambda a - \cosh \lambda (a+c)]}{\lambda^2 GJ} \qquad \ldots(127)$$

From Eqs. (118) and (127):

$$A_3 = \frac{m_s^- [\cosh \lambda a - \cosh \lambda (a+c) \cosh \lambda l]}{\lambda^2 GJ \cdot \sinh \lambda l} \qquad \ldots(128)$$

From Eqs. (122) and (126):

$$A_2 - A_3 = - \frac{m_s^- \sinh \lambda (a+c)}{\lambda^2 GJ} \qquad \ldots(129)$$

From Eqs. (128) and (129):

$$A_2 = - \frac{m_s^- [\cosh \lambda a - \cosh \lambda (a+c)] \cosh \lambda l}{\lambda^2 GJ \cdot \sinh \lambda l} - \frac{m_s^- \sinh \lambda (a+c)}{\lambda^2 GJ} \qquad \ldots(130)$$

From Eqs. (125) and (130):

$$A_1 = -\frac{m_s^- [\cosh \lambda a - \cosh \lambda (a+c)] \cosh \lambda l}{\lambda^2 GJ \cdot \sinh \lambda l}$$

$$+ \frac{m_s^- \sinh \lambda a}{\lambda^2 GJ} - \frac{m_s^- \sinh \lambda (a+c)}{\lambda^2 GJ} \qquad \ldots(131)$$

Substituting the six constants found in Eqs. (131), (130), (128), (117), (124), and (127) into Eqs. (114), (115), and (116) correspondingly, we have the expression $\bar{\phi}$.

Region I:

$$M_{\bar{w}}^{\circ} = \frac{c \cdot m_s^- \cdot h}{l} \bar{x}$$

$$GJ\bar{\phi} = M_{\bar{w}}^{\circ} + GJ(A_1 \sinh \lambda \bar{x} + B_1 \cosh \lambda \bar{x})$$

$$= \frac{m_s^-}{\lambda^2} \left\{ \lambda^2 \cdot \frac{c \cdot h}{l} \cdot \bar{x} - \left[\frac{(\cosh \lambda a - \cosh \lambda (a+c)) \cosh \lambda l}{\sinh \lambda l} \right.\right.$$

$$\left.\left. + \frac{\sinh \lambda (a+c) \sinh \lambda l - \sinh \lambda a \sinh \lambda l}{\sinh \lambda l} \right] \sinh \lambda \bar{x} \right\}$$

Using the relationships

$$\cosh \lambda (a+c) = \cosh \lambda (l-b) = \cosh \lambda l \cosh \lambda b - \sinh \lambda l \sinh \lambda b$$

$$\sinh \lambda (a+c) = \sinh \lambda (l-b) = \sinh \lambda l \cosh \lambda b - \cosh \lambda l \sinh \lambda b$$

$$\cosh \lambda a = \cosh \lambda [l-(b+c)] = \cosh \lambda l \cosh \lambda (b+c) - \sinh \lambda l \sinh \lambda (b+c)$$

$$\sin \lambda a = \sinh \lambda [l-(b+c)] = \sinh \lambda l \cosh \lambda (b+c) - \cosh \lambda l \sinh \lambda (b+c)$$

we have:

$$GJ\bar{\phi} = \frac{m_{\bar{s}}}{\lambda^2}\left\{\lambda^2 \cdot \frac{c.n.\bar{x}}{\ell} - \left[\frac{\cosh a \cosh\lambda\ell - \cosh\lambda b - \sinh\lambda a \sinh\lambda\ell}{\sinh\lambda\ell}\right]\sinh\lambda\bar{x}\right\}$$

or

$$GJ\bar{\phi} = \frac{m_{\bar{s}}}{\lambda^2}\left\{\lambda^2 \frac{c.n}{\ell} \cdot \bar{x} - \left[\frac{\cosh\lambda(b+c) - \cosh\lambda b}{\sinh\lambda\ell}\right]\sinh\lambda\bar{x}\right\} \quad \ldots(132)$$

From Eq. (113) we can write

$$GJ = \lambda^2 EA_{\bar{w}\bar{w}} \quad \ldots(133)$$

Differentiating Eq. (132) with respect to $\bar{X}$ twice and substituting the obtained expression of $\bar{\phi}''$ and Eq. (133) into Eq. (94) we have

$$M_{\bar{w}} = -EA_{\bar{w}\bar{w}}\bar{\phi}''$$

$$= \frac{m_{\bar{s}}}{\lambda^2}\,\frac{\cosh\lambda(b+c) - \cosh\lambda b}{\sinh\lambda\ell}\,\sinh\lambda\bar{x} \quad \ldots(134)$$

Equations (132) and (134) are the expressions of the rotation $\bar{\phi}$ and warping moment integral $M\bar{W}$ in Region I.

Region II:

$$M^{o}_{\bar{w}} = m_{\bar{s}}\left[\frac{c.n}{\ell}\bar{x} - \frac{(\bar{x}-a)^2}{2}\right]$$

(see Fig. 12.c)

From Eqs. (115), (130) and (124):

$$GJ\bar{\phi} = M^{o}_{\bar{w}} - \frac{m_{\bar{s}}}{\lambda^2} + GJ(A_2 \sinh\lambda\bar{x} + B_2 \cosh\lambda\bar{x})$$

$$= \frac{m_{\bar{s}}}{\lambda^2}\left\{\lambda^2\left[\frac{c.n}{\ell}\bar{x} - \frac{(x-a)^2}{2}\right] - 1 - \left[\frac{\cosh\lambda a - \cosh\lambda(a+c)\cosh\lambda\ell}{\sinh\lambda\ell} + \sinh\lambda(a+c)\right]\sinh\lambda\bar{x} + \cosh\lambda a \cosh\lambda\bar{x}\right\}$$

using the following formulas to simplify the above expression:

$$\cosh\lambda(a+c) = \cosh\lambda(\ell-b) = \cosh\lambda\ell\cosh\lambda b - \sinh\lambda\ell\sinh\lambda b$$

$$\sinh\lambda(a+c) = \sinh\lambda(\ell-b) = \sinh\lambda\ell\cosh\lambda b - \cosh\lambda\ell\sinh\lambda b$$

then

$$GJ\bar{\phi} = \frac{m_{\bar{s}}}{\lambda^2}\left\{\lambda^2\left[\frac{c.n}{\ell}\bar{x} - \frac{(\bar{x}-a)^2}{2}\right] - 1 - \left[\frac{(\cosh\lambda a\cosh\lambda\ell - \cosh\lambda b)}{\sinh\lambda\ell}\sinh\lambda\bar{x} - \frac{\sinh\lambda\ell\cosh\lambda b\cosh\lambda\bar{x}}{\sinh\lambda\ell}\right]\right\}$$

$$= \frac{m_{\bar{s}}}{\lambda^2}\left\{\lambda^2\left[\frac{c.n}{\ell}\bar{x} - \frac{(\bar{x}-a)^2}{2}\right] - 1 + \left[\frac{\cosh\lambda b\sinh\lambda\bar{x}}{\sinh\lambda\ell} + \frac{\cosh\lambda a}{\sinh\lambda\ell}\cdot\sinh\lambda(\ell-\bar{x})\right]\right\}$$

therefore:

$$GJ\bar{\phi} = \frac{m_{\bar{s}}}{\lambda^2}\left\{\lambda^2\left[\frac{c.n.\bar{x}}{\ell} - \frac{(\bar{x}-a)^2}{2}\right] - 1 + \frac{\cosh\lambda a\sinh\lambda\bar{x}' + \cosh\lambda b\sinh\lambda\bar{x}}{\sinh\lambda\ell}\right\}$$

and

$$M_{\bar{w}} = \frac{m_{\bar{s}}}{\lambda^2}\left(1 - \frac{\cosh\lambda a\sinh\lambda\bar{x}' + \cosh\lambda b\sinh\lambda\bar{x}}{\sinh\lambda\ell}\right)$$

...(136)

Region III:

Similarly, the following expressions can be derived for Region III.

$$GJ\bar{\phi} = \frac{m\bar{s}}{\lambda^2}\left[\lambda^2 \cdot \frac{c.n'}{\ell} \cdot \bar{x}' - \frac{\cosh\lambda(a+c) - \cosh\lambda a}{\sinh\lambda\ell} \cdot \sinh\lambda\bar{x}'\right] \quad \ldots(137)$$

$$M_{\bar{w}} = \frac{m\bar{s}}{\lambda^2} \frac{\cosh\lambda(a+c) - \cosh\lambda a}{\sinh\lambda\ell} \cdot \sinh\lambda\bar{x}' \quad \ldots(138)$$

For the special case; i.e. when c = 1 and a = b = 0 the following expressions can be obtained from Eqs. (135) and (136):

$$GJ\bar{\phi} = \frac{m\bar{s}}{\lambda^2}\left[\lambda^2\left(\frac{\ell}{2}\bar{x} - \frac{\bar{x}^2}{2}\right) - 1 + \frac{\sinh\lambda\bar{x} + \sinh\lambda\bar{x}'}{\sinh\lambda\ell}\right] \quad \ldots(139)$$

$$M_{\bar{w}} = \frac{m\bar{s}}{\lambda^2}\left(1 - \frac{\sinh\lambda\bar{x} + \sinh\lambda\bar{x}'}{\sinh\lambda\ell}\right) \quad \ldots(140)$$

B. Concentrated Torque

The expressions of ϕ in each of the regions of the analogous beam (Fig.) can be written as

Region I:

$$GJ\bar{\phi} = M^{o}_{\bar{w}} + GJ(A_1\sinh\lambda\bar{x} + B_1\cosh\lambda\bar{x}) \quad \ldots(141)$$

Region II:

$$GJ\bar{\phi} = M^{\circ}_{\bar{w}} + GJ(A_2 \sinh \lambda\bar{x} + B_2 \cosh \lambda\bar{x}) \qquad \ldots(142)$$

Applying the boundary conditions to determine the constants A1, A2, B1, and B2 appearing in Eqs. (141) and (142)

At $\bar{x} = 0$, $\bar{\phi} = 0$. from Eq. (141)

$$0 + GJB_1 = 0 \qquad \therefore B_1 = 0 \qquad \ldots(143)$$

At $\bar{x} = \ell$, $\bar{\phi} = 0$. from Eq. (142)

$$0 = GJ(A_2 \sinh \lambda\ell + B_2 \cosh \lambda\ell)$$

or $$A_2 = -\frac{B_2 \cosh \lambda\ell}{\sinh \lambda\ell}$$

At $x = a$, $\bar{\phi}_I = \bar{\phi}_{II}$ $\ldots(144)$

$$(M^{\circ}_{\bar{w}})_a + GJ(A_1 \sinh \lambda a + B_1 \cosh \lambda a) = (M^{\circ}_{\bar{w}})_a + GJ(A_2 \sinh \lambda a + B_2 \cosh \lambda a)$$

or $$(A_1 - A_2) \sinh \lambda a + (B_1 - B_2) \cosh \lambda a = 0 \qquad \ldots(145)$$

At $\bar{x} = a$, $\bar{\phi}'_I = \bar{\phi}'_{II}$

$$(M^{\circ}_{\bar{SP}}) + \lambda GJ(A_1 \cosh \lambda a + B_1 \sinh \lambda a) = (M^{\circ}_{\bar{SP}})_a + \lambda GJ(A_2 \cosh \lambda a + B_2 \sinh \lambda a$$

Referring to Fig. B.14, we obtain the following

$$M.\frac{b}{\ell} + \lambda GJ(A_1 \cosh \lambda a + B_1 \sinh \lambda a) = -M.\frac{a}{\ell} + \lambda GJ(A_2 \cosh \lambda a + B_2 \sinh \lambda a)$$

Substituting Eqs. (143) and (144) in the above equation and rewriting:

$$M\frac{(b+a)}{l} + \lambda GJ(A_1 \cosh \lambda a) = \lambda GJ B_2 \left[\sinh \lambda a - \frac{\cosh \lambda l}{\sinh \lambda l} \cosh \lambda a\right]$$

or

$$M + A_1 \lambda GJ \cosh \lambda a = -B_2 \lambda GJ \frac{\cosh \lambda b}{\sinh \lambda l} \qquad \ldots(146)$$

Substituting Eqs. (143) and (144) into Eq. (145) and simplifying:

$$A_1 \sinh \lambda a \sinh \lambda l = B_2 \sinh \lambda b \qquad \ldots(147)$$

Solving Eqs. (146) and (147) simultaneously we obtain

$$A_1 = -\frac{M \sinh \lambda b}{\lambda GJ \sinh \lambda l} \qquad \ldots(148)$$

$$B_2 = -\frac{M}{\lambda GJ} \sinh \lambda a \qquad \ldots(149)$$

Therefore, from Eq. (144)

$$A_2 = -\frac{B_2 \cosh \lambda l}{\sinh \lambda l} = \frac{M \sinh \lambda a \cosh \lambda l}{\lambda GJ \sinh \lambda l} \qquad \ldots(150)$$

Substituting the four constants found in Eqs. (148), (150) (143) and (149) into Eqs. (141) and (142) correspondingly, we have the expression of $\bar{\phi}$

Region I:

$$M^{\circ}_{\tilde{w}} = M.\frac{b}{l}.\bar{x} \qquad \text{(see Fig. B.14C)}$$

$$GJ\bar{\phi} = M^{\circ}_{\bar{w}} + GJ(A_1 \sinh\lambda\bar{x} + B_1 \cosh\lambda\bar{x})$$

$$= M \cdot \frac{b}{l} \cdot \bar{x} - \frac{M}{\lambda} \frac{\sinh\lambda b \sinh\lambda\bar{x}}{\sinh\lambda l}$$

$$= \frac{M}{\lambda}\left[\frac{b}{l} \cdot \lambda\bar{x} - \frac{\sinh\lambda b}{\sinh\lambda l} \cdot \sinh\lambda\bar{x}\right]$$

$$M_{\bar{w}} = -EA_{\bar{w}\bar{w}}\phi'' \qquad \ldots(151)$$

$$= \frac{M}{\lambda} \frac{\sinh\lambda b}{\sinh\lambda l} \cdot \sinh\lambda\bar{x}$$

$$\ldots(152)$$

Region II:

$$GJ\phi = \frac{M}{L}\left[\frac{a}{L} \cdot \lambda\bar{x}' - \frac{\sinh\lambda a}{\sinh\lambda l} \cdot \sinh\lambda\bar{x}'\right] \qquad \ldots(153)$$

$$M_{\bar{w}} = \frac{M}{\lambda} \frac{\sinh\lambda a}{\sinh\lambda l} \cdot \sinh\lambda\bar{x}' \qquad \ldots(154)$$

C. Redundant Warping Moment Integral

The redundant warping moment integral, denoted by M_{W1} (Fig.B.15) of an analogous beam corresponds to the redundant moment of a "real" beam. The $\bar{\phi}$ and $M_{\bar{w}}$ due to this integral, M_{W1} can be obtained as follows:

Using Eq. (111), the expression of $\bar{\phi}$ is

$$GJ\bar{\phi} = M^{\circ}_{\bar{w}} + GJ(A \sinh\lambda\bar{x} + B\cosh\lambda\bar{x}) \qquad \ldots(155)$$

At $x = 0$, $\phi = 0$

hence,

$$0 = 0 + GJB \qquad \therefore B = 0 \qquad \ldots(156)$$

At $\bar{x} = l$, $\bar{\phi} = 0$

hence, $\bullet =$

$$0 = M_{\bar{w}1} + GJ(A \sinh \lambda l + B \cosh \lambda l) \qquad \ldots(157)$$

Substituting Eq. (156) into Eq. (157) and rewriting,

$$A = - \frac{M_{\bar{w}1}}{GJ \sinh \lambda l} \qquad \ldots(158)$$

At a distance X from the left support

$$M^{\circ}_{\bar{w}} = M_{\bar{w}1} \cdot \frac{\bar{x}}{l} \qquad \text{(See Fig)} \qquad \ldots(159)$$

Substituting Eqs. (156), (158) and (159) into Eq. (155) we have,

$$GJ\bar{\phi} = M_{\bar{w}1}\left(\frac{\bar{x}}{l} - \frac{\sinh \lambda \bar{x}}{\sinh \lambda l}\right) \qquad \ldots(160)$$

Therefore,

$$M_{\bar{w}} = - E A_{\bar{w}\bar{w}} \bar{\phi}''$$

$$= M_{\bar{w}1} \cdot \frac{\sinh \lambda \bar{x}}{\sinh \lambda l} \qquad \ldots(161)$$

Similarly, we obtain the following equations for the case of Fig.

$$GJ\bar{\phi} = M_{\bar{w}2}\left(\frac{\bar{x}'}{l} - \frac{\sinh \lambda \bar{x}'}{\sinh \lambda l}\right) \qquad \ldots(162)$$

$$M_{\bar{w}} = M_{\bar{w}2} \frac{\sinh \lambda \bar{x}'}{\sinh \lambda \ell} \qquad \ldots(163)$$

D. Torsion of Continuous Beams

Using the formulas of items (A), (B) and (C) of this article we are able to derive the formula of the warping moment integra, $M_{\bar{W}}$ of a continuous beam. The method of superposition is used to obtain these formulas.

1. Uniform Torque

By the method of superposition, the structure shown in Fig.B.17a can be represented by the sum of structures of Fig.B.17a and c , where M_{W1} is a redundant warping moment integral. The relation between the loading M and the redundant M_{W1} can be obtained by setting equal the first derivative of ϕ at the left hand side of the middle support and that at the right hand side of the middle support. (Analogy: the slope at the left side of the support is equal to the slope at the right side of the same support for a continuous beam under flexural beiding). I.e. $\bar{\phi}'_{\text{left}} = \bar{\phi}'_{\text{right}}$. From Eqs. (137), (160) and (162):

$$\frac{m_{\bar{S}}}{\lambda}\left[-\lambda\frac{c(\ell - n)}{\ell} + \frac{\cosh \lambda(a+c) - \cosh \lambda a}{\sinh}\right] + M_{\bar{w}1}\left(-\frac{1}{d} + \frac{\lambda \cosh \lambda d}{\sinh \lambda d}\right)$$

$$= M_{\bar{w}1}\left(\frac{1}{d} - \frac{\lambda \cosh \lambda d}{\sinh \lambda d}\right)$$

$$\bar{M}_{w1} \cdot \lambda\left[\frac{1}{\lambda\ell} + \frac{1}{\lambda d} - \frac{1}{\tanh\lambda\ell} - \frac{1}{\tanh\lambda d}\right]$$

$$= \frac{\bar{m}_S}{\lambda}\left[-\lambda\frac{c(\ell-n)}{\ell} + \frac{\cosh\lambda(a+c)-\cosh\lambda a}{\sinh\lambda\ell}\right]$$

Therefore,

$$\bar{M}_{w1} = \frac{\bar{m}_S}{2} K \qquad \ldots(164)$$

where

$$K = \frac{-\left[c(\ell-n)\lambda + \frac{\cosh\lambda(a+c)-\cosh\lambda a}{\sinh}\right]}{\frac{1}{\lambda\ell} + \frac{1}{\lambda d} - \frac{1}{\tanh\lambda\ell} - \frac{1}{\tanh\lambda d}}$$

$$= \frac{\tanh\lambda\ell \cdot \tanh\lambda d\left[\lambda c(\ell-n)\sinh\lambda\ell + \cosh\lambda a - \cosh\lambda(a+c)\right]}{\ell\sinh\lambda\ell \cdot \left[\tanh\lambda\ell + \tanh\lambda d - \left(\frac{1}{\lambda d} + \frac{1}{\lambda\ell}\right)\tanh\lambda\ell \cdot \tanh\lambda d\right]} \qquad \ldots(165)$$

Region I

From Eqs (134) and (161):

$$\bar{M}_w = \frac{\bar{m}_S}{2} \cdot \frac{\cosh\lambda(b+c)-\cosh\lambda b}{\sinh\lambda\ell} \cdot \sinh\lambda\bar{x} - \bar{M}_{w1} \cdot \frac{\sinh\lambda\bar{x}}{\sinh\lambda\ell}$$

$$= \frac{\bar{m}_S}{\lambda^2}\left[\frac{\cosh\lambda(b+c)-\cosh\lambda b}{\sinh\lambda\ell} \cdot \sinh\lambda\bar{x} - K\frac{\sinh\lambda\bar{x}}{\sinh\lambda\ell}\right]$$

$$= \frac{\bar{m}_S}{2} \cdot \frac{\cosh\lambda(b+c)-\cosh\lambda b - K}{\sinh\lambda\ell} \cdot \sinh\lambda\bar{x} \qquad \ldots(166)$$

Region II

From Eqs. (136) and (161):

$$M_{\bar{w}} = \frac{m_{\bar{s}}}{\lambda^2}\left(1 - \frac{\cosh \lambda a.\sinh \lambda \bar{x}' + \cosh \lambda b.\sinh \lambda \bar{x})}{\sinh \lambda \ell}\right) - M_{\bar{w}1}.\frac{\sinh \lambda \bar{x}}{\sinh \lambda \ell}$$

$$= \frac{m_{\bar{s}}}{\lambda^2}\left[1 - \frac{\cosh \lambda a.\sinh \bar{x}' + (K+\cosh \lambda b)\sinh \lambda \bar{x}}{\sinh \lambda \ell}\right] \quad \ldots(167)$$

Region III

From Eqs. (138) and (161):

$$M_{\bar{w}} = \frac{m_{\bar{s}}}{\lambda^2}.\frac{\cosh \lambda(a+c)-\cosh \lambda a}{\sinh} . \sinh \lambda \bar{x}' - M_{w1} . \frac{\sinh \lambda \bar{x}}{\sinh \lambda \ell}$$

$$= \frac{m_{\bar{s}}}{\lambda^2} . \frac{[\cosh \lambda(a+c)-\cosh \lambda a] \sinh \lambda \bar{x}' - K \sinh \lambda \bar{x}}{\sinh \lambda \ell} \quad \ldots(168)$$

Region IV

From Eq. (163):

$$M_{\bar{w}} = -M_{\bar{w}1} . \frac{\sinh \lambda \bar{x}'d}{\sinh \lambda d} = \frac{m_{\bar{s}}}{2} . K . (- \frac{\sinh \bar{x}'d}{\sinh \lambda d}) \quad \ldots(169)$$

2. Concentrated Torque

Similarly, we can derive the formulas of $M_{\bar{w}}$ for the structure shown in Fig. . The result is given as follows:

$$M_{w1} = \frac{M}{\lambda} . K$$

$$K = \frac{\tanh \lambda d \tanh \lambda \ell (a \sinh \lambda \ell - \lambda \ell \sinh \lambda a)}{\lambda \ell \sinh \lambda \ell (\tanh \lambda d + \tanh \lambda \ell) - (1+\frac{\ell}{d}) \sinh \lambda \ell - \tanh \lambda d - \tanh \lambda \ell} \quad \ldots(171)$$

Region I

$$M_{\bar{w}} = \frac{M}{\lambda} \cdot \frac{\sinh \lambda b - K}{\sinh \lambda \ell} \cdot \sinh \lambda \bar{x} \quad \ldots(172)$$

Region II

$$M_{\bar{w}} = \frac{M}{\lambda} \cdot \frac{\sinh \lambda a \cdot \sinh \lambda \bar{x}' - K \sinh \lambda \bar{x}}{\sinh} \quad \ldots(173)$$

Region III

$$M_{\bar{w}} = \frac{M}{\lambda} K(- \frac{\sinh \bar{x}' d)}{\sinh \lambda d} \quad \ldots(174)$$

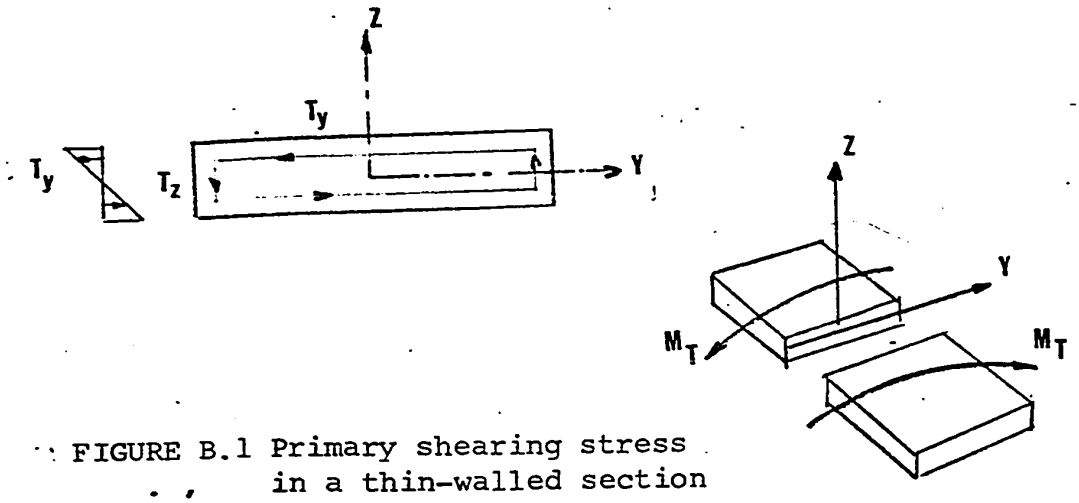

FIGURE B.1 Primary shearing stress in a thin-walled section

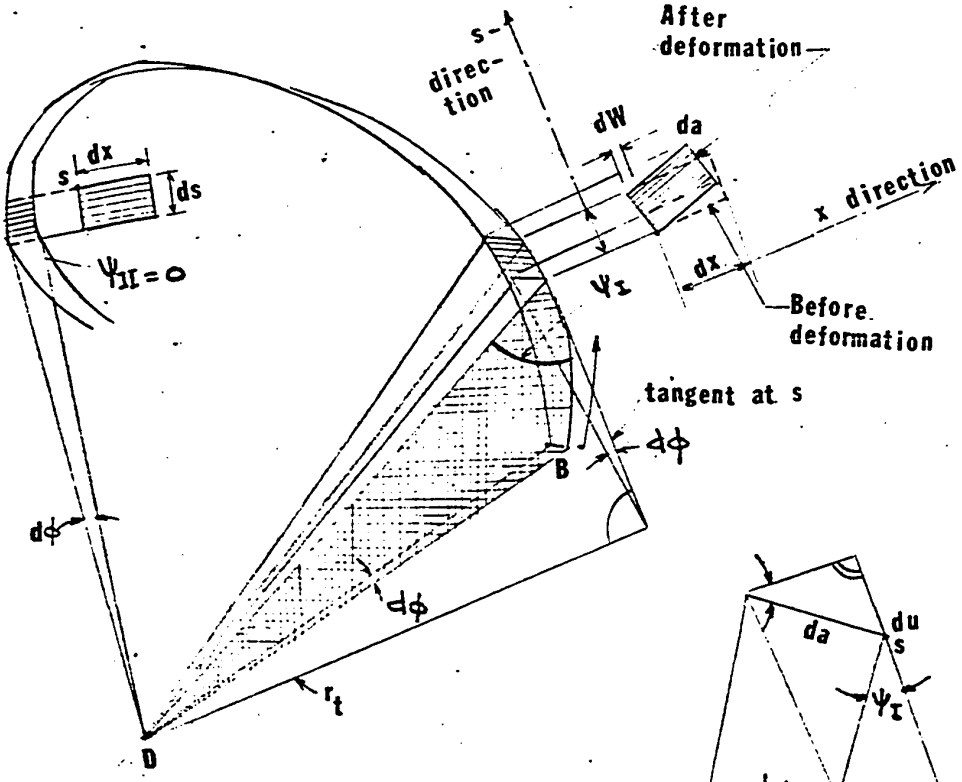

FIGURE B.2(a) Deformed middle plane of an open section of length dx

FIGURE B.2(b)

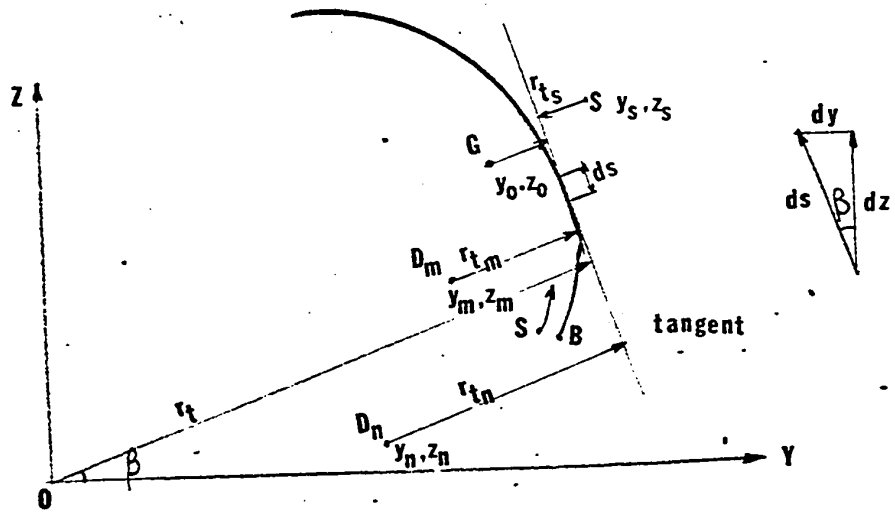

FIGURE B.3(a) Effect on warping of a displacement of rotation centre

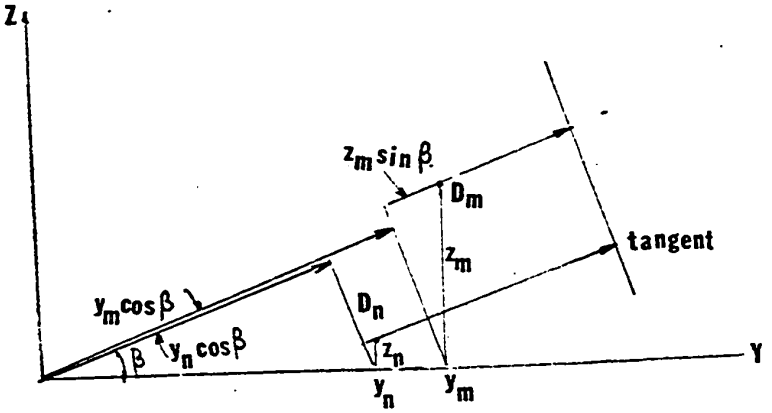

FIGURE B.3(b) Effect on warping of a displacement of rotation centre

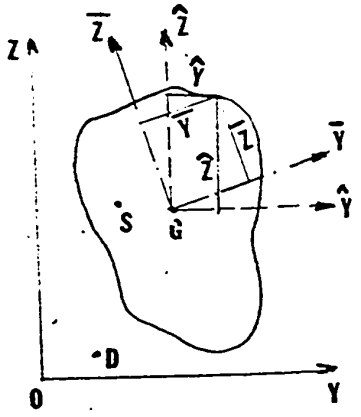

FIGURE B.4 Rotation of coordinates

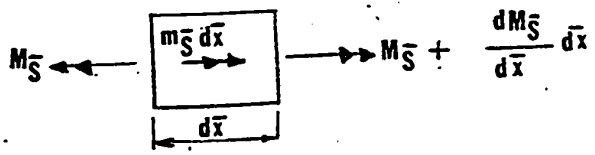

FIGURE B.5 Twisting moment on an element

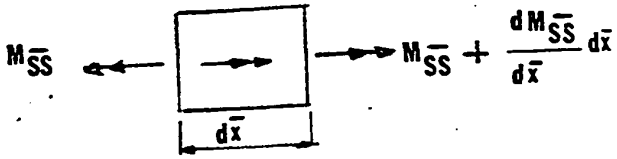

FIGURE B.6 Twisting moments on an element

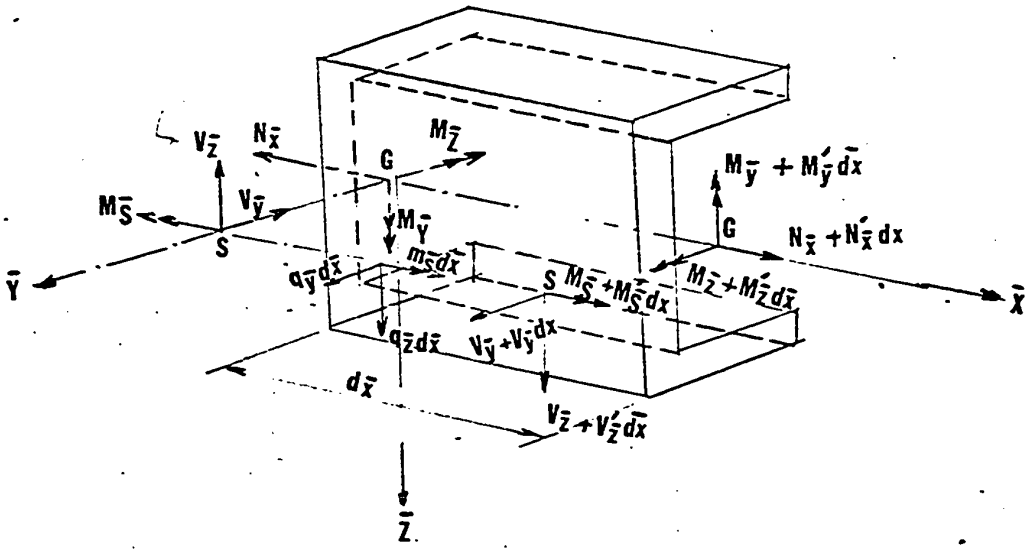

FIGURE B.7 Element of a twisted bar

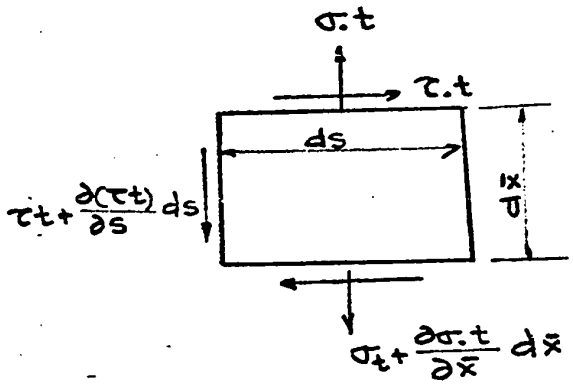

FIGURE B.8 Element subjected to both twisting and bending

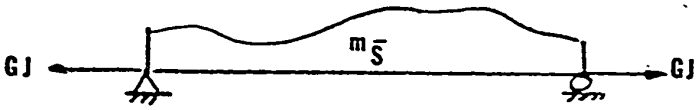

FIGURE B.9 Analogous beam column

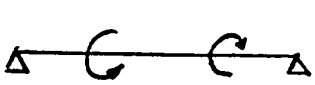

FIGURE B.10 Beam subjected to torque

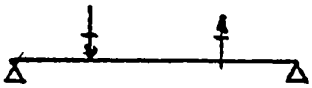

FIGURE B.11 Vector convention for beam subjected to torque

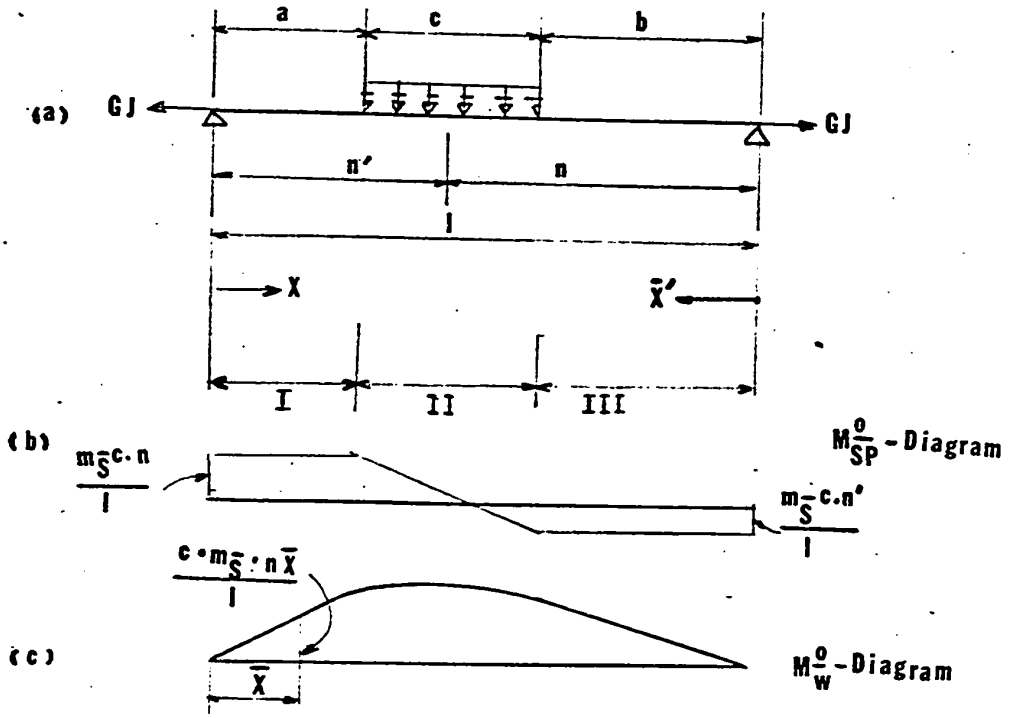

FIGURE B.12 Analogous beam column loaded with uniform torque

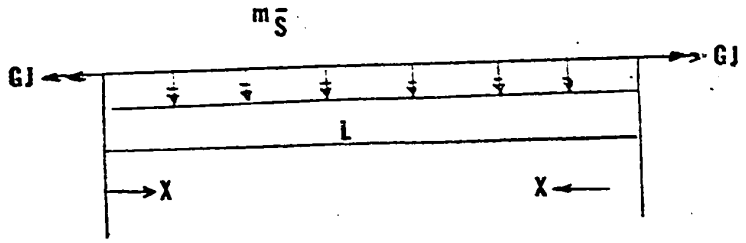

FIGURE B.13 Analogous beam column loaded with uniform torque for all length

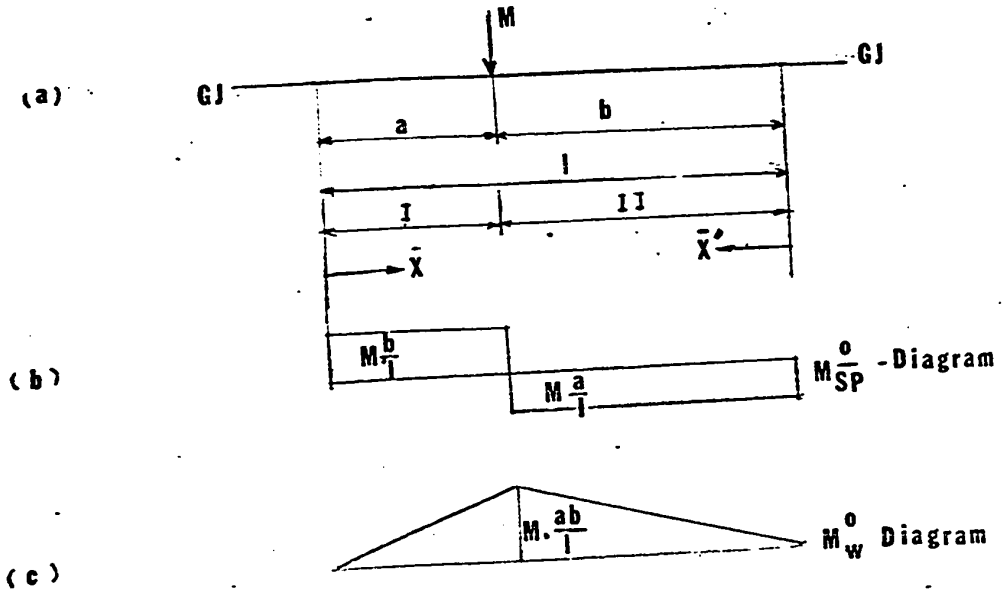

FIGURE B.14 Analogous beam column subjected to concentrated torque

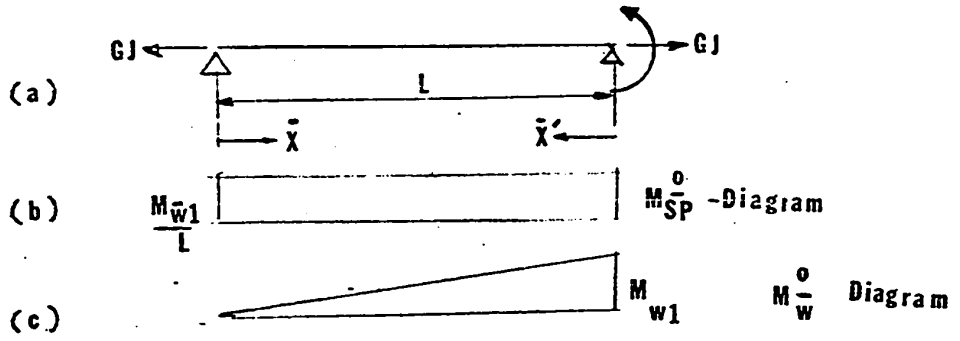

FIGURE B.15 Analogous beam subjected to redundant warping moment integral

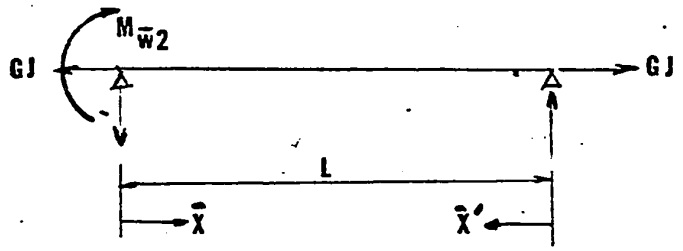

FIGURE B.16 Analogous beam subjected to redundant warping moment integral

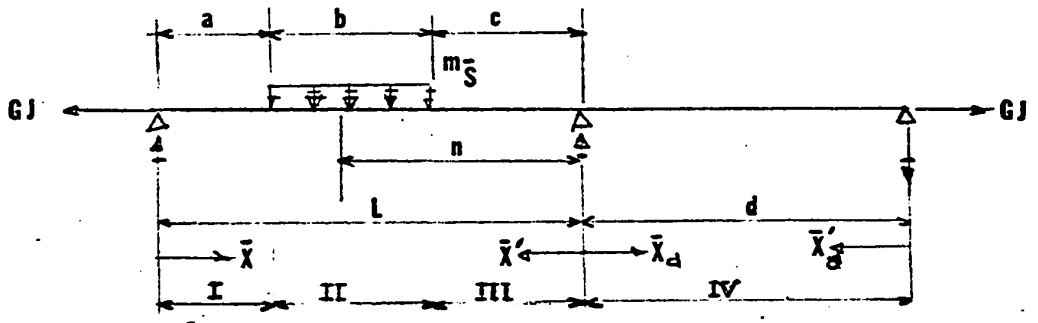

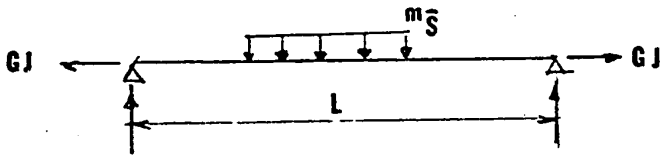

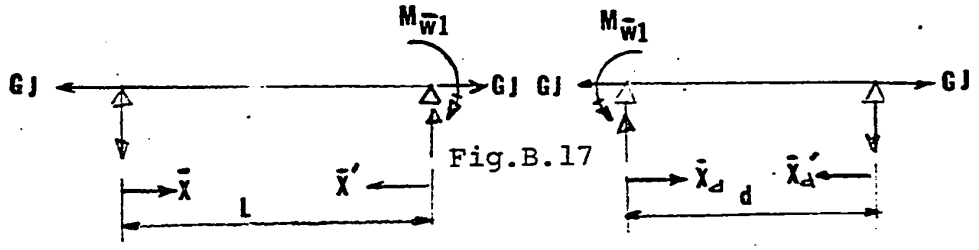

Fig.B.17

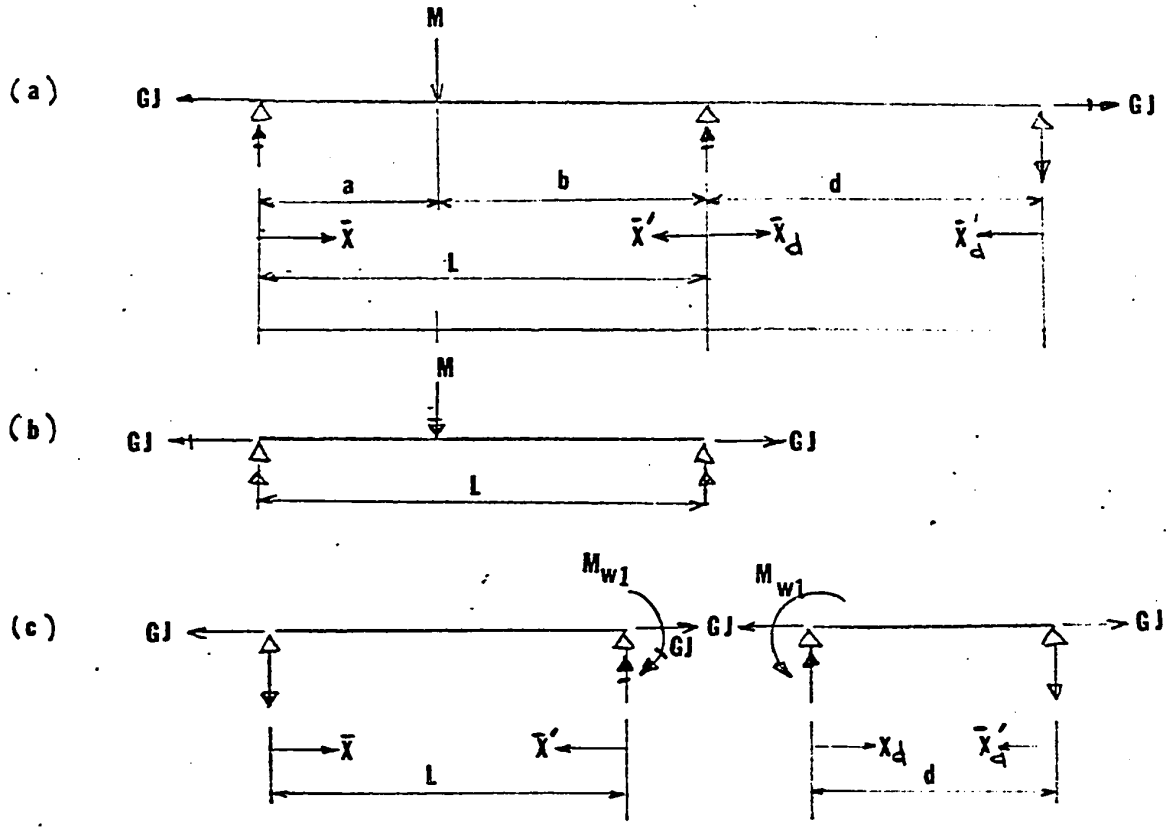

FIGURE B.18 Analogous continuous beam subjected to concentrated torque

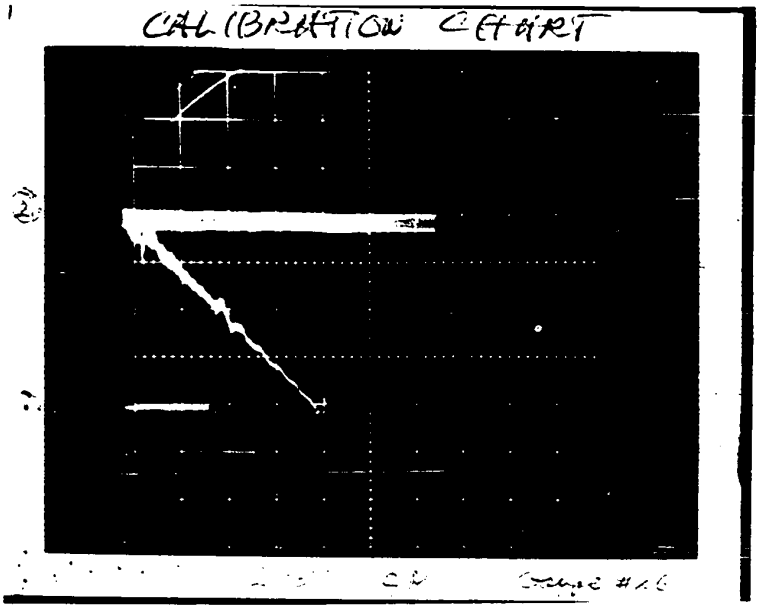

Photograph 1. Calibration of Oscilloscope for Known Strain

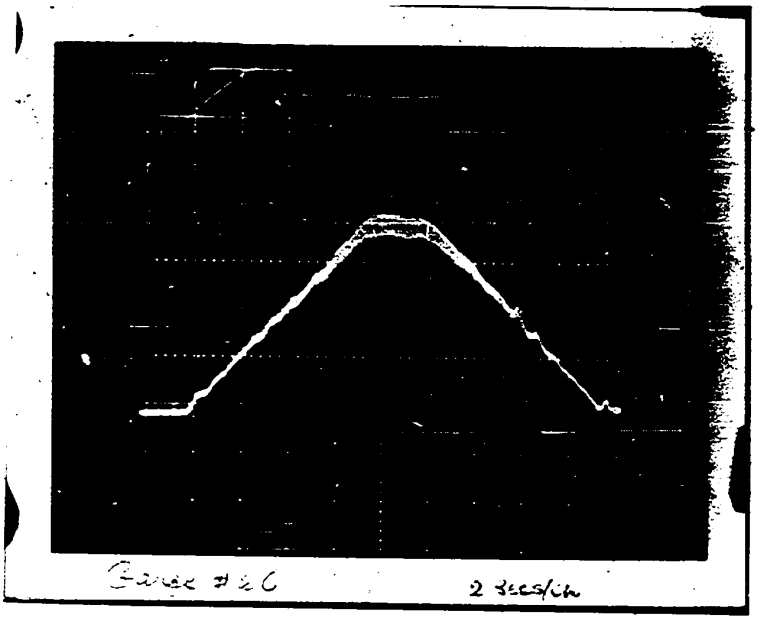

Photograph 2. Oscilloscope Response for Strain Gauge No. 26 subjected to Moving Load

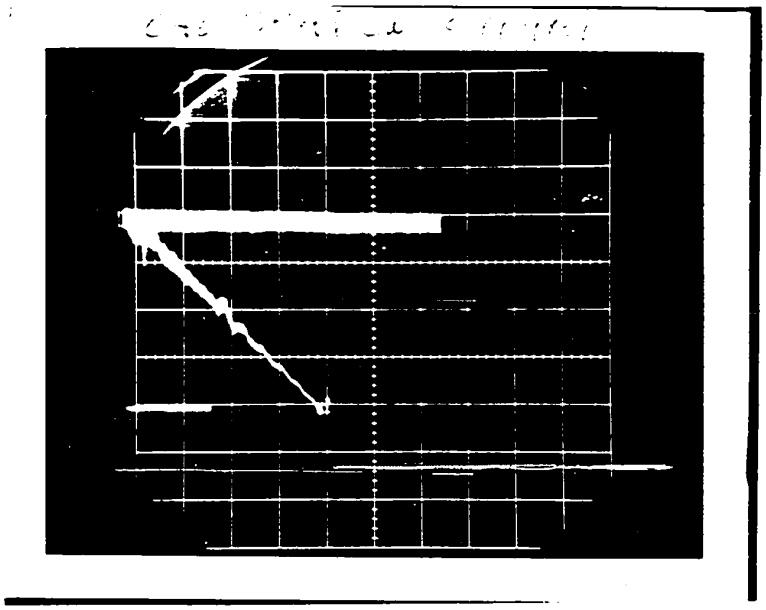

Photograph 1. Calibration of Oscilloscope for Known Strain

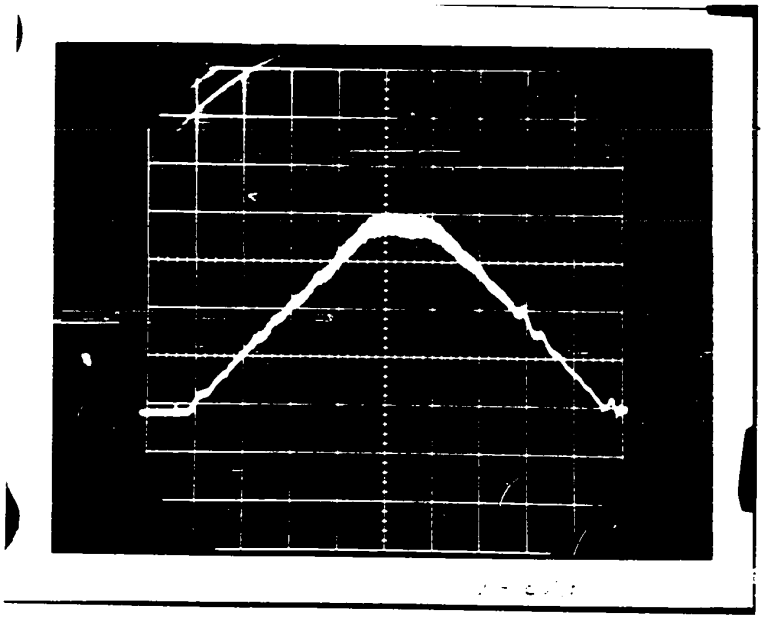

Photograph 2. Oscilloscope Response for Strain Gauge No. 26 subjected to Moving Load

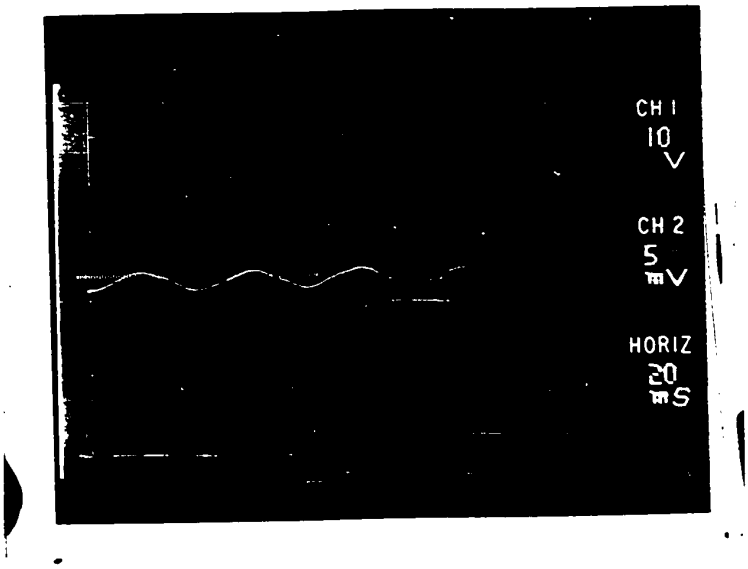

Photograph 3. Oscilloscope Response showing the period of Oscillation

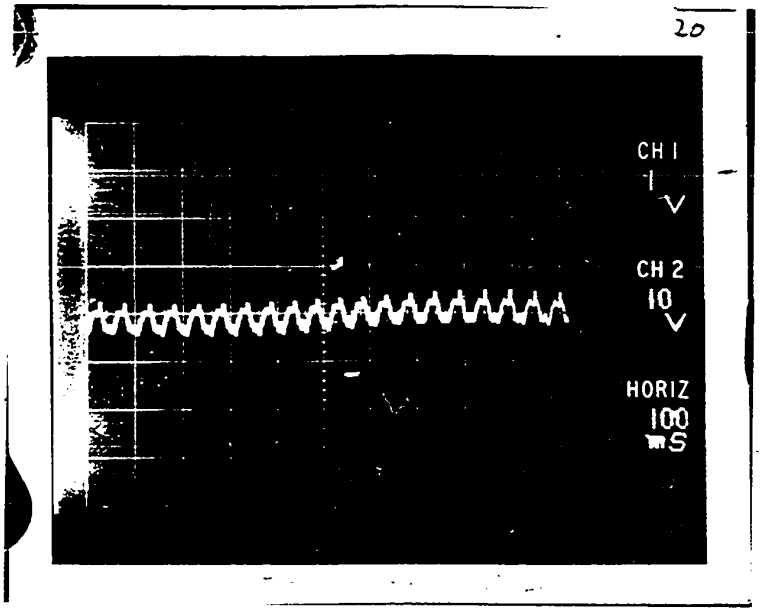

Photograph 4. Oscilloscope Response when Gilmore Actuator is at 20 cycles/sec

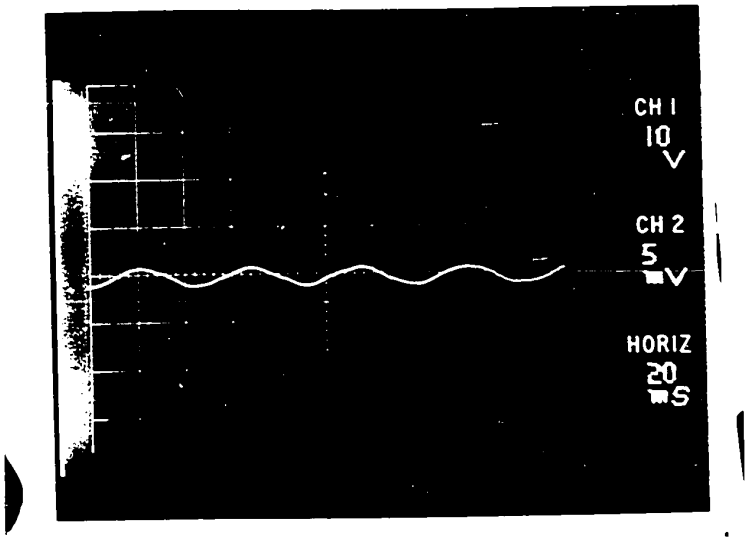

Photograph 3. Oscilloscope Response showing the period of Oscillation

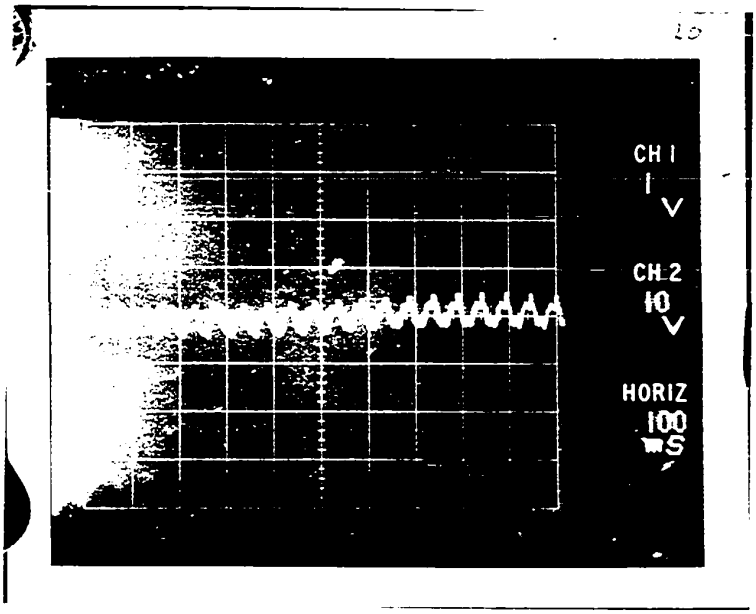

Photograph 4. Oscilloscope Response when Gilmore Actuator is at 20 cycles/sec

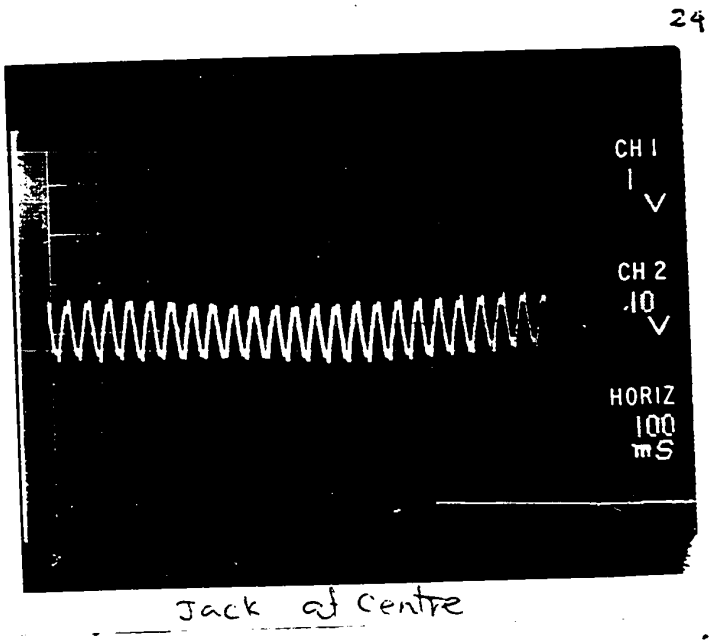

Photograph 5. Oscilloscope Response when Gilmore Actuator is at 24 cycles/sec

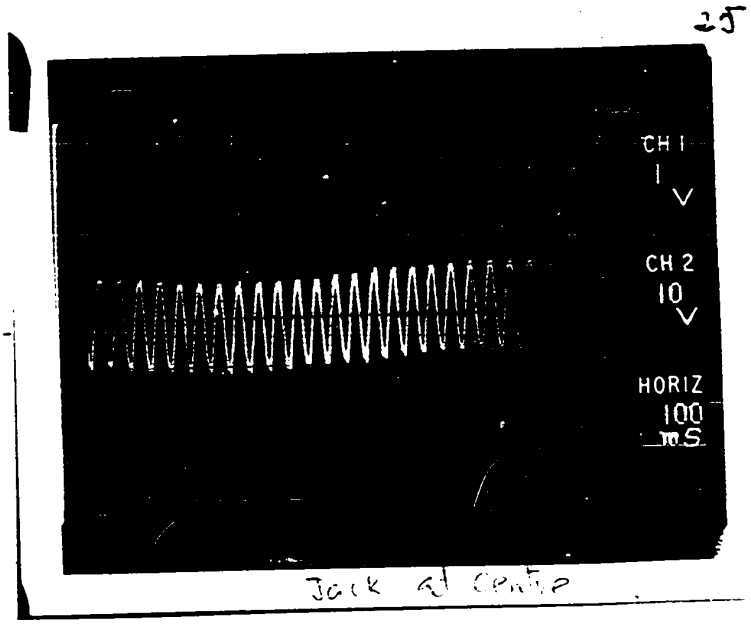

Photograph 6. Oscilloscope Response when the Gilmore Actuator is at 25 cycles/sec

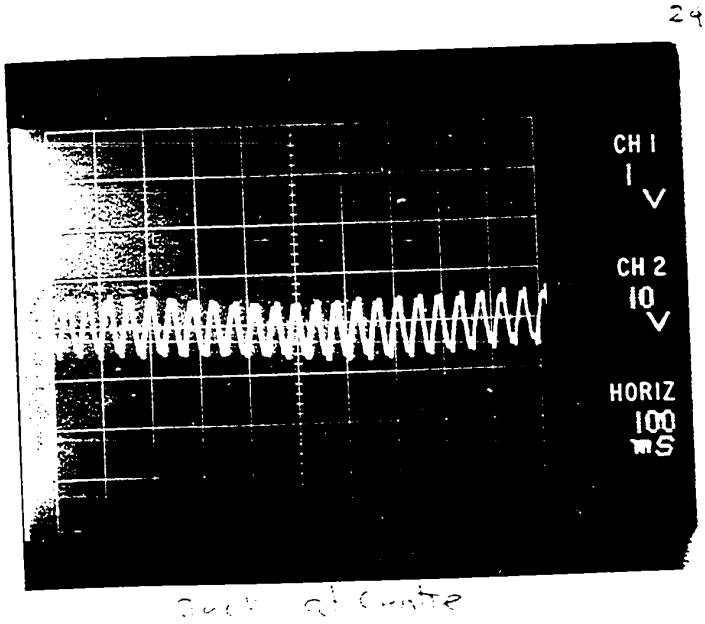

Photograph 5. Oscilloscope Response when Gilmore Actuator is at 24 cycles/sec

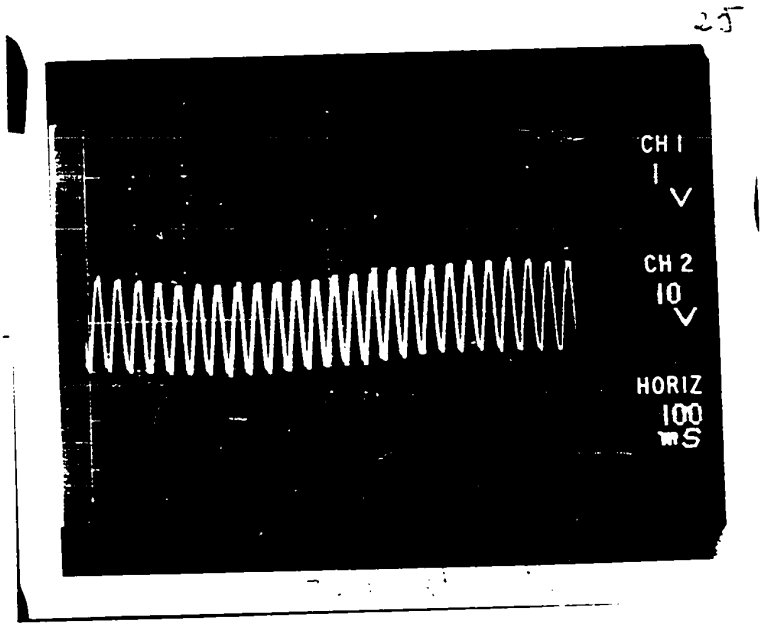

Photograph 6. Oscilloscope Response when the Gilmore Actuator is at 25 cycles/sec

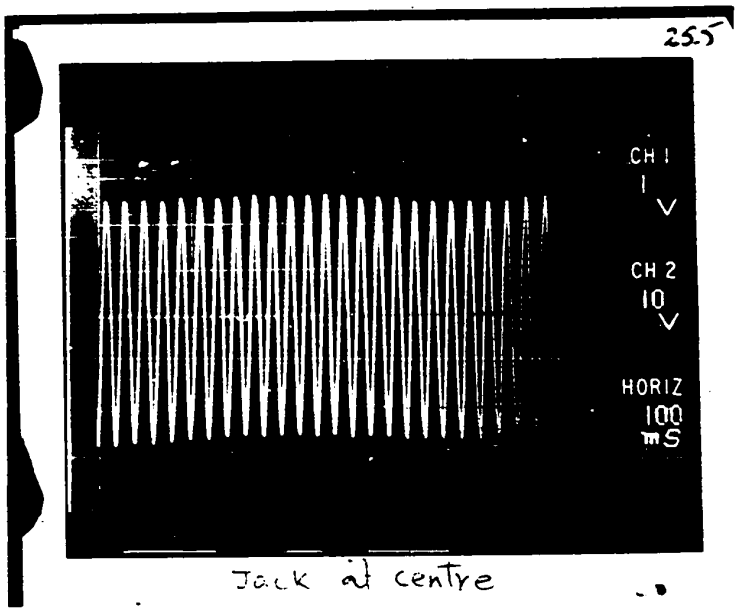

Photograph 7. Oscilloscope Response when Gilmore Actuator is at 25.5 cycles/sec

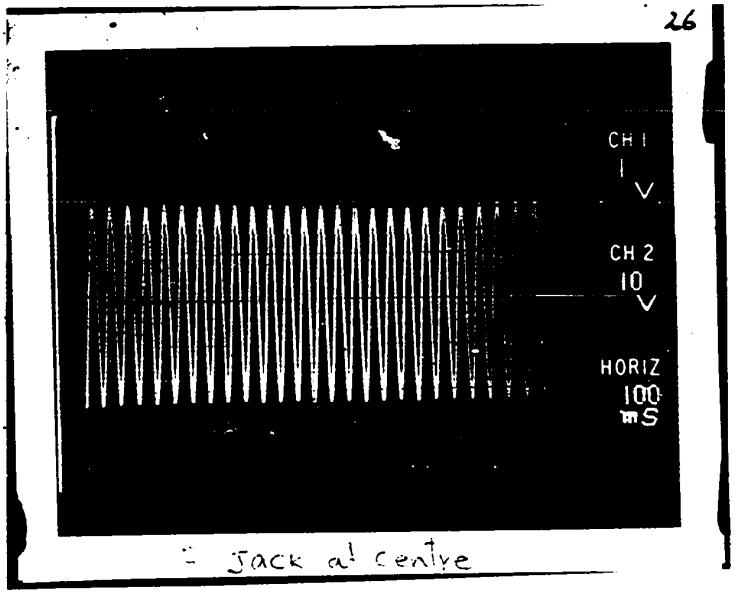

Photograph 8. Oscilloscope Response when Gilmore Actuator is at 26 cycles/sec

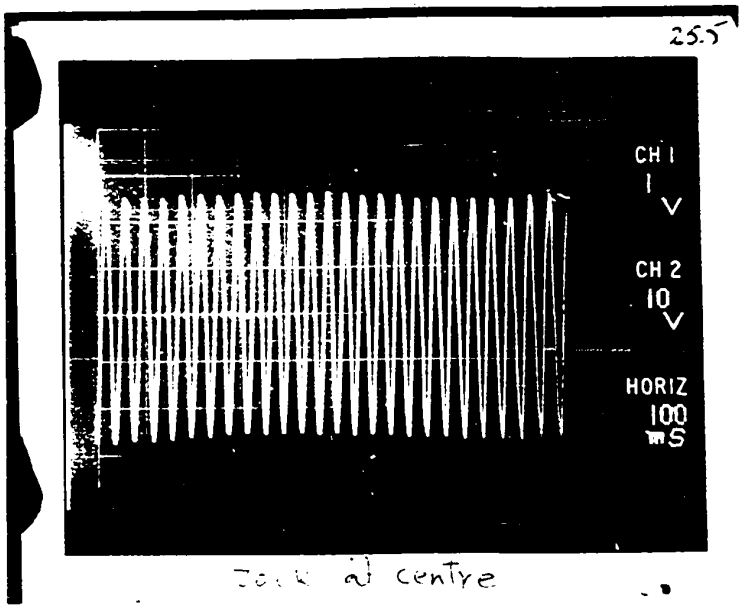

Photograph 7. Oscilloscope Response when Gilmore Actuator is at 25.5 cycles/sec

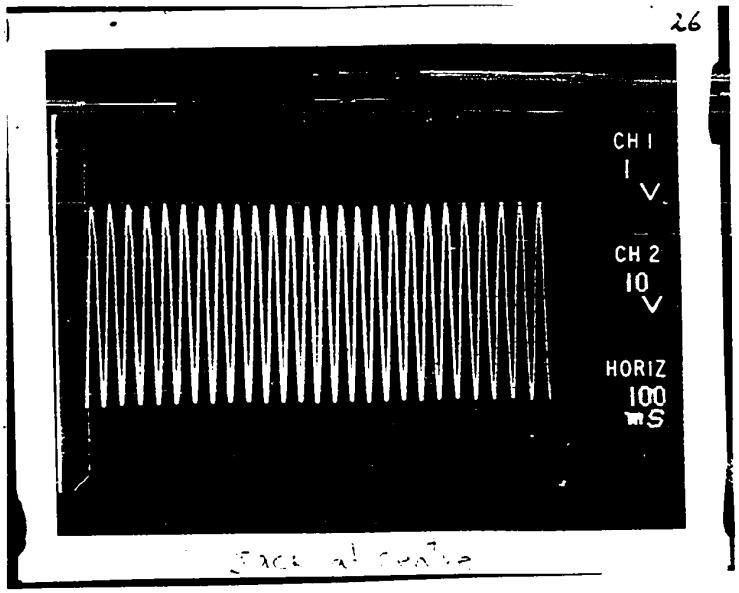

Photograph 8. Oscilloscope Response when Gilmore Actuator is at 26 cycles/sec

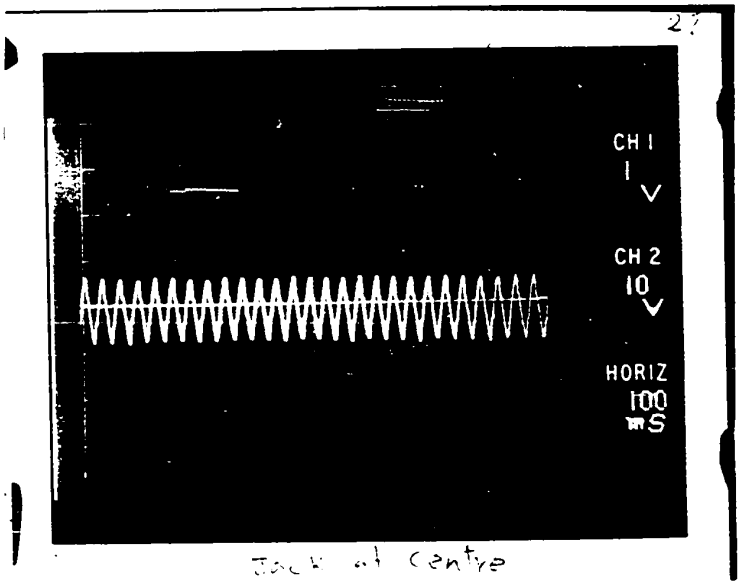

Photograph 9. Oscilloscope Response when Gilmore Actuator is at 27 cycles/sec

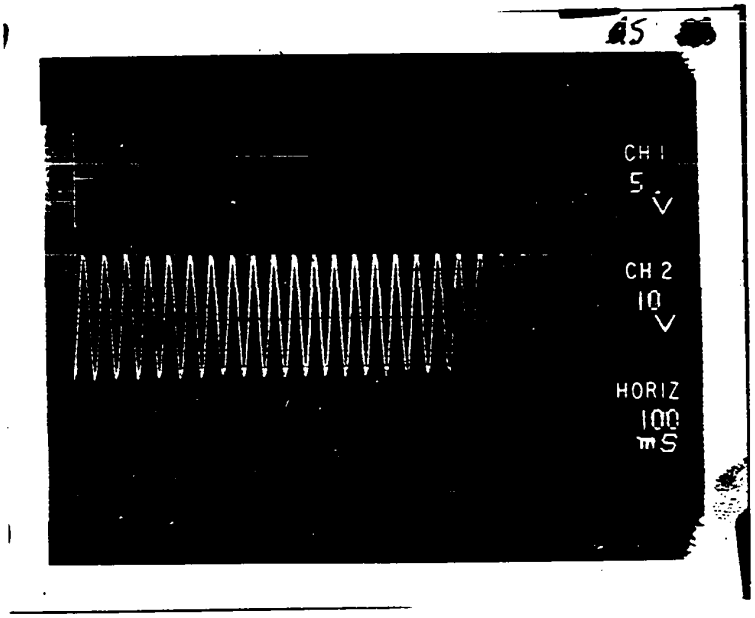

Photograph 10. Oscilloscope Response when Gilmore Actuator is at 64 cycles/sec

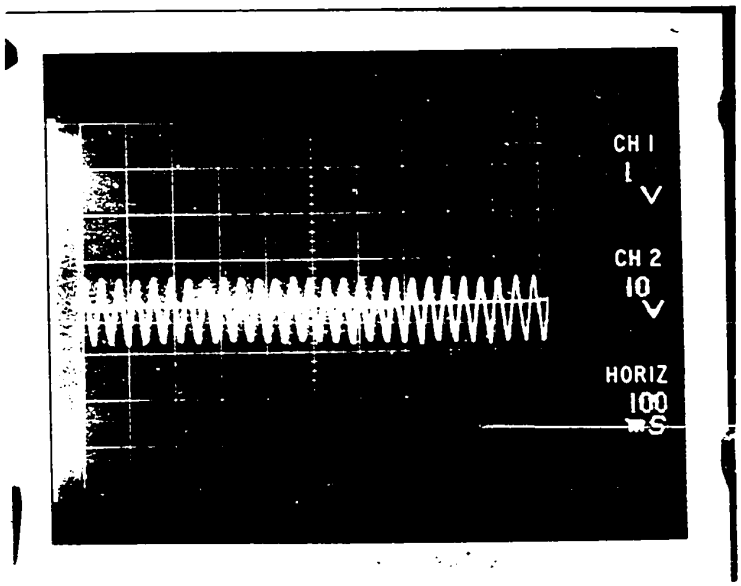

Photograph 9. Oscilloscope Response when Gilmore Actuator is at 27 cycles/sec

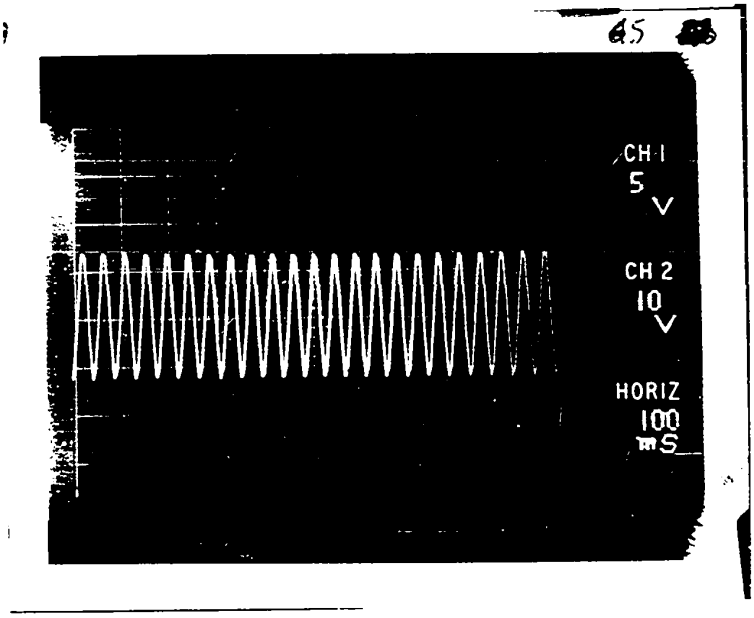

Photograph 10. Oscilloscope Response when Gilmore Actuator is at 64 cycles/sec

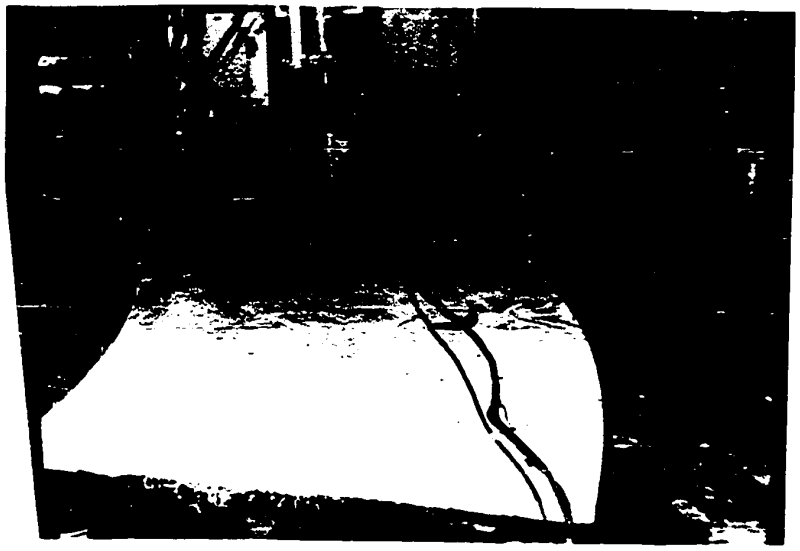

Photograph 11. Model

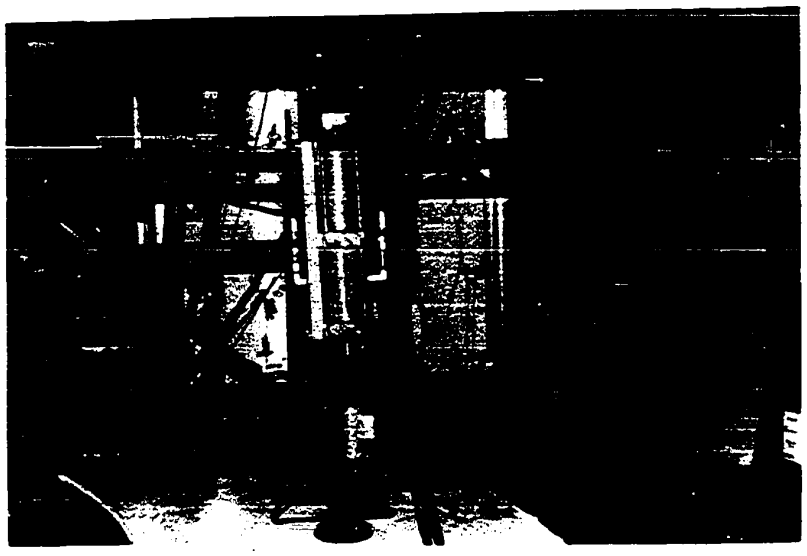

Photograph 12. Model with Gilmore Actuator and Loading Frame

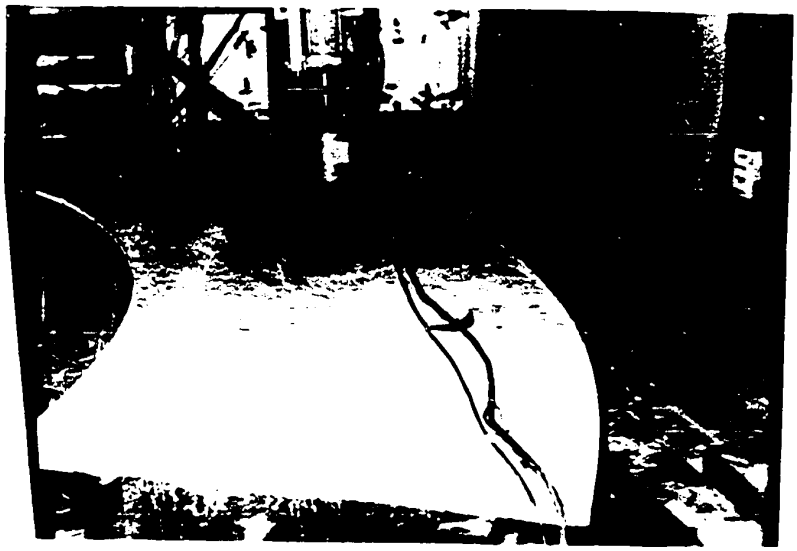

Photograph 11. Model

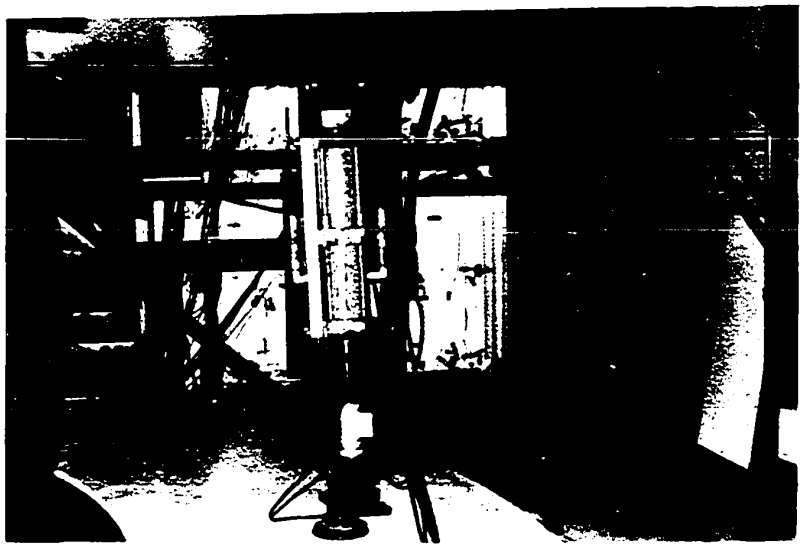

Photograph 12. Model with Gilmore Actuator and Loading Frame

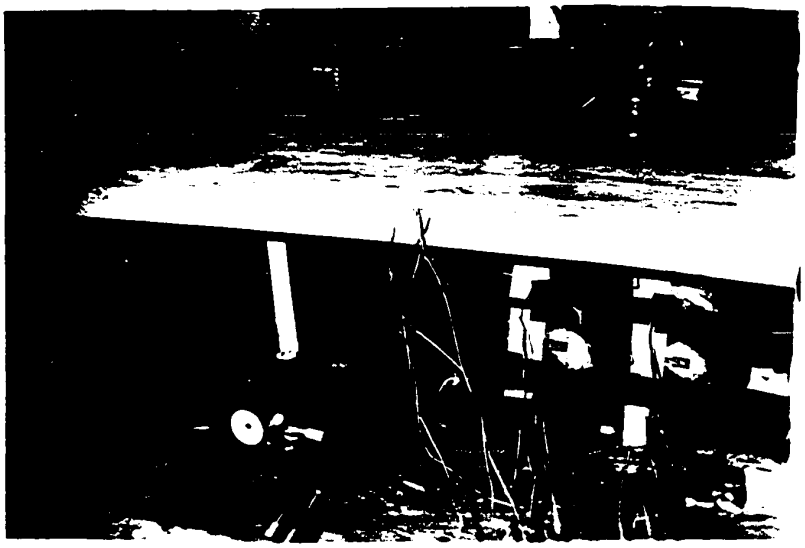

Photograph 13. Model with Strain Gauges and Dial Indicators

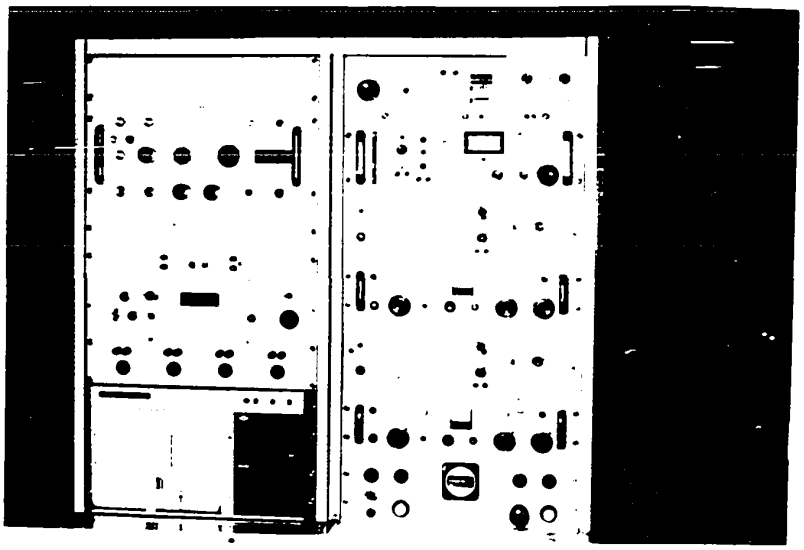

Photograph 14. Gilmore Loading System

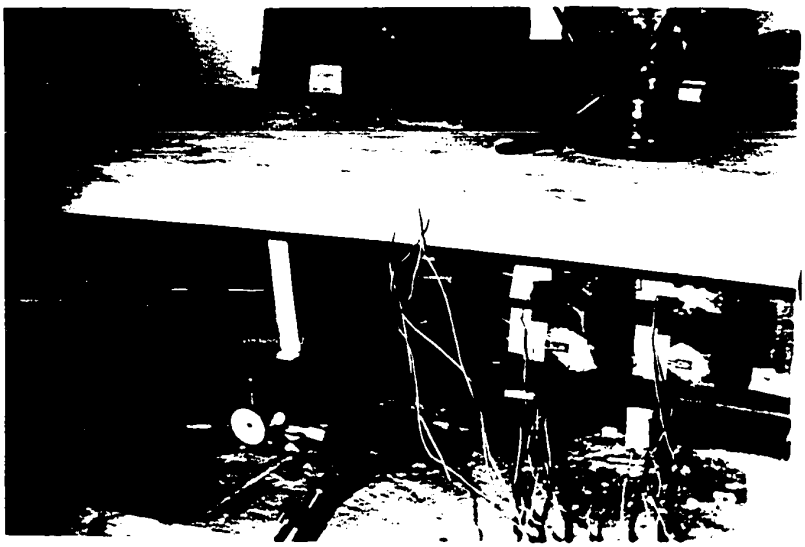

Photograph 13. Model with Strain Gauges and Dial Indicators

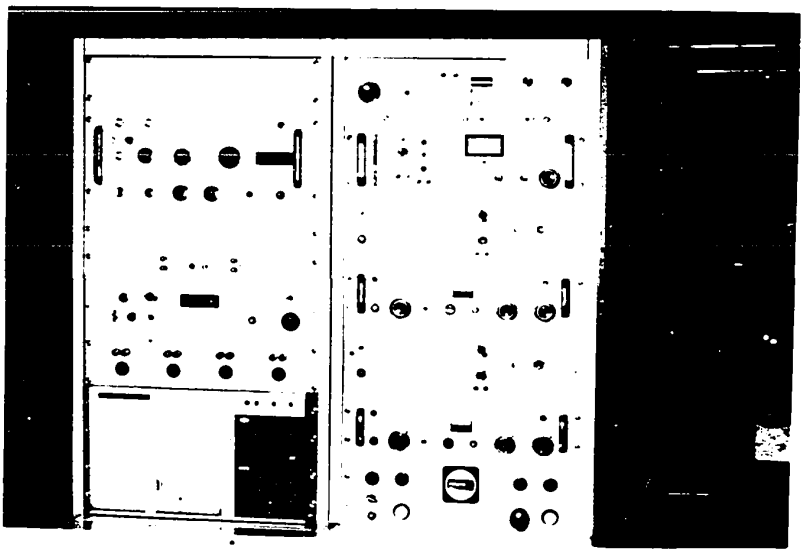

Photograph 14. Gilmore Loading System

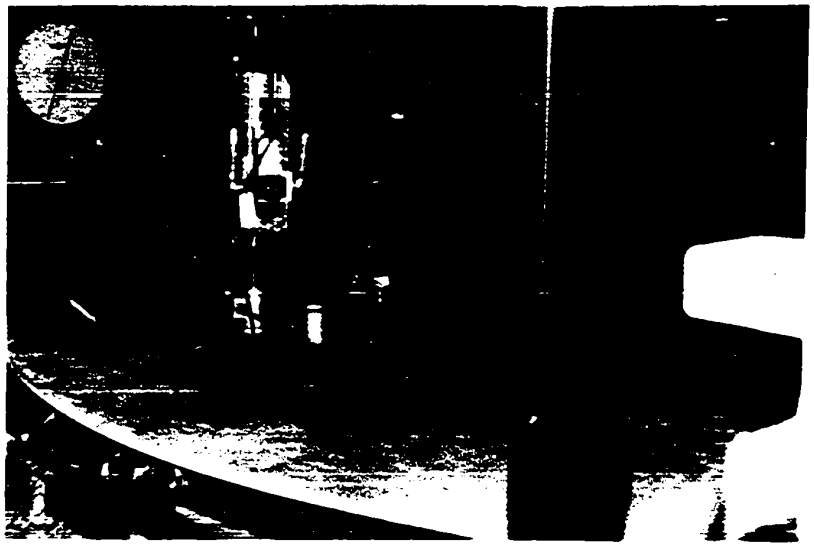

Photograph 15. Model with Gilmore Actuator

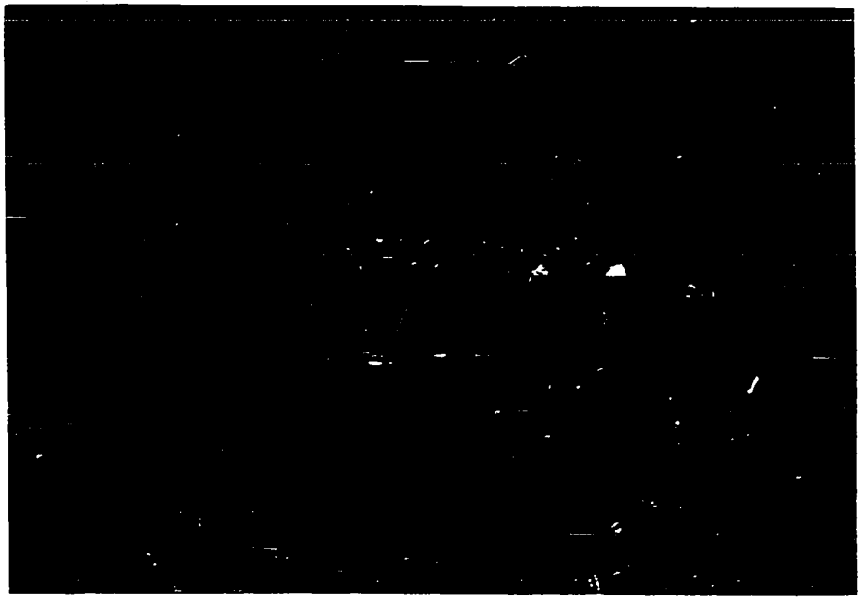

Photograph 16. Load Carriage

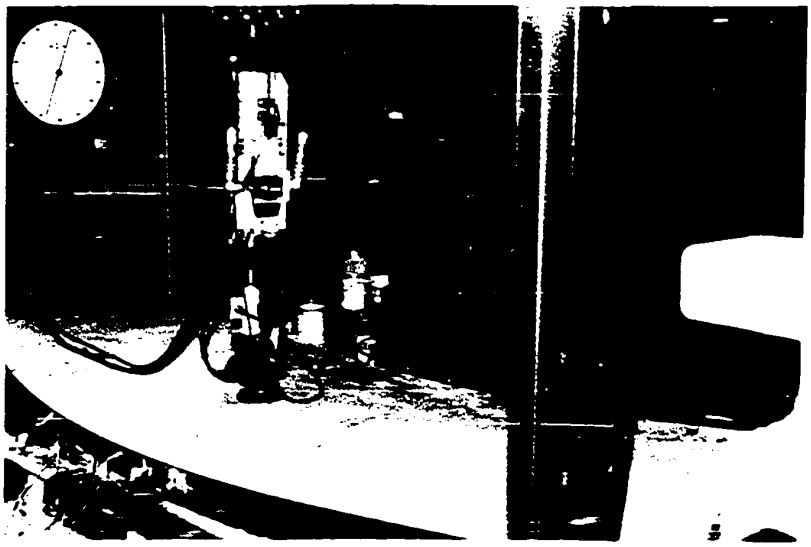

Photograph 15. Model with Gilmore Actuator

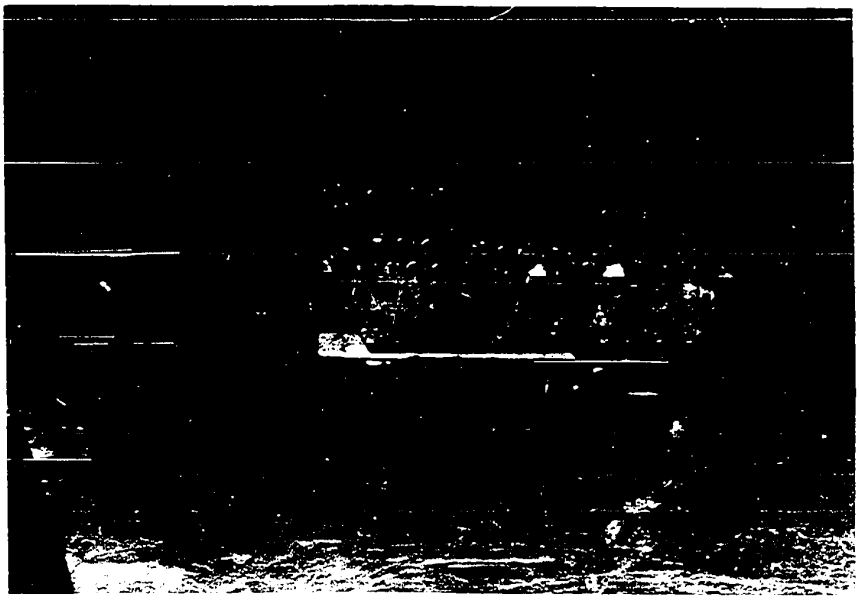

Photograph 16. Load Carriage